Theory of
Breaking of a Polymer Molecule
under Tension

A Thesis

Submitted in partial fulfilment of the

requirements for the Degree of

Doctor of Philosophy

in the Faculty of Science

by

Rosabella K. Puthur

Department of Applied Chemistry
Cochin University of Science and Technology
Kochi — 682 022 (INDIA)

October 2001

Certificate

Certified that the thesis entitled 'THEORY OF BREAKING OF A POLYMER MOLE-CULE UNDER TENSION' submitted by Mrs. Rosabella K. Puthur, is based on the bonafide work carried out by her under our joint supervision in the Department of Applied Chemistry, Cochin University of Science and Technology and that no part thereof has been included in any other thesis submitted previously for the award of any degree.
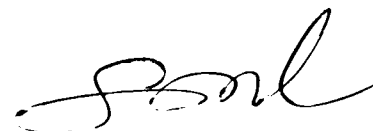
Prof. K. L. Sebastian (Guide)

Professor

Dept of Inorganic and Physical Chemistry

IISc Bangalore

Prof. S. Sugunan (Co-guide)

Head

Dept of Applied Chemistry

CUSAT Kochi

Contents

Chapter 1

Fracture in Polymers

1.1 Introduction

The wide usage of polymeric materials in engineering is largely due to their valuable mechanical properties and especially due to their high strength coupled with large recoverable deformability. This unique combination of properties arises from the specific structure of polymers, namely, the presence in them of two kinds of linkages differing sharply in energy and length; strong chemical bonds between the atoms of the chain and much weaker intermolecular ones between the chains. Fracture is the rupture of the bonds between the elements of a body (atoms, molecules or ions) resulting in breakage or cleavage of the specimen into parts. In mathematical terms we may define a fracture processs [1] as one by which the sum of the degrees of connectedness of the parts of a sample or a structural element is increased by at least one. This definition includes the piercing of films and tubes, but excludes minute damages as caused by crazing or chain scission. The term fracture process is meant to describe the whole development of a fracture from its initiation through crack growth and propagation to completion of the fracture. In contrast to thermal or environmental degradation and failure, the fracture process is understood as stress-biased material disinetegration. It carries on if and only if a drivng force exists, which has literally to be a force. Forces, however, will give rise to deformations. This means that fracture initiation will always be preceeded by specimen deformation. The

resistance of a material to fracture is called strength or mechanical strength.

In the absence of flow, chain scission and chain strength determine the mechanical properties of polymers. In fact, there are a number of observations which support this assumption:

1. with increasing number n of chain atoms, a saturated linear hydrocarbon will turn from gas to liquid and to solid; the solid will attain technically useful strength if n is around 2000; with increasing moleculear weight and chain orientation that strength may still be increased 50-fold [2];

2. the mechanical loading and rupture of virtually all natural and synthetic polymers leads to the scission of molecular chains and the formation of free radicals [3];

3. the strength and the hardness of solids increase with volume concentration of primary bonds [4];

4. in a number of uniaxial tensile fracture experiments the energy of activation of sample fracture coincided with the activation energy for main chain bond scission [3].

In materials such as highly oriented or liquid-crystalline polymers, the overall strength of the solid is likely to be governed by the strength of the chemical bonds linking chain segments and the calculation demands treatment on a quantum mechanical level [5]. In this case, a formalism at the atomic scale is more appropriate, and at non-zero temperatures, one expects thermal fluctuations to cause the chemical bonds to break. It is found that the axial tensile modulus is an appreciable fraction (0.2 - 0.80) of the value expected for an assembly of parallel chains. Hookean behaviour has been assumed for strains up to 0.13 by Chevychelov [6]. A number of empirical anharmonic potential functions have been used to treat the homolytic scission of a bond in an overstressed chain. While Morse or Lennard-Jones functions have been used most frequently [6, 7] other functions have been assumed to account for bond angle deformation [8].

Because the interactions between atoms in a polymer are either intramolecular or intermolecular, the failure of a macroscopic sample of such a material can be described

on the molecular scale by two types of events [9]: the breaking of intermolecular van der Waals, hydrogen or electrostatic bonds (chain slippage or peeling apart of neighbouring chains), and the breaking of intramolecular covalent bonds (chain scission).

The measured tensile strengths of solids are much lower than the theoretical strengths as calculated from the atomic binding forces. For organic polymers, the maximum theoretical strength is that of a carbon-carbon bond. In practice, the tensile strength of a carbon-carbon bond cannot be approached unless the molecules are highly oriented in the direction of the applied tensile force. Usually all polymer samples contain structural irregularities at which the local stress and strain are higher than the average measured stress and strain. Fracture occurs at the most defective point.

1.2 Theories of Fracture

1.2.1 Statistical Theory of Fracture

Based purely on statistical considerations, Coleman and Marquardt [10] developed their important theory of breaking kinetics of fibers. They especially investigated the distribution of lifetimes of fibers under constant or periodic load and the effects of fiber length, rate of loading and bundle size on the strength of filaments or bundles thereof. Two statistical effects should be noted: (1) the lower strength of a bundle as compared with that of a monofilament (due to the accelerating increase in failure probability K after rupture of the first filament within a bundle) and (2) the increase of strength with loading rate here derived from the reduced time each filament spends at each load level. The large scatter of strengths and the dependency on sample geometry may be explained by introducing the concept of flaws of different degrees of severity. When being stressed, the flaw since it is the weak region, may fail, leading to a void, a craze, and or to a propagating crack and macroscopic failure. Following Epstein's statistical theory of extreme values [11], the strength of a material volume element depends on the 'severeness' of the most critical flaw being present within that volume element. The third statistical argument is that fracture is the result of a large number of molecular processes. Its application

to polymers definitely was stimulated from many sides including fracture and fatigue of metals [12] or glasses [13] and the thermodynamics of reactions [14]. This interpretation of fracture necessitates a consideration of the correlation of the individual steps and of the final failure criterion.

Recently Huang [15] has studied the general properties of failure of polymeric materials using Markov theory and has given a statistical theory of fracture of general molecular bonds of polymeric materials. He obtained a general rigorous relation between the number of the molecular bonds of the polymeric components and the effective life time of the loaded components and discovered that the relation (relative to stress, temperature etc.) is just the probable statistical mean one.

1.2.2   Griffith's Theory

If the strength of a material is limited by macroscopic flaws, then a formalism based on continuum mechanics is commonly used to investigate the distribution and time evolution of these flaws. The principal continuum theory of brittle fracture is that first proposed by Griffith [16]. In his phenomenological theory of strength, Griffith pointed out that one could acccount for the large difference between experimentally observed rupture strengths in solids and theoretically expected values by presupposing that stress and associated strain energy are not uniformly distributed in a test specimen, but are concentrated in the neighbourhood of preexisting microcracks. Rupture or brittle fracture then occur by propagation of these preexisting microcracks – which presumably develop as a result of the preparation procedures – under the action of the high localised stresses at the crack tips. According to Griffith, a crack would propagate and a sample would fail in brittle fashion when the work required to extend the crack and create new surfaces was just balanced by an equal reduction in the strain energy of the specimen associated with the applied stress. Under these conditions, no increase in total potential energy of the system occurs and the energy to make the crack self-propagating comes from the elastic energy stored near the crack tips.

Griffith used the Inglis equation [17] for the local stress, σ_{max}, occuring at the edge of

a narrow elliptical crack in a uniformly stressed thin plate, namely,

$$\sigma_{\max} = 2\sigma_0 \sqrt{\frac{c}{\rho}} \qquad (1.1)$$

where σ_0 is the applied stress, $2c$ is the length of the elliptical crack, and ρ is the radius of curvature. Griffith was able to show that the critical applied tensile stress, σ_c, required to cause such a transversely oriented crack to spread was given by

$$\sigma_c = \sqrt{\frac{2E\gamma}{\pi c}} \qquad (1.2)$$

where E is Young's modulus of elasticity, and γ is the specific surface energy, that is, the energy required to form a unit area of fracture surface. Thus the stress to propagate the crack and produce brittle fracture decreases with increase of preexisting crack size, but increases with increase of modulus or with the surface energy. Griffith investigated the validity of the above equation by carrying out experiments on glass tubes and hemispheres in which he purposely introduced cracks of various sizes by use of a diamond cutter. He also determined E and γ from separate experiments. He was able to show that, for these materials, his theoretical equation was approximately satisfied and that σ_c did vary as the crack size to the negative one-half power. He also estimated that the radius of curvature need not be much larger than atomic dimensions and under these conditions the estimated local stress at the crack tip does become comparable to the expected theoretical stresses based on the magnitude of interatomic forces.

The Griffith theory was further developed and generalised by Irwin [18] and others, but the general form of the rupture stress and crack length relation remained the same. The principal difficulty in applying the Griffith criterion to polymers, or even to specific glassy and relatively brittle polymers like polystyrene is that a considerable amount of energy can be dissipated in these materials by localised molecular orientation and plastic deformation process that occur in the vicinity of the crack, and in the craze regions preceding the crack tips. The propagation of the crack thus involves not only breaking of the interatomic bonds in the already crazed region but conversion of mechanical energy

to heat energy by additional viscous and plastic deformation accompanying extension of the crazes. The extent of crazing, and of local regions of plastic flow and chain orientation in the neighborhood of crack tips, has been studied by Kambour [19] and others.

1.2.3 Continuous Viscoelastic Models

The model of a common 'failure envelope' proposed by Smith [20] is based on a consideration of the viscoelastic behaviour of continuous high polymer bodies, i.e., on the concept that a reduction according to the time-temperature superposition principle of the environmental parameters stress, strain-rate and temperature should lead to corresponding molecular states. If a fracture criterion refers to unique limits of molecular load-carrying capability, then the plotting of reduced stress at break versus strain at break for different experimental conditions should lead to one master curve, the failure envelope. For a large number of natural and synthetic rubbers and vulcanizates under similar modes of mechanical excitation, this concept was found to hold. It thus generally allows the extrapolation of the ultimate behaviour into unknown regimes of time, strain-rate or temperature. This model, however, does not allow prediction of the shape of the fracture envelope or the conversion of data obtained under different modes of excitation (uniaxial, equal biaxial or other multiaxial loading).

Blatz, Sharda and Tschoegl [21] have proposed a generalized strain energy function as a constitutive equation of multiaxial deformation. They incorporated more of the nonlinear behaviour in the constitutive relation between the strain energy density and the strain. They were then able to describe simultaneously by four material constants the stress-strain curves of natural rubber and styrene-butadiene rubber in simple tension, simple compression or equibiaxial tension, pure shear and simple shear.

The theory of rubber elasticity and the time-temperature superposition principle are adopted in the continuous elastic models. These models implicitly recognize the molecular origin of the viscoelastic behaviour of a material, but explicitly they do not refer to noncontinuous quantities such as the discrete size, structure and arrangement of molecules, anisotropy of molecular properties or the distribution of molecular stresses or stored strain

energy. A representation of a solid as a continuum is quite adequate where individual molecular events or discontinuities of stress or strain are either not discernible or not of particular importance.

1.2.4 Rate Process Theories of Fracture

Contrary to the continuum mechanical theories, 'molecular' rate process theories of fracture recognise the presence of discrete particles or elements forming the material body. Rate process theories formulate a relationship between breakage, displacement and reformation of these elements to deformation, defect development and fracture of the structured material. It is assumed that macroscopic failure is a rate process, that the basic fracture events are controlled by thermally activated breakage of secondary and or primary bonds and that the accumulation of these events leads to crack formation and or to break-down of the loaded sample. Here the basic events are defined in a general manner and not experimentally related to particular morphological changes.

A stress-biased thermodynamically irreversible displacement of molecules past each other results in the flow of a liquid, melt or solid. A molecule in thermal equilibrium with its surroundings is in thermal motion, which in the case of a liquid or solid is predominantly a vibration around a temporary equilibrium position. The amplitude of vibration is constantly changing. Eyring [22] postulated that a displacement (or jump) of a molecule from an initial to a neighbouring equilibrium position may occur if the thermal energy of the molecule is sufficient to reach the activated stage, i.e., the top of the energy barrier separating the initial and the final equilibrium positions. The rate of decay of activated states towards the final position was obtained by him as

$$k_0 = \kappa \frac{k_B T}{h} \exp(-u_0/kT) \exp \Delta s/k_B. \tag{1.3}$$

Here κ is the transmission constant which indicates how many of the activated complexes actually disintegrate, k_B is Boltzmann's, h Planck's, and R the gas constant, T is absolute temperature, u_0 the height of potential barrier, and Δs the difference in entropy between ground state and activated state. In the absence of external forces initial and

final equilibrium states are assumed to have the same potential energy. Then the rates of flow of particles across the dividing potential barrier are the same in the forward and backward directions. Under the influence of external forces, however, local stress fields are generated. A particle thermally activated to move in the direction of , say, stress Ψ by a distance $\lambda/2$ then gains an amount of energy

$$w = \Psi \lambda q / 2 \tag{1.4}$$

where q is the average cross section occcupied by the particle normal to the direction of motion. A particle moving in the $-\Psi$ direction will lose the same amount of energy. The first particle, therefore, needs less thermal energy to reach the activated state than the second particle. Consequently the rates of flow of particles across an energy barrier in opposite directions are biased by the local stress:

$$k_1 = k_0 \exp(w/kT) \tag{1.5}$$

$$k_2 = k_0 \exp(-w/kT). \tag{1.6}$$

The net flow rate, therefore, is

$$K = k_1 - k_2 = 2k_0 \sinh(w/kT). \tag{1.7}$$

In 1943, Tobolsky and Eyring applied the concept of slipping of secondary bonds to the breaking of polymeric threads under uniaxial load [14]. The rate of decrease of the number N of such bonds per unit area under constant uniaxial stress Ψ_0 is obtained as

$$-\frac{1}{N}\frac{dN}{dt} = 2k_0 \sinh(\Psi_0 \lambda / 2NkT) \cdot \tag{1.8}$$

For large values of stress, the flow of bonds takes place almost exclusively as breakage and not as reformation. In that case one may use Eq. (1.5) instead of Eq. (1.7). If one substitutes there $\Psi_0 \lambda / 2NkT$ by y one obtains a solution in terms of the exponential

integral

$$-Ei(-y) = \int_{y_0}^{\infty} dy' \exp(-y')/y' = k_0 t_b. \tag{1.9}$$

The lower limit of integration is $y_0 = \Psi_0 \lambda / 2 N_0 kT = w/kT$. Eq. (1.9) offfers an implicit relation between the expectation value of the time to fracture of the thread t_b, the rate of flow of unstressed secondary bonds, k_0, and the stress Ψ_0 acting on the N_0 initial bonds. With $w \gg kT$ the exponential integral may be approximated by

$$-Ei(-y) = [(\exp -y)/y](1 - 1/y). \tag{1.10}$$

Within the range of validity of this approximation, the logarithm of lifetime $\log t_b$, is almost linearly related to w; i.e., to the applied stress. Exactly this behaviour is exhibited by a large number of stressed metals, ceramics or polymers.

Independently from each other Zhurkov et al. [23] in the USSR and Bueche [24] in the USA expressed the idea that in fracture of polymers – and also of metals – the breakage of primary (chemical) bonds play an important role. As a result of detailed investigations of the life time $\tau(\sigma, T)$, at various stresses σ and temperatures T, it was established [3] that the following relationship exists, applicable to all polymeric solids

$$\tau(\sigma, T) = \tau_0 e^{(U_0 - \gamma\sigma)/RT} \tag{1.11}$$

when σ remains constant. Here T is absolute temperature, R is the gas constant and U_0, γ and τ_0 are constants. The constant τ_0 proves to be practically the same for all solid bodies and equal to $10^{-12} - 10^{-13}$sec. The constant U_0 for polymers is close to the activation energy of thermal degradation E, of the macromolecules. The constant γ is very sensitive to the structure of the polymeric body and varies considerably during crystallisation, plasticisation and other changes in the physical structure of the polymeric body.

Analysis of data on the life time of polymeric bodies leads to the conclusion that failure of a body is a complex aggregate of processes among which the leading one, in the long run, is that of thermal degradation of macromolecules, accelerated by the action

of the mechanical stress. The constant γ in the equation reflects the efffect of the stress on the rate of thermal degradation of the polymer. The higher the stress and higher the temperature, the lower the life time of the polymer. Raising the value of γ enhances the effect of the stress on the rate of thermal degradation. Thus, mechanical breakdown of a polymeric body is a mechanochemical process

It can be easily seen from the Eq. (1.11) that at sufficiently low temperatures the dependence of the life time on the stress (at T = constant) becomes very prominent. Therefore, a minor rise in stress under these conditions may change the life time by many orders from very high values to negligibly small ones. This leaves the impression that there exists a stress separating infinitely long-lived stressed bodies from those that fail instantaneously. Therefore, at sufficiently low temperatures a critical stress value may be used for practical purposes.

The Arrhennius expressions of Bueche and Zhurkov do not contain dependence on N. The Zhurkov equation asserts that τ, the mean lifetime of a solid, is the same as what one might expect to be the mean lifetime of a single bond. In fact, a number of bonds are expected to break prior to τ. The consequence is that the remaining bonds are subjected to even greater stress, and the breaking process accelerates rapidly. The mean breaking time of a bond under the initial stress per bond is therefore taken to be a good estimate of the lifetime of the solid. There is no dependence on sample size, and since Zhurkov proposes the theory as working for any solid, there cannot be dependence on the degree of polymerisation. However, in a fiber of highly aligned polymer chains, the stress-bearing units are long segments of the chains, each of which can break at any one of its bonds. Thus one expects some dependence on N.

Following the earlier works of Eyring, Zhurkov and Bueche, these and other authors have continued to develop different aspects of the kinetic theory of fracture. Particularly in the USSR, fracture data have been interpreted in terms of the failure of regular non-morphological model lattices [25, 26]. Gubanov et al. [25] and Bartenev [26] focussed on the potential energy of interaction between adjacent members of a polymer chain and Dobrodumov [27] on the increase of the load and – consequently – of the rate of scisssion

of bonds adjacent to a broken bond.

Hsiao and Kausch [28, 29] studied the effect of orientation-dependent local strain on the total rate of chain scission and Salganik [30] analysed the amount of thermal energy and the direction of relative motion imparted by statistically fluctuating phonons to adjacent segments. Different statistical aspects of the accumulation of molecular defects were treated by Goikhman [31] and Gotlib [32] who simulated the isolated production, growth, interaction and coalescence of defects. An energy probability theory was forwarded by Valanis [33] who combined the role of strain energy density, the stochastic nature of fracture and the fracture hypothesis of Zhurkov. The model suggested by Termonia and Smith [34] explicitly takes into account the role of the weak attractive forces between chains as well as chain slippage through entanglements. Stress-strain curves calculated for polyethylene agree quantitatively with experiment.

Wheras all of the above theories refer in one way or another to the thermally activated breakage of one kind of molecular bonds as primary fracture event, the Bueche-Halpin theory for the tensile strength of gum elastomers [35] employs the idea that the viscoelastic straining of rubber filaments together with the degree of their ultimate elongation determine the kinetics of crack propagation in an elastomeric solid.

To the molecular processes specified above one has to add the unspecified ones, internal destruction, damage or crack formation probability. In analogy to the molecular description of deformation used by Blasenbrey and Pechhold [36] all of these molecular processes can be referred to the four physical rearrangements that can occur between neighbouring chain segments with parallel chain axes: change of conformation (segment rotation, gauche-trans transformation), cavitation, slip and chain scission. Of these chain scission and − to some extent − cavitation and slip are potentially detrimental to the load-bearing capacity of a polymer network. Conformational changes on the other hand, appear to be 'conservative' processes, which by themselves will modify and delay but never generate any progress in the development of a fracture process.

1.3   Simulation Studies of Fracture

Since the task of estimating the lifetime of a solid under stress is difficult to perform analytically, attempts have been made to investigate this property using molecular dynamics simulations. Wang et al. [37] performed molecular dynamics simulations on a two-dimensional set of atoms interacting through Lennard-Jones forces and found a strong dependence of the time until a break occurs on the applied stress. As expected, there is a range of stress for which the material can be seen to relax to a metastable equilibrium and then suddenly fail. For larger stresses, the material fails immediately, and at smaller stresses, the finite duration of the simulation prevented failure from appearing. This simulation confirms the metastability of the unbroken state. Finally, the critical load is found to decrease significantly with temperature. This latter result, especially in the context of explicit microscopic simulation of the failure of single crystals, provides many additional insights into the role of thermal fluctuations in metastable solids. They also found that failure is sometimes preceded by a crystal-crystal phase transition that corresponds to a physically allowed lattice invariant (PALI) strain. At sufficiently high temperatures they observed direct failure of the system via stress-induced melting [38].

Welland et al. [39] and Manevitch et al. [40] each studied the breaking behaviour of single polymer chains. Manevitch was concerned with the role solitons might play in causing a polymer chain to break. He investigated these solitons using a molecular dynamics simulation of a chain of atoms connected by Morse potentials. The position and time dependent statistical probability for fracture of a one-dimensional string of Lennard-Jones atoms has been evaluated by Welland et al. [39] as a function of the temperature, tension and length. A surprising exponential dependence of the fracture-site probability with distance from a string end is observed.

In a recent review, [41] Baljon et al. discussed the molecular mechanisms of rupture in the light of recent computational simulation studies. When the bonds in a crystalline solid or a polymer are pulled apart at constant velocity, they rupture through a series of sudden yield events during which the material reorganises. Yield events are separated by perioids of elastic deformation where the stress builds until the system becomes unstable.

The nature of the structural change at yield events varies from system to system; small cavities form in the polymer film, an additional atomic layer is formed in the crystal and hydrogen binding sites rearrrange in the biological system.

Knudsen et al. [42] applied the technique of Brownian dynamics simulation for the study of the fracture process of flexible polymer chains when they encounter an extensional flow field of transient character. The simulation results showed that the fracture yield depended strongly on flow rate and on molecular weight. The distribution of the resulting fragments is interpreted in terms of the conformation of the chain prior to fracture.

Sheng Yu-Jane et al. [43] studied the static and non equilibrium dynamic properties of a single linear chain under an attraction force f , by Monte Carlo simulations using a continuous model and by scaling calculations. Chain lengths from $N = 10$ to $N = 100$ are considered. For these static results, the simulation data show that the average end-to end distance $\langle R_f \rangle \sim N^{2\nu} f$ at weak tension forces and for strong forces $\langle R_f \rangle \sim N^{1/\nu - 1} f$ which are consistent with previous studies. The nonequal relaxation behaviour is studied for an initially stretched polymer chain, when the stretching force is removed. Detailed chain configuration during the relaxation process are analysed from the simulation data. Different relaxation dynamics are found for three regions, the linear, pincus and model dependent regimes. The non-equilibrium relaxation time τ is derived in the linear ($\tau \sim N^{1+2\nu}$), pincus ($\tau \sim N^2 f^{1/\nu - 2}$) and model-dependent regimes. These results are compared and are discussed in the light of scaling theories.

Fracture of perfectly oriented polymer fibers was studied [44] by computer simulation technique based on the ultimate structure model to establish the upper limit of the tenacity of polymers with finite molecular weight. The fracture mechanism was also investigated in terms of average molecular weight and different nature of interchain interaction. The tenacity of the model fibers increased with molecular weight and tended to approach the theoretical limit for infinite molecular weight. In the lower molecular weight cases, significant broadening of the stress distribution was observed under elevated stress, and the fracture behaviour was plastic. In the higher molecular cases, the stress distribution was quite narrow until a significant number of bond-cleavage occurrred, and the failure

was brittle. The primary factor of fracture was chain slippage in the lower molecular weight cases, and chain scission in the higher molecular weight cases. Higher tenacity was marked when polar ineractions were introduced, especially in lower molecular weight cases. This can be attributed to the enhancement of chain binding by the polar interaction and suppression of chain-slippage.

A new model [45] for simulating dynamic fracture in impact loaded solids was based on the traditional molecular dynamics procedure, but accounted for the irreversible nature of the fracture process by deleting the attractive part of the particle interaction potential when the bond between two particles was stretched beyond a critical length. This critical length was determined by comparison with Griffith theory. The model was applied to a two-dimensional homogenous solid in the absence of a microstructure. When the impact zone is much smaller than the size of the sample, or the impact zone is wide and the impact amplitude is large, the first crack forms a finite distance ahead of the impact zone. Static continuum elasticity theory showed that the position of this first crack occured at the position of maximum tensile stress. This crack then propagates back to the edges of the impact zone and forward into the sample, thereby creating an x-shaped crack pattern. The tips of the x-shaped crack propagate more slowly than the stress wave; hence, strong deviations from this pattern are observed when the stress wave passes the crack tips. When the predominantly compressive stress wave reflects off the back free surface, a tensile wave propagates back into the sample creating even more damage. This damage occurs in bands parallel to and set back from the back surface.

Oliveira and Taylor [46] performed extensive simulations in order to determine the conditions under which an anharmonic chain will break. The dynamics of a rectilinear chain of 100 monomers interacting via a Lennard-Jones potential were followed by solving a set of simultaneous Langevin equations. There are two principal results from this study; (1) In order for irreversible breaking to occur in a stretched chain, a bond must be extended to a length considerably greater than the length at which the restoring force is maximised. (2) The breaking rate of a bond may be expressed in terms of the product of an attempt frequency and an Arrhenius factor. While the Arrhenius factor may be

satisfactorily described in terms of the height of an effective energy barrier, the attempt frequency is found to be several orders of magnitude smaller than the dominant phonon frequencies. Later, Oliveira [47] presented a microscopic theory for fracture nucleation in finite chains, which may account for results found in simulations. He showed that the expression obtained for the characteristic breaking time scaled well and that the activation energy agreed with the analytical results. The delay in the fragmentation is a consequence of the long-range time correlation in the relative motion of two adjacent particles. This correlation is responsible for the origin of a self-organised memory as well as the large elongation necessary for irreversible break to occur.

A one-dimensional monoatomic chain under tensile stress has been studied by molecular dynamics by Bolton et al. [48]. Chains of 2–20 atoms have been simulated. A simple transition state theory, equivalent to a nucleation theory for one-dimensional fluids, gives the main features of the decay rate coefficient as a function of the applied stress. For finite chain lengths, an anharmonic RRKM theory provides a more accurate rate coefficient, but chain healing (reversible decay) in the simulated motion causes a significant deviation, particularly at high chain energy. The simulaton is extended to chain arrays which show greatly increased nonstatistical effects. Starting with atoms randomly distributed on a triangular lattice Chakrabarti et al. [49] had found that the stress needed for fracture seems to vanish and the time to complete fracture seems to diverge at the percolation threshold, whereas the elastic modulus vanishes at a different concentration.

Nyden and Noid [50] investigated the kinetic stability of model polymers as a function of temperature, secondary structure and molecular weight. The rate constants for random scission of the carbon-carbon bonds were obtained from simulations starting from both planar zigzag and coiled conformations. The coiled polymers were found to be more stable than planar zigzag polymers with the same primary structure. The computer-generated rates correlated reasonably well with the functional predictions of the Rice, Ramsperger and Kassel theory of unimolecular reactivity; however, deviations were observed for some of the short-chained polymers. Computer movies revealed pronounced coiling in the vicinity of dissociating bonds. This behavior was examined in the light of proposed

mechanisms for intramolecular hydrogen transfer.

The dynamics of Rouse chains and Morse chains was simulated both without and with hydrodynamic interaction between chain elements by Cascales and Torre [51]. From the simulated trajectories, steady-state properties such as chain dimensions and elongated viscosities were calculated. When hydrodynamic interaction is acccounted for by using the Rotne-Prager-Yamakawa tensor, the calculated dimensions and viscosities are appreciably lower than when it is neglected. Carrying out simulations with varying elongational rate, it is possible to observe stretching and finally the fracture of polymer chains. The critical elongational rate, corresponding to infinite elongation in the case of Rouse chains, and the fracture of the Morse chain is characterised as a function of chain length. When the short length of the simulated chain is accounted for adequately, the elongated rate needed for fracture ϵ_f scales with molecular weight M as $\epsilon_f \propto M^{-2}$. This result, predicted rigorously without hydrodynamic interactions, holds in practice as well as when hydrodynamic interaction is considered.

The macroscopic fracture response of real materials originates from the competition and interplay of several atomic scale mechanisms of decohesion and shear, such as interplanar cleavage and dislocation nucleation and motion. These phenomena involve processes over a wide range of length scales, from the atomic to the macroscopic. Cleri Fabrizio et al. review [52] the attempts to span these length scales in dislocation and fracture modeling by (1) fully atomistic large-scale simulations of millions of atoms or more, approaching the continuum limit from the 'bottom-up' (2) directly coupling atomic scale simulations and continuum mechanics, in a 'top-down' approach and (3) by defining a set of variables common to atomistic simulations and continuum mechanics models in the form of constitutive relations. A case study of the constitutive-relation approach is presented for the problem of dislocation nucleation from a crack tip in a crystal under stress; a comparison of the results of atomic simulations to the Pierls-Nabarro continuum model is made.

1.4   Models Used to Study Polymer Fracture

1.4.1   Spin Model

Blumberg-Selinger et al. [53] used a one-dimensional model to explore the idea that the unbroken state of a solid under stress is actually metastable. The model consists of N bonds in parallel subjected to a stress or strain. The condition of each bond was mapped into a spin state, an unbroken bond corresponding to an up spin and a broken bond corresponding to a down spin. The free energy of this model has a global minimum when all the bonds are broken and for small enough stress, it has a local minimum, which corresponds to a metastable state with some surviving bonds. For larger stresses the local mimimum disappears. One might call the stress at which this local minimum disappears, 'the breaking stress' of the sample. However, just before the stress is large enough to make this minimum disappear entirely, the lifetime of the metastable state may be quite small, since the height of the barrier between the global and local minima will be small compared to k_BT. Therefore, the concept of breaking stress becomes somewhat ill-defined. The extension of this model to higher dimensions required numerical calculations [54] which produced similar metastable behaviour.

1.4.2   Network Models

Numerical studies that modeled solids with a network of bonds (or fuses or springs) have also been performed [55]. The material is represented by a network of mechanical elements (bonds, springs, beams) that have their own mechanical properties. These properties depend on the purpose for which the model is intended. In models that are used to represent in detail the behaviour of specific materials, each element in the network may have quite complex, time-dependent properties. In most of the models, the network elements can exist in two mechanical states and the kinetics of failure and deformation are controlled by the strain-dependent transition rate between these two states. In most cases one of the two states corresponds to complete failure (removal) of the network elements. This processs may be reversible, but in most models material failure is considered an

irreversible process.

In a typical Monte Carlo simulation, an element of the networks selected at random with a probability $P(\Omega)$ that depends on the local configuration Ω. After an element has been selected, it is removed from the network (or its properties are changed) and the network is allowed to partially or completely relax to a new mechanical equilibrium (subject to appropriate mechanical boundary conditions). The new network element bond-breaking probabilities (rates) are then calculated and the process of transition between mechanical states and relaxation is repeated many times to simulate the material failure or deformation process.

The rate of failure of many materials increases very rapidly with increasing stress or strain. It seems natural to suppose that this macroscopic behaviour has a microscopic origin and that the failure of individual network elements also depends strongly on the local stress or strain. Consequently, models in which the failure or modification rate constant R_f is related to the local force f associated with these elements by relations such as

$$R_f \sim f^\eta \tag{1.12}$$

or

$$R_f \sim \exp(af^n) \tag{1.13}$$

have been explored. However, the assumption that the rate of failure or modification depends only on the local stress cannot be justified quantitatively and may have to be modified if an acccurate simulation of the properties of real materials is required. The form given by Eq. (1.13) is supported by the absolute reaction rate theory for chemical reactions. According to this theory, the rate constant of a chemical process can be written as

$$R = b(T)\exp(-E_a/k_B T) \tag{1.14}$$

where E_a is the activation energy, k_B is the Boltzmann constant,T is the temperature,

and $b(T)$ is a weakly temperature-dependent preexponential factor. For stress-induced failure, Eq. (1.14) can be written as

$$R = b(T, f) \exp(-E_a(f)/k_B T) \qquad (1.15)$$

In most cases $E_a \gg k_B T$ and the preexponential factor $b(T, f)$ can be approximated by a constant. The main effect of exerting an external force on the system is to reduce E_a by an amount that depends on f (or the local bond length displacement δ). For a simple harmonic potential the elastic energy stored in a distorted bond is given by

$$E_s = k\delta^2/2 = f^2/2k \qquad (1.16)$$

where k is the bond force constant.

It is assumed that E_a for bond breaking is reduced by an amount proportional to E_s, then a value of 2 is obtained for the exponent n in Eq. (1.13). It might also be argued that the bond has broken when δ has reached a critical value δ_0 and that the energy required to reach this displacement will be reduced by an amount proportional to f. These simple ideas are not realistic, and at this stage Eq. (1.13) must be regarded as an empirical relation. For polymers a considerable amount of experimental data support the idea that E_a is reduced by an amount that is proportional to the stress (σ) [56, 1]. Under these circumstances the bond-breaking rate constant can be expressed by the form

$$R = \nu_0 e^{-(E_a - \beta\sigma)/k_b T} \qquad (1.17)$$

where ν_0 is a thermal vibration frequency. For three-dimensional systems, the parameter β in Eq. (1.17) can be interpreted as an activation volume. For the breaking of a bond in a network, β can be interpreted as an activation length (β') and σ can be replaced by f.

It might be inferred from the above discussion that the elements in the network should be interpreted on a molecular level. However in most cases a more macroscopic interpretation in which the elements of the netwok represent physical structures such as grains, dislocations or other extended structures seems to be more appropriate. In other cases,

the elements in the network may represent the material in a characteristic volume of size (length) determined by the fracture process itself (the size of the plastic zone, for example [57, 58]).

The Hookian-spring model has the disadvantage that it has a zero Poisson ratio for a square lattice which is physically unreasonable. This has been overcome in a number of different ways. The first is to add a term to the Hamiltonian which penalizes bond bending [59]. The second is to replace the spring lattice with two-dimensional elements (based on Hookean springs) which results in two independent Lame constants [60]. A third approach is to employ Born springs which penalize rotation of the springs away from lattice directions [61, 62]. Hassold and Srolovitz [63] employed a Born-spring model to study the effects of a random distribution of defects on the fracture of an elastic model loaded in pure tension. The springs fail completely and irreversibly once a critical strain energy is exceeded. The Born potential provides an effective bending force that yields realistic crack microstructures, which are analyzed in detail. As the defect density increases, the crack becomes increasingly ramified, even though fewer spring failures are required for complete breakdown. The failure stress and Young's modulus approach zero as the system approaches the percolation threshold.

Random fluctuations appear to be an ingredient in material deformation and failure processes. However, in the Monte Carlo models outlined above, randomness enters the models in a relatively uncontrolled fashion. The degree of randomness can be controlled by methods such as noise reduction in which a network element must be selected m times before it finally fails or is modified [64, 65]. Disorder can also be introduced in a quite different way. The elements in the network can be considered to be 'damaged' at rates given by Eqs. (1.12), (1.13) or (1.15) and to fail when the damage associated with the ith element reaches a threshold value (T_i). Apart from the random distribution of threshold values that are assigned at the start of a simulation, models of this type with 'quenched' disorder are completely deterministic. When the damage associated with one of the elements in the system reaches its T_i, it is removed or modified. The system is then relaxed to a new mechanical equilibrium and new damage rates are calculated.

The damage associated with each of the bonds is then increased at the new damage rates until the next bond reaches its damage threshold. The simulation proceeds by a sequence of damage growth, network modification and relaxation steps until the 'material' fails completely or a preselected number of network elements have been modified. In these models the disorder can be controlled via the distribution of threshold values. In many cases the introduction of disorder via random bond selection or quenched disorder (random damage thresholds) leads to very similar damage patterns and kinetic behaviour. This behaviour is similar to that found for the closely related (DLA) model [66] described below. In this case, simulations carried out with the use of deterministic models with quenched disorder [67] lead to patterns that are similar to those obtained with the standard DLA model.

1.4.3 The Diffusion-Limited Aggregation (DLA) Model and Related Models

This corresponds to the random selection of growth sites with probabilities given by a scalar field ϕ that obeys the Laplace equation

$$\nabla^2 \phi = 0 \qquad (1.18)$$

with adsorbing boundary conditions ($\phi = 0$) on the surface of the growing pattern and a fixed value for ϕ ($\phi = 1$) at infinity. This model has been found to describe quite well both kinetics [68] and the structure [69] of fluid-fluid displacement in a porous medium (an esentially deterministic process that takes place in a random medium with 'quenched' disorder). Quenched disorder can also be introduced via a random distribution of strain, stress or elastic energy thresholds. In models of this type, the network element that most exceeds its threshold may be modified [70] or more complex criteria that include 'memory' effects may be used [71].

In the DLA process [66], particles are added one at a time to a growing cluster or aggregate via random walk trajectories originating from outside the region occupied by

the cluster. Structures covering a wide range of length scales can be generated with improved DLA algorithms [72, 73, 74]. The DLA model is closely related to simple models for the growth of cracking patterns. Processes such as dielectric breakdown and fluid-fluid displacement are closely related to other material 'failure' processes such as cracking.

The close relation between DLA and material failure is also exhibited quite explicitly by the dielectric breakdown version of this model [75]. In this model the Laplace Eq. (1.18) is discretized to give

$$\phi_{ij} = 1/4(\phi_{i-1,j} + \phi_{i+1,j} + \phi_{i,j-1} + \phi_{i,j+1}) \tag{1.19}$$

and is solved numerically (with appropriate boundary conditions) on a lattice to obtain the growth probabilities (in Eq. (1.19). The discretized Laplace equation is given for a square lattice where ϕ_{ij} is the value of the scalar harmonic field associated with the lattice site with cordinates (i,j)). Unoccupied perimeter sites are selected randomly with probabilities that are given by

$$P(i,j) \sim \phi(i,j)^{\eta} \tag{1.20}$$

or

$$P(i,j) \sim n\phi(i,j)^{\eta} \tag{1.21}$$

and filled to represent the growth process. In Eq. (1.21), n is the number of filled sites adjacent to the unoccupied perimeter site. The simple homogerous (power law) relation betwen the growth probabilities (P) and the scalar field (ϕ) in Eqs. (1.20) and (1.21) is motivated primarily by theoretical considerations. A simple homogerous relation between P and ϕ is expected to generate patterns with relatively simple fractal scaling properties, whereas more inhomogerfous complex relations between P and ϕ will lead to structures with more complex geometric scaling behaviour. For the case $\eta = 1$, this model generates random patterns that are very similar to those associated with the DLA model.

1.4.4 Surface Cracking Models

A model for surface cracking [76] can be constructed from a triangular network of Hookean bonds with central force interactions. For this system the elastic energy is given by

$$E = 1/2 \sum_{ij} k_{ij}(l_{ij} - l_0)^2 \tag{1.22}$$

where l_{ij} is the distance between the ith and jth nodes and $k_{ij} = k$ if the nodes are connected and $k_{ij} = 0$ if the bond between the ith and jth nodes is broken. In addition, each node in the network is attached to the (rigid) substrate by a weak bond. The force exerted by this weak bond on the ith node is given by

$$\mathbf{f} = k_2(\mathbf{r}_i^0 - \mathbf{r}_i) \tag{1.23}$$

where $\mathbf{r}_i$ is the position in the ith node and $\mathbf{r}_i^0$ is the position of attachment to the substrate (its position at the start of the simulation). In this model only the high modulus bonds in the surface layer are allowed to break (all the nodes remain attached substrate). The bond-breaking probabilities are given by

$$P_i \sim R_i = \exp(k\delta_i^2/2). \tag{1.24}$$

(Eq. (1.13) with a value of 2 for the exponent n). The simulation proceeds via a sequence of bond-breaking and relaxation steps.

1.5 Mechanical Strength and Molecular Mass

The effect of molecular weight on fiber strength has been widely investigated by Bartenev and Zuyev [77]. In low molecular weight material, chain slip occurs readily so that the sample strength depends solely on the strength of intermolecular attraction. Noticeable macroscopic strength is only obtained if the molecular weight is sufficient to permit physical cross-links through entanglements or chain folds between several chains. In the

range of molecular weights between 1.5 and 3×10^4 g/mol, fiber strength increases with molecular weight, whereas at still higher molecular weights, the effect of the increasing number of defects introduced in processing such a fiber, tends to outweigh the effect of the decreasing number of chain ends. Also it is found that high strength with a high degree of orientation (e.g., obtained at higher drawing temperatures) requires high molecular weights [78, 63].

A stochastic model was presented by Mikos and Peppas [79] to predict the molecular mass dependence of the polymer fracture energy and strength for polymers with molecular masses higher than the critical value corresponding to the onset of entanglements. A chain scission criterion is invoked for the polymer chain segments crossing the fracture plane and being entangled about it. The presence of dangling ends was responsible for the change of the fracture properties with molecular mass. The predictions of the model agreed with experimental data of the fracture energy and strength of PMMA and polystyrene.

Experimentally, Sambasivam et al. [80] could find the different possible mechanism responsible for the failure of polystyrene films. It was found that for polystyrene films, at very low molecular weights, substantially 100% pull out occcurs. At the middle molecular weight range, chain scission and chain pull out contribution to the total energy are approximately equal. For very high molecular weights, the chain scission contribution is about 90 %. A scaling relationship is proposed between the molecular weight of the polymer and the fraction of chains undergoing scission.

Huai and Kamer [81] investigated criteria for craze failure at a crack tip and the dependence of craze failure on the molecular weight of the polymers. Their micromechanics model is based on the presence of cross-tie fibrils in the craze microstructure. These cross-tie fibrils give the craze some small lateral load bearing capacity so that they can transfer stress between the main fibrils. This load transfer mechanism allows the normal stress in the fibrils directly ahead of the crack tip in the centre of the craze to reach the breaking stress of the polymer chains. They have solved for stress field near the crack tip and used it to relate craze failure to the external loading and microstructural quantities such as the craze widening (drawing) stress, the fibril spacing, the molecular weight and

the force to break a single polymer chain. The relationship between energy flow to the crack tip due to external loading and the work of local fracture by fibril breakdown is also obtained. The analysis shows that the normal stress acting on the fibrils at the crack tip increases linearly as the square root of the craze thickness, assuming that the normal stress distribution is uniform and is equal to the drawing stress acting on the craze-bulk interface. The critical crack opening displacement and hence the fracture toughness is shown to be proportional to $1 - (M_e/qM_n)^2$ where M_e is the entanglement molecular weight, M_n is the number average molecular weight of the polymer before crazing and q is the fraction of engaged strands that do not undergo chain scission in forming the craze.

1.6   Some Other Important Results from the Studies on Polymer Fracture

Using a rigorous ab initio method Crist et al. [82] have evaluated the energy of covalent bond deformation of a $-CH_2-CH_2-$ ethylene repeat unit at strains upto 0.6. The computational scheme involves subtracting energies of axially strained normal parafffins differing in length by one ethylene unit. At small strains it is found that the deformation is contributed to equally by C–C bond stretch and by C–C–C bond angle opening. At higher strains the majority of the deformation is accomplished by C–C stretch.

Crist Jr. et al. [83] modeled the chain as a series of truncated harmonic oscillators, each of which has a critical extension x_c^h to break and argued that the chain of N such oscillators will require an overall displacement of exactly Nx_c^h, since the equally stretched situation will always be of lowest potential for any given chain extension. In an actual polymer backbone, the bond anharmonicity will cause this behaviour to alter; above a certain critical extension, the potential can be minimised by extending some bonds and shortening others and it is this critical extension which corresponds to the energy criterion for fracture.The authors have presented a simple model based upon a coupled chain of N Morse oscillators, to characterise the fracture of a single polymer chain. There exists a critical overall extension ΔL_c below which the fracture is energetically unfavorable

but above which fracture is favoured both energetically and kinetically. This elongation ΔL_c scales as $N^{1/2}$. For the critically stretched chain, the activation energy for rupture increases with N. Long chains must be stretched beyond this critical value to fail within experimentally meaningful times. Chains of all lengths subjected to the same force will fail with the same activation energy, provided this force is large enough to stretch each chain to $\Delta L > \Delta L_c$. Observed activation energies are less than $\frac{1}{3}D_c$, where D_c is the bond energy. It is proved mathematically by Liu Yongning [84] that if the strain is larger than a critical strain, the atomic thermal movement can contribute to fracture; otherwise it has no influence on fracture.

Pla Oscar [85] proposed a discrete model of linear springs for studying fracture in thin and elastically isotropic brittle films. The method enables us to draw a map of the stresses in the material. Cracks generated by the model, imposing a moving thermal gradient in the material, can branch or wiggle depending on the driving parameter. It was also found that [86] whenever the interfiber spacing was too small, breaks in one fiber caused breaks in the adjacent fiber.

Starting from a model of microcrack propagation in craze on a mesoscale, the kinetic process of microcrack propagation resulting from fibril breakdown in the crack tip zone is mathematically formulated by a combination of fracture mechanics and fracture kinetics [87]. A microcrack evolution equation involving both the geometric structure parameters of craze and the meso-mechanical quantities is obtained. After solving this evolution equation, a statistical distribution function of microcrack size which evolves with time and the moment generating function of microcrack size are derived. Any-order averaged damage function can be therefore deduced. Specifically, the analytic expressions of the first order averaged damage function and its damage rate are presented which correspond to a similar definition of damage mechanics.

A new method [88] for predicting the time to brittle fracture of polyethylene includes a model which is based on the concept of the crack layer, i.e. a system consisting of the strongly interacting crack and process zone and the kinetic equations which govern the crack-layer growth. The processs zone in polyethylenes usually appears to be a thin strip

of drawn material extending along the crack line. This permits a characterisation of the crack layer by two parameters: the crack and process-zone lengths. The two parameter crack-layer kinetic model allows description of slow crack growth as the discontinuous process which is commonly observed in the brittle fracture of polyethylenes. The model also predicts a relationship between time to failure and applied stress, identical to that established experimentally. The material parameters of the kinetic model can be determined by experiments on smooth specimen, i.e. are independent of slow crack growth and require relatively short-term observations. Thus the combination of the material testing and the mathematical modeling of the crack layer evolution are proposed as a method for lifetime prediction in the brittle fracture of polyethylene.

A model study of brittle fracture of polymers [89] shows that the relation $v = v(F)$ between the crack-tip velocity v and the driving force F exhibit discontinuous transition and hysterisis. For short polymers, at the onset of crack propagation the polymer chains separate by pulling out the molecular chains. Rapid crack motion occurs at higher driving force, where the polymer chains break. This is in contrast with brittle materials and the difference is attributed to inertia, which is less important during pull out of molecular chains, than the models where the crack motion involves breaking strong short-ranged bonds.

Levitov and Shytovand [90] argue that breaking of an atomic chain under stress is a collective many-particle tunneling phenomenon. They have studied classical dynamics in imaginary time by using a conformal mapping technique and derived an analytic formula for the probability of breaking. The result covers a broad temperature interval and interpolates between two regimes: tunneling and thermal activation. Also, they have considered the breaking induced by an ultrasonic wave propagating in the chain, and proposed to observe it in a scanning tunneling microscopy experiment.

Sambasivam et al. [91] have studied extensively the fracture behaviour of polystyrene films and latex. They found that the most probable deformations in polystyrene films included the scissor-like opening of the 109^0 C–C–C angle and the extension of the original 1.54A distance between carbon atoms. They have also determined experimentally the

molecular friction coefficients and the energy for chain pull-out for a polystyrene latex and compared with the theoretical values. They found that [92] in fracture behaviour, the main effects are chain scission and chain pull-out. With increasing molecular weight and annealing times, chain scission becomes more important. Mechanical properties such as fracture energy, generally increase with annealing.

Sjoerdsma and Boyens [93] developed a theory to describe the fracture probability of high impact polystyrene. By assuming that fracture initiation is a consequence of the impingement of crazes due to the craze thickening process, an equation for the fracture probability as a function of the strain is derived. Experiments support the validity of this equation qualitatively while the stress and temperature dependence of the fracture probability correlate in the expected manner with the strain rate. An approximation shows the calculation of the fracture probability as a function of time.

Doerr and Taylor [94] analysed the concept of the breaking strength of a polymer chain by means of a study of the dynamics of a rectilinear chain of monomers connected by Hookian bonds. A formalism is then developed whereby the average time to breaking of the chain can be calculated as a function of temperature and strain. Correlations in space and time in the motion of the chain lead to breaking times that are not simple functions of the chain length. The predicted breaking times are appreciably smaller than those that would be found in a chain in which the thermal motions of the monomers were uncorrelated.

It is found that [95] at low temperature and or high strain rates the polyethylene fibre shows brittle failure, displaying a pronounced strain rate and temperature dependence of the tensile strength. At high temperatures and or low strain rates a transition from a brittle to a ductile failure mode could be observed. This brittle-to-ductile transition is analysed in terms of competitive failure modes, which leads to a simple model that can be used to predict the strain-rate dependence of the transition temperature. In the brittle failure mode it is observed that an increase in strain rate and or decrease in temperature leads to a reduction in work of fracture.

Chapter 2

Transition State Theory

2.1 Introduction

The problem of escape from metastable states is ubiquitous in almost all scientific areas. Reaction-rate theory has received major contributions from fields as diverse as chemical kinetics, the theory of diffusion in solids, homogenous nucleation and electrical transport theory, to name a few. The theory originated with Arrhenius [96], who, inspired by van't Hoff, demonstrated that the temperature dependence of the rate of change of optical isomers is characterized by an activation energy $E^{\ddagger}$. Forty years of intensive research on activated reactions culminated with Eyring's famous paper on the absolute rate theory [97] and the deceptively simple expression

$$\Gamma = \Gamma_0 e^{-E_a/k_B T} \tag{2.1}$$

where Γ_0 is known as the prefactor, whose dimensions are time^{-1} and k_B is Boltzmann's constant. Perhaps Eyring's main contribution to chemistry and physics was his demonstration that the transition state theory (TST) formula (2.1) is applicable to a wide variety of chemical and physical processes, particularly for larger systems.

In this chapter we review the different approaches for calculating the rate of reactions. Since we use the classical as well as the quantum transition state theory in our polymer breaking problem, we discuss these theories somewhat in detail. A brief account of the

other theories are also given.

2.2 Classical Transition State Theory

The relationship between transition state theory and dynamical theories was first discussed by Wigner [98] who emphasised that the theory was a model essentially based on classical mechanics. The following assumptions are made in deriving the TST rate expression.

1. There exists a transition state which can be identified as a dividing surface separating reactants from products, or more generally, any two physical states that are separated by a bottleneck in phase space.

2. Thermodynamic equilibrium must prevail throughout the entire system for all degrees of freedom. All effects that result from a deviation from the thermal equilibrium distribution, such as the Boltzmann distribution are neglected.

3. The rate of an elementary process is identified with the crossing of the representative point across the critical surface in the direction of the reaction products.

4. The electronic and nuclear motions can be separated (equivalent to the Born-Oppenheimer approximation in quantum mechanics).

5. Any orbit crossing the dividing surface will not recross it.

The TST rate is proportional to the total flux of classical trajectories from reactant to product side of the dividing surface. This flux is calculated either with the Boltzmann weighting function at a given temperature T (canonical TST) or with a delta-function weighting accounting only for the trajectories of a given total energy E (microcanonical TST). Canonical TST was originally put forward by Polanyi and Wigner [99] and developed further by Petzer and Wigner [100], Eyring [97], Wynne-Jones and Eyring [101], and Evans and Polanyi [102]. Microcanonical TST was devoloped mainly by Rice and Ramsperger [103], Kassel [104] and Marcus [105]. When applied to unimolecular reactions, it is known as the RRKM theory [106].

2.2.1   Canonical Transition State Theory

Now we give the details of the canonical transition state theory (see Nikitin [107]). Consider a system of n interacting atoms. The Hamiltonian is given by

$$H = \frac{1}{2} \sum_{ij}^{3n} a_{ij} \, \dot{q}_i \dot{q}_j \; + U(q_1, q_2, \ldots, q_{3n}) \qquad (2.2)$$

where q_i are the generalised coordinates characterising the position of the atoms. We can also express Eq. (2.2) in terms of the generalised momenta as

$$H = \frac{1}{2} \sum_{ij}^{s} g_{ij} p_i p_j \; + U(q_1, q_2, \ldots, q_{3n}). \qquad (2.3)$$

where s is the number of degrees of freedom and the kinematic coefficients a_{ij} are connected with the g_{ik} by the relation $\sum_j a_{ij} g_{ik} = \delta_{ik}$. An element of phase volume $d\Gamma$ has the form $d\Gamma = \prod_i^s dp_i dq_i$, and the number of states in the volume element $d\Gamma$ is $d\Gamma / h^s$. The reaction coordinate q_r is chosen in such a way that it is normal to the dividing surface and on it takes a given value q_r^*. Since the number of particles in phase space is proportional to the partition function, the normalised distribution function on the critical surface must have the form:

$$f^* = \frac{\exp\left[-\beta H^*(p_i, q_i)\right]}{Q}. \qquad (2.4)$$

where $H^* = H\left(p_i, q_i\right)\big|_{q_r = q_r^*}$, and $\beta = 1/k_B T$. The partition function Q is defined as

$$Q = \frac{1}{h^s}\!\int \exp\left[-\beta H(p_i, q_i) d\Gamma\right]. \qquad (2.5)$$

The current of particles along q_r will be proportional to the mean rate of change of phase volume $\left\langle \frac{d\Gamma}{dt} \right\rangle$, at points of intersection of the critical surface by the reaction coordinate, i.e. at $q_r = q_r^*$. Now the averaging can be done by integrating the distribution function $f(p_i, q_i)$, over all momenta and coordinates. The limits of integration for p_r are determined by the condition that the current is taken into account only in one direction. i.e. $\dot{q}_r = \sum_i g_{ri} p_i \geq 0$

(see assumption 3) and for all other momenta and coordinates over the interval from $-\infty$ to $+\infty$. Thus we obtain the following basic formula for the rate constant of the process

$$k = \int_{\dot{q}_r=0}^{\infty} \frac{\dot{q}_r \, dp_r}{h^s} \int_{-\infty}^{\infty} \frac{\exp\left[-\beta H^* d\Gamma^*\right]}{Q} \tag{2.6}$$

where $d\Gamma^* = \prod_{i \neq r} dp_i dq_i$. If we assume that in the expression for the kinetic energy in H^*, the part corresponding to the motion of q_r is separable, we can write H^* as

$$H^* = E_t + H_0^*. \tag{2.7}$$

where $E_t = \frac{1}{2}m_r \, \dot{q}_r^2$, $H_0^* = \frac{1}{2} \sum_{n,m \neq r} a_{nm} \, \dot{q}_n \dot{q}_m + U^*$ and $U^* = U(q_1, q_2, \ldots, q_r^*, \ldots, q_s)$. Then the Eq. (2.6) can be written in the form

$$k = \frac{1}{Q} \int_0^{\infty} \frac{dE_t}{h} \exp\left(-\beta E_t\right) \int \exp\left(-\beta H_0^*\right) d\Gamma^* = \frac{kT}{h} \frac{Q^*}{Q} \exp\left(-\frac{E_0}{k_B T}\right), \tag{2.8}$$

where E_0 denotes the minimum potential energy of the activated complex.

$$E_0 = \min\left[U(q_1, \ldots, q_s)\right]_{q_r = q_r^*}, \tag{2.9}$$

Q^* is the total partition function of the activated complex, the energy of which is measured from the level E_0. i.e.

$$Q^* = \frac{1}{h^{s-1}} \int \exp\left[-\beta\left(H_0^* - E_0\right)\right] d\Gamma^*. \tag{2.10}$$

2.2.2   Microcanonical Transition State Theory

Microcanonical TST is particularly useful for unimolecular reactions. In this approach, a rate constant is determined for the microcanonical ensemble of reactant molecules [108, 109, 110] i.e., an assemby of molecules, for which there is an equal population of all states at a particular energy. The microcanonical rate constant $k(E)$ is for reactants whose total energy is E. The canonical TST rate constant $k(T)$ is a Boltzmann average over $k(E)$ and is given by

$$k(T) = \int_0^\infty k(E)P(E)dE \qquad (2.11)$$

where the reactants have energy E, $P(E) = N(E)\exp\left(-E/k_B T\right)/Q$ is the normalised Boltzmann probability, and the microcanonical TST rate constant $k(E)$, is the specific rate constant for reactants with total energy between E and $E + dE$.

Microcanonical transition states are reactive systems which have a total energy $H = E$ and a value for the reaction coordinate q_r which lies between q_r^* and $q_r^* + dq_r^*$. The reaction coordinate potential at the transition state is E_0. For a bimolecular reaction, the combined states of the reactant molecules at total energy E define a supermolecule.The fraction of supermolecules that lie at the transition state (i.e., at q_r ranging from q_r^* to $q_r^* + dq_r^*$) with reaction coordinate momenta in the range from p_r^* to $p_r^* + dp_r^*$ may be found from statistical mechanics. This fraction is

$$\frac{dN(q_r^*, p_r^*)}{N} = \frac{dq_r^* dp_r^* \int_{H=E-E_t^*-E_0} d\Gamma^*}{\int_{H=E} d\Gamma}. \qquad (2.12)$$

All supermolecules that lie within q_r^* and $q_r^* + dq_r^*$ and with positive p_r^* will cross the transition state towards products in the time interval $dt = \mu_r dq_r^*/p_r^*$. Also $dp_r^* = \frac{\mu_1}{p_r^*}dE_t^*$. Thus, from Eq. (2.12), the reactant-to- product flux through the transition state for momentum $p_1^\ddagger$ is

$$\frac{dN(q_r^*, p_r^*)}{dt} = \frac{NdE_t^* \int_{H=E-E_t^*-E_0} d\Gamma^*}{\int_{H=E} d\Gamma}. \qquad (2.13)$$

To find the total reaction flux, Eq. (2.13) must be integrated between the limits $E_t^* = 0$ and $E_t^* = E - E_0$ which gives

$$\frac{1}{N}\frac{dN}{dt} = k(E) = \frac{\int_0^{H=E-E_0} d\Gamma^*}{\int_{H=E} d\Gamma} = \frac{G^*(E-E_0)}{hN(E)}. \qquad (2.14)$$

where $G^*(E - E_0)$ is the sum of states at the transition state.

2.2.3 Variational Transition State Theory

Classical transition state theory gives the exact rate constant if the net rate of reaction equals the rate at which trajectories pass through the transition state. These two rates are equal, however, only if trajectories do not recross the transition state: any recrossing makes the reactive flux smaller than the flux through the transition state. Thus, the classical transition state theory rate constant may be viewed as an upper bound to the correct classical rate constant.

One can consider different positions for the transition state along the reaction path and calculate the rate constant corresponding to each. The minimum rate so obtained is the closest to the truth, assuming that quantum effects related to tunneling and non-separability are negligible. This procedure is called variational transition state theory [111, 112, 113, 114]. There are both canonical and microcanonical versions of variational transition state theory. The microcanonical approach involves calculating $k(E)$, and finding the minimum rate constant that is obtained when the position of the dividing surface is varied. This minimum is then inserted into Eq. (2.11) and $k(T)$ is obtained by numerical integration. In the canonical approach, the values of $k(T)$ are calculated by numerical integration of Eq. (2.11). The minimum value of this $k(T)$, when the dividing surface is varied, is then accepted as the best estimate of the rate constant.

2.3 Quantum Mechanical Transition State Theory

A basic difficulty in the generalisation of classical transition state theory to quantum mechanics is that the reaction criterion cannot be formulated as the condition that a trajectory pass through a critical surface. This is connected with the fact that, in a quantum mechanical observation, the coordinates and momenta of a system cannot be asssigned simultaneously. The uncertainty in the value of the reaction coordinate at the transition state must be at least the size of the wavelength associated with the motion along the reaction coordinate; i.e., the transition state is not localised.

In classical transition state theory, the potential energy is constant and the reaction coordinate motion is separated from the remaining internal motions at the localised position along the reaction coordinate which defines the transition state. Quantum mechanical delocalisation of the transition state along the reaction coordinate can lead to two problems.

1. In the region Δq, the potential will not be flat and it is incorrect to treat the reaction coordinate as being a classsical translational motion. Also since the potential is usually having a concave-down shape, quantum mechanical tunneling will occur through the potential.

2. If there is curvature along the reaction coordinate in the region Δq, the reaction coordinate is not separable from the remaining internal degrees of freedom [108, 111, 115, 116]. Thus, the rate constant expression cannot be factored into a frequency $k_B T/h$ for the reaction coordinate and a partition function for the remaining degrees of freedom. Also, since the curvature couples the reaction coordinate with the remaining modes, tunneling cannot be treated as a one-dimensional reaction coordinate barrier-penetration problem. Instead, there will be a multitude of tunneling paths which involve all the coordinates[117, 118, 119].

Clearly, then, there are many difficulties in deriving a quantum mechanical transition state theory expression which does not include the separable reaction coordinate approximation. To obtain a working transition state theory expression, the separable approximation is asssumed and corrections are made to the classical rate constant of Eq. (2.8) to account for quantum effects. It is well known that quantum partition functions are required for most vibrational motions. This effectively leads to a barrier for reaction which is not the classical barrier, but the difference in zero-point energies between the transition state and the reactants. Also in the transit of the representative point over the potential barrier, there is a probability of over-barrier reflection and tunnel transmission. As a result of these, in calculating the current along the reaction coordinate, in Eq. (2.6) the integral $\int_{\dot{q}_r=0}^{\infty} \frac{\dot{q}_r}{h} e^{-p_r^2/2\mu_r k_B T} dp_r$ should be replaced by $\int_{-\infty}^{\infty} P(E_t) e^{-E_t/k_B T} \frac{dE_t}{h}$ where $P(E_t)$

is the transmission probability. Integration over E_t extends into the region of negative energy also, since in quantum theory the probability of tunnel transition can be taken into account. To maintain the maximum analogy between the classical and quantum formulae, the TST rate constant is multiplied by an energy or temperature dependent 'transmission coefficient' to correct for nonclassical motion along the reaction coordinate. We rewrite Eq. (2.8) as

$$k = \chi \frac{k_B T}{h} \frac{Q^{\ddagger}}{Q_A Q_B} e^{(-E_0/k_B T)} \qquad (2.15)$$

where χ is known as the transmission coefficient. From the above arguments we see that

$$\chi \frac{k_B T}{h} = \int_{-\infty}^{\infty} P(E_t) e^{-E_t/k_B T} \frac{dE_t}{h}. \qquad (2.16)$$

We can calculate χ for a one-dimensional potential barrier with one maximum [107]. For this, the first step is to get an expression for the transmission probability.

The problem of the calculation of $P(E_t)$ can be put in the following way. In the region I (see Fig. 2.1) there is an incident current of unit amplitude, which is described by the wavefunction

$$\Psi_1^+(q_r) = e^{i \frac{p_r q_r}{\hbar}}, \qquad q_r < q_r'. \qquad (2.17)$$

In the same region there is also the reflected current with unknown amplitude X,

$$\Psi_1^-(q_r) = X e^{-i \frac{p_r q_r}{\hbar}}, \qquad q_r < q_r'. \qquad (2.18)$$

In region II there is only the transmitted current with amplitude Y,

$$\Psi_{II}^+(q_r) = Y e^{i \frac{p_r q_r}{\hbar}}, \qquad q_r > q_r''. \qquad (2.19)$$

The explicit assignment of the wavefunction in region 1 and II is equivalent to the imposition of boundary conditions on the solution of the wave equation describing the motion of the representative point in terms of the coordinate q_r.
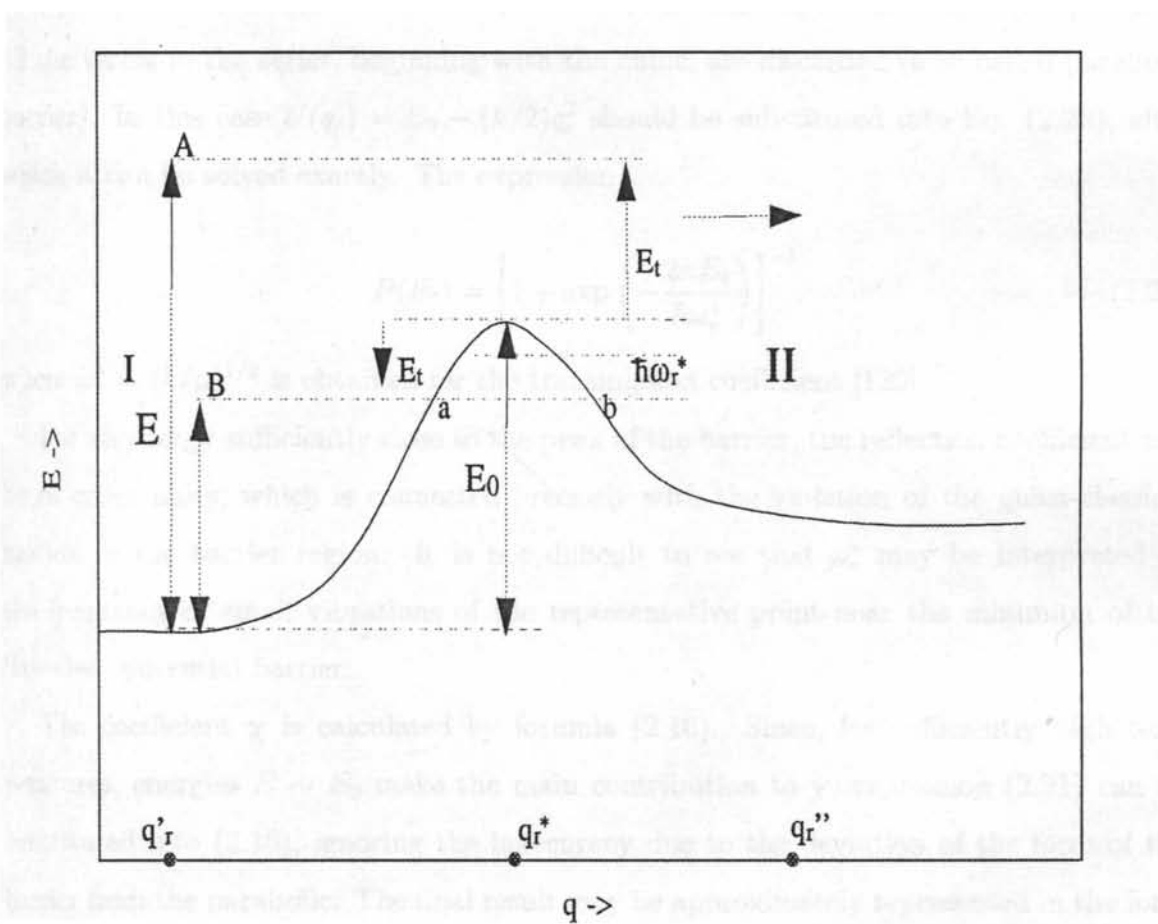
Figure 2.1: Penetration of a one-dimensional potential barrier by a particle; state A–above barrier transmission ($E_t > 0$); state B–tunnel transmission ($E_t < 0$).

$$-\frac{\hbar^2}{2\mu}\frac{\partial^2 \Psi}{\partial q_r^2} + U(q_r)\Psi = E\Psi. \tag{2.20}$$

The solution of this equation in the region of the potential barrier, with the specified boundary conditions, allows well-defined amplitudes X and Y to be determined, and hence the transmission coefficient $P = |X|^2$ and the reflection coefficient $Q = |Y|^2$.

Now consider a particular case. Suppose the energy of the particle is such that, in the region near the top of the barrier, the conditions for classical motion are violated, but, in the range of variation of E_t under consideration, the potential energy in this region can be represented in the form of a series, about the maximum, in the coordinate q_r, where all the terms in the series, beginning with the cubic, are discarded (a so-called parabolic barrier). In this case $U(q_r) = E_0 - (k/2)q_r^2$ should be substituted into Eq. (2.20), after which it can be solved exactly. The expression

$$P(E_t) = \left[1 + \exp\left(-\frac{2\pi E_t}{\hbar \omega_r^*}\right)\right]^{-1} \tag{2.21}$$

where $\omega_r^* = (k/\mu)^{1/2}$ is obtained for the transmission coefficient [120].

For an energy sufficiently close to the peak of the barrier, the reflection coefficient will be of order unity, which is connected precisely with the violation of the quasi-classical motion in the barrier region. It is not difficult to see that ω_r^* may be interpreted as the frequency of small vibrations of the representative point near the minimum of the 'inverted' potential barrier.

The coefficient χ is calculated by formula (2.16). Since, for sufficiently high temperatures, energies $E \sim E_0$ make the main contribution to χ, expression (2.21) can be substituted into (2.16), ignoring the inaccuracy due to the deviation of the form of the barrier from the parabolic. The final result may be approximately represented in the form

$$\chi = \frac{x}{\sin x} \tag{2.22}$$

where $x = \frac{\hbar \omega_r^*}{2kT}$. This value of χ is used in the next chapter for calculating the rate of breaking of the polymer.

2.4 Kramers' Theory

A very different approach to the theory of activated rate processes was suggested by Kramers in his serminal paper of 1940 [121]. An interesting review of the development of the theory may be found in Ref. [122]. In contrast to TST, which at best allows for the solvent to modify the free energy of activation, Kramers suggested that the solvent (or other medium) applies a frictional force on the reacting solute. The frictional force dissipates energy from the system to the bath; this is counteracted by random force which arises from fluctuations in the bath. The friction and the random fluctuations are related by a fluctuation dissipation relation. The existence of friction and random fluctuations causes two opposing effects. In the low friction limit, Kramers argued that without any external source of energy reaction cannot occur. Reactants must cross an energy barrier, and without any source of energy they wiil not have the necessary energy. The interaction of the solvent with the solute is the mechanism of energy transfer. In this underdamped regime, any increase in the damping strength implies an increase in the fluctuational force and will result in an increase in the reaction rate.

In the limit of moderate to strong damping, the frictional force is substantial enough to cause a fast exchange of energy between solute and solvent so that the solute is maintained in thermal equilibrium. However, the frictional force makes it difficult for the particles to move and the rate is limited by the spatial diffusion of the particle across the barrier separating reactants and products. As the damping increases, the diffusion time increases and the rate decreases. In Kramers' theory, friction plays a critical role. The dependence of the rate on friction is described in terms of a bell-shaped function. Only its maximum value is given by a TST expression which does not include any dependence of the rate on friction. Kramers' modification of the rate expression in the spatial diffusion limit is often referred to as a dynamical recrossing correction induced by the solvent.

Kramers modeled the interaction in terms of a one-dimensional Langevin equation

$$m\frac{d^2q}{dt^2} + \frac{dw(q)}{dq} + m\gamma\frac{dq}{dt} = \xi(t)$$ (2.23)

where the the reaction co-ordinate q has a mass m and feels a potential $w(q)$. The random force $\xi(t)$ is Gaussian with zero mean, and its correlation function is related to the damping constant γ through the second fluctation dissipation theorem:

$$< \xi(t)\xi(t^{'}) >= mk_BT \times 2\gamma\delta(t - t^{'}) \qquad (2.24)$$

where $\delta(x)$ is the Dirac delta function.

Kramers' model is simple. It is one-dimensional and assumes that the friction is Markovian. He derived an expression for the rate in the underdamped and spatial diffusion limits. He did not derive a uniform expresson for the rate valid for all values of the damping strength. This is the Kramers' turnover problem, which was solved only in the late eighties by Pollak, Grabert and Hanggi [123] and is known as PGH theory. A multidimensional generalisation of Kramers' problem in the spatial diffusion limit was proposed and solved by Langer [124]. The multidimensional energy diffusion limit was solved by Matkowsky, Schuss and coworkers [125, 126]. A multidimensional turnover theory has been recently formulated [127].

It has been recognised for some time that the Markovian property of the random force in the Langevin equation is often violated and so a generalised version of the Langevin equation incorporating memory effects into the random force has been developed. Use of this model along with dynamic corrections led to the development of the Grote-Hynes [128] theory of activated reaction rates. This elegant correction to the Kramers' theory is accurate when the frictional forces are moderate to high and the harmonic approximation to the reaction barrier is appropriate. In addition, because the theory is classical, any quantum mechanical effects are excluded.

Progress in the activated rate theory has been made possible by an observation of Zwanzig [129] that a generalised Langevin equation can be formally related to a microscopic Hamiltonian system in which a discrete harmonic bath is bi-linearly coupled to a system coordinate:

$$H = \frac{P_s^2}{2m_s} + V_0(s) + \sum_k \frac{P_k^2}{2m_k} + \frac{1}{2}m_k\omega_k^2 \left(q_k - \frac{c_k s}{m_k\omega_k^2} \right)^2 . \qquad (2.25)$$

The harmonic bath with bi-linear coupling allows the classical bath degrees of freedom to be analytically integrated out to yield an effective potential which is formally identical to a generalised Langevin equation in which the dependent friction is given by the cosine transform of the spectral density of the bath. This spectral density is the most basic description of the external bath. For the discrete Hamiltonian above it is given by

$$J\left(\omega\right) = \frac{\pi}{2} \sum_k \frac{c_k^2}{m_k \omega_k} [\delta(\omega - \omega_k)] \ . \tag{2.26}$$

Using this formal device of the microscopic Hamiltonian leading to a generalised Langevin equation, along with variational transition state theory, Pollak and co-workers [130] have developed a body of work in which it is shown that applying variational transition state theory to the discrete Hamiltonian in Eq. (2.25), and then passsing to a continuum limit can reproduce Grote-Hynes theory, and also potentially predict corrections. In addition, Pollak, Grabert, and Hanggi [123] have developed a 'turnover' theory which can describe reaction rates out of the range of applicability of Grote-Hynes theory from low to high frictional regimes. Voth and co-workers [131] have numerically studied more complicated classical Hamiltonians in which friction is spatially dependent.

Recently, Schwartz [132] used a methodology in which he defines the rate in terms of the flux autocorrection function and proceeds via the recently developed interaction representation for nonadiabatic corrections to adiabatic evolution operators to study the rate of a chemical reaction when the reaction is placed in a dissipative bath. This methodology is an infinite order resummation of nonadiabatic corrections to evolution operators. The approach produces an analytic expression which yields accurate results over a range of temperatures, viscosities and system parameters through the Kramers turnover region.

2.5 Centroid Approach

The theory of Feynman path centroid dynamics can be applied to the calculation of quantum barrier crossing rates. The formulation starts from the exact definition of the quantum survival probability of the reactant state and the reaction rate is then defined

as the steady-state limit of the decay rate of the survival probability. Voth, Chandler and Miller [133] have used this approach to develop a 'quantum transition state theory' which has been further developed by Voth [134] to provide an approximate quantum rate theory for condensed phase reactions. The centroid approach has the great advantage that it is relatively simple to apply. One needs to compute only diagonal matrix elements, a computation which is feasible using quantum Monte Carlo techniques.

A variational formulation of the centroid theory, has also been presented [135] and found to improve the resulting estimates. A recent numerical development has been the application by Topaler and Makri [136] of their adiabatic propagator algorithm to the Hamiltonian of Eq. (2.25). Numerical calculations can then produce rates of reaction as a function of viscosity of the solution. Finally Georgievskii and Pollak [137] have recently developed an approximate quantum theory that seems to be able to reproduce the numerical results of Makri and Topaler [136] in the high friction limit.

Based on an approximation for the initial reactant state and the centroid molecular dynamics (CMD) approximation for the dynamics, Jang and Voth [138] recently obtained a new approximate rate expression which is equal to the path integral quantum transition state theory (PI-QTST) expression multiplied by a transmission factor of order unity. This factor varies with the choice of the dividing surface in the low temperature limit, but it is invariant to that choice at higher temperatures. It is then shown that the PI-QTST rate expression results from the quadratic barrier approximation for the calculation of the transmission factor only. The potential to use the new rate expression as an improved version of the PI-QTST is also tested for model systems. For certain choices of the dividing surface, it is shown that the new reaction rate expression results in improvement over the PI-QTST results. The overall formulation also yields a better understanding of the barrier crossing dynamics viewed from the centroid perspective and the rigorous origin of the PI-QTST formula.

2.6   Flexible Transition State Theory

The first version of quantum TST to satisfactorily account for large amplitude motion was flexible transition state theory (FTST) which was introduced by Wardlaw and Marcus [139]. Like all variational theories, FTST allows the transition state to be 'mobile' and not associated with any particular potential energy surface (PES) feature − it typically occurs at larger interfragment separations for low energies and angular momenta, and at smaller separations for high energies and angular momenta. However, FTST also treats the transition state as 'floppy' and not associated with any particular geometry − there are large amplitude motions (transitional modes) which are coupled to each other and to overall rotation of the molecular system. Typically transitional modes correspond to free rotations of the separated fragments that evolve into vibrational motions of the parent molecule. The strength of FTST is the avoidance of approximations concerning the transitional modes by inclusion of the full transitional mode potential (or, the entire PES, if available) and by an exact enumeration of the transitional mode contribution to the transition state sum of states. This enumeration can only be feasibly acccomplished by a classical treatment of the transitional modes through phase space integrals, which neglects quantum effects (like zeropoint energy) and which makes an individual variational location of the reaction bottleneck for each quantum state impossible. A thorough discussion of the advantages, limitations, and approximations of FTST is provided in recent review articles [140]. Subsequent fundamental developments in FTST have been made by Aubanel and Wardlaw [141], Klippenstein and Marcus [142], Klippenstein [143] and Smith [144].

A simple formula for the canonical flexible transition state theory expression for the thermal reaction rate constant is derived by Robertson, Wagner and Wardlaw [145] that is exact in the limit of the reaction path being well approximated by the distance between the centres of mass of the reactants. This formula evaluates classically the contribution to the rate constant from transitional degrees of freedom (those that evolve from free rotations in the limit of infinite separation of the reactants). As a result of this treatment, the formula contains the product of two factors: one that exclusively depends on the collision kinematics and one that exclusively depends on the potential energy surface that controls

the transitional degrees of freedom. This second factor smoothly varies, in the classical limit, from harmonic oscillator to hindered rotor to free rotor partition functions as the potential energy surface varies from quadratic to sinusoidal to a constant in its dependence on the relative orientation angles of fragments. Recently they have got a completely general canonical and microcanonical (energy-resolved) flexible transition state theory (FTST) expression for the rate constant for an arbitrary choice of reaction coordinate [146]. The derivation is thorough and rigorous within the framework of FTST and replaces their previous treatments which implicitly involved some significant assumptions. The rate expressions apply to any definition of the separation distance between fragments in a barrierless recombination (or dissociation) that is held fixed during hindered rotations at the transition state, and to any combination of fragment structure (atom, linear top, nonlinear top). The minimization of the rate constant with respect to this definition can be regarded as optimizing the reaction coordinate within a canonical or microcanonical framework. The expression is analytic except for a configuration integral whose evaluation generally requires numerical integration over internal angles (from one to five depending on the fragment structures). The form of the integrand in this integral has important conceptual and computational implications. The primary component of the integrand is the determinant of the inverse G-matrix associated with the external rotations and the relative internal motion of the fragments.

Chapter 3

Transition State Theory of Breaking of a Polymer

3.1 Introduction

In this chapter we use Quantum Transition State Theory (QTST) to derive an expression for the rate of breaking of a polymer subjected to a force at one of its ends. We make use of a multidimensional version that has been applied successfully to calculate the rate in a variety of problems [147, 148, 122]. It uses the harmonic approximation for all the vibrations and the reaction coordinate, and has the advantage of having tunneling contributions included in the rate. The expression for the rate is [107]:

$$R = \frac{\Omega}{4\pi \sin(\hbar\beta\Omega/2)} \frac{Q^{\ddagger}}{Q} e^{-\beta E_a} \,. \tag{3.1}$$

E_a is the activation energy of the reaction. $Q^{\ddagger}$ denotes the partition function for the transition state, with only the stable modes included. Q is the partition function for the initial state and $\beta = 1/(k_B T)$. Ω is the frequency of the unstable mode and $\frac{\Omega}{4\pi \sin(\hbar\beta\Omega/2)}$ is the contribution of this mode to the rate. It includes tunneling contributions too [107]. Under the harmonic approximation for all the modes, the rate is

$$R = \frac{\Omega}{4\pi \sin(\frac{\hbar\beta\Omega}{2})} \frac{\prod_j \sinh\left(\frac{\hbar\beta\omega_j}{2}\right)}{\prod_j^\ddagger \sinh\left(\frac{\hbar\beta\omega_j^\ddagger}{2}\right)} e^{-\beta E_a} \tag{3.2}$$

ω_j is the frequency of the mode for the initial state and $\omega_j^\ddagger$ is the corresponding frequency for the transition state. In the above equation, the product for the transition state does not include the unstable mode and this is indicated by the superscript $\ddagger$ on the product. While the above expressions are fully quantum mechanical, taking the temperature to be large, and assuming $\frac{\hbar\beta\omega_j}{2} \ll 1$, we can get the classical limit for the rate. The result is

$$R_{classical} = \frac{1}{4\pi} \frac{\prod_j \omega_j}{\prod_j^\ddagger \omega_j^\ddagger} e^{-\beta E_a}. \tag{3.3}$$

3.2 The Model

The model that we consider is the following: A single polymer molecule has one end fixed and a force is acting on the other end, as shown in Fig. 3.1. We imagine the polymer to be a chain of units of mass m joined together by bonds obeying the Morse potential. Thus, denoting the position of the nth atom as u_n and taking the number of bonds to be N, we can write the potential energy of the system to be

$$V_{total}(u_1, u_2, u_3, ... u_N) = \sum_{n=1}^{N} V_M(u_n - u_{n-1} - b) - Fu_N. \tag{3.4}$$

We take u_0 to be fixed and equal to zero. In the above, the Morse potential V_M is defined by

$$V_M(u_n - u_{n-1} - b) = D_e(1 - e^{-a(u_n - u_{n-1} - b)})^2, \tag{3.5}$$

D_e, a and b are parameters characterizing the Morse potential. The force acting on the last atom is F and it causes the last term in the potential energy in the Eq. (3.4). From the variables u_n, it is convenient to change over to a new set of variables y_n, the distortion of the nth bond from its equilibrium length b. Putting $y_n = u_n - u_{n-1} - b$, we can write
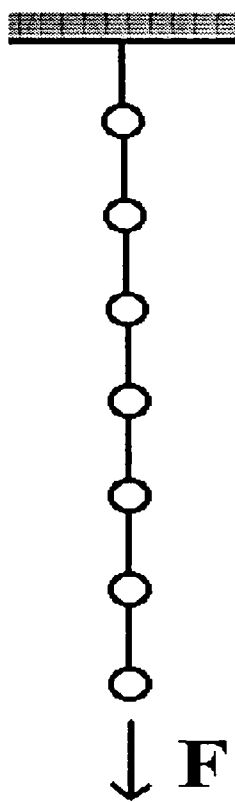
Figure 3.1: The model investigated consists of N units each of mass m, joined together by bonds obeying the Morse potential. It is fixed at one end and is acted upon by a force F acting at the other end.

the potential energy as

$$V_{total}(y_1, y_2, y_3, ...y_N) = \sum_{n=1}^{N} V_M(y_n) - F \sum_{n=1}^{N} y_n - NbF. \qquad (3.6)$$

The last term in the above equation is a constant and is of no consequence in the dynamics and hence we shall omit this term. The above potential energy is a sum of N separate terms:

$$V_{total}(y_1, y_2, y_3, ...y_N) = \sum_{n=1}^{N} V(y_n) \qquad (3.7)$$

with the modified potential for each bond, $V(y)$ defined by

$$V(y) = D_e(1 - e^{-ay})^2 - Fy. \qquad (3.8)$$

Thus we see that the effect of an externally applied force at one end is just to change the potential of each bond from the Morse potential to this new modified Morse potential, $V(y)$. To understand the form of this potential, we give plots of $V(y)/D_e$ for different values of F_1 in the Fig. 3.2, where F_1 is the dimension-less force defined by $F_1 = 2F/(D_e a)$. The figure shows that for any nonzero value for the force F, the potential has two extrema, one being a minimum and the other a maximum. We denote the values of y for the two as $y_\pm$.

3.2.1 Expression for $y_\pm$

These can be obtained using the condition for extrema. i.e. the first derivative is zero. Differentiating (3.8) we get

$$\frac{dV}{dy} = 2aD_e \left(1 - e^{-ay}\right) e^{-ay} - F. \qquad (3.9)$$

At the extrema,

$$\frac{dV}{dy} = 2aD_e \left(1 - e^{-ay}\right) e^{-ay} - F = 0$$
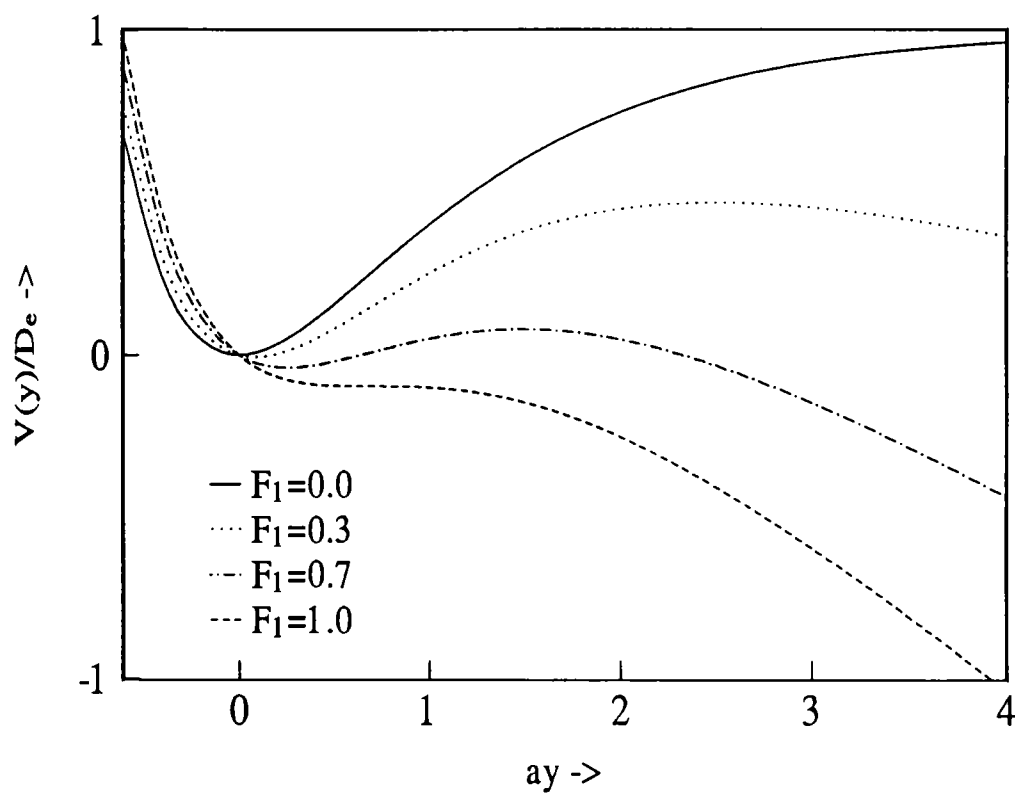
which on solving gives

Figure 3.2: Shapes of the modified Morse potential plotted against ay, for different values of F_1.

$$y_{\pm} = \frac{1}{a} \ln \left[\frac{2}{1 \pm \sqrt{1 - F_1}} \right]. \tag{3.10}$$

Note that the above definition implies $y_+ < y_-$. For any $F_1 < 1$, each bond is metastable (see Fig. 3.2). It can go over the barrier if it gets a certain activation energy, resulting in the breaking of the bond and consequently of the polymer.

3.2.2 Expression for Activation Energy

The activation energy for breaking any one of the bonds is given by

$$E_a = V(y_-) - V(y_+). \tag{3.11}$$

Substituting the value of y_+ and y_- in Eq. (3.8),

$$E_a = D_e \left[\sqrt{1 - F_1} + \frac{F_1}{2} \ln \left\{ \frac{1 - \sqrt{1 - F_1}}{1 + \sqrt{1 - F_1}} \right\} \right]. \tag{3.12}$$

As one increases F_1, the values of y_+ and y_- get closer. Also, there is lowering of the barrier for dissociation. If the dimensionless force $F_1 = 1$, $y_+ = y_-$ and the activation energy is zero. The breaking of the polymer is no longer an activated process. This limiting force is $F = D_e a / 2$.

3.3 The Single Bond Breaking Rate

The simplest approach to the calculation of the rate would be the following: We consider the vibrational motion of just one bond that may break and neglect coupling to the rest of the system. This is obviously a crude approximation. As the motion involves stretching of the bond between two units, each unit having a mass m, the reduced mass for the vibrational motion is $m/2$. The potential energy for the vibration in the neighborhood of the minimum of the potential is $\frac{1}{2}V''(y_+)(y - y_+)^2$ where $V''(y_+)$ is the second derivative of $V(y)$ with respect to y evaluated at y_+. $V''(y_+)$ can be easily found to be

$$V''(y_+) = D_e a^2 (\sqrt{1 - F_1} + 1 - F_1). \tag{3.13}$$

So the frequency of vibration of the diatomic molecule is

$$\omega_s = a\sqrt{2D_e/m} \left(\sqrt{1 - F_1} + 1 - F_1 \right)^{1/2}. \tag{3.14}$$

In a similar manner, the frequency of the unstable mode is

$$\Omega_s = a\sqrt{2D_e/m} \left(\sqrt{1 - F_1} - 1 + F_1 \right)^{1/2}. \tag{3.15}$$

Since we are interested in only one mode, the product in the numerator of Eq. (3.2) will be containing only one factor and that in the denominator, no factor. Substituting $\Omega = \Omega_s$ and $\omega_j = \omega_s$ in Eq. (3.2), we get the rate to be

$$R_s = \frac{\Omega_s \sinh \left(\frac{\hbar \beta \omega_s}{2} \right)}{4\pi \sin(\frac{\hbar \beta \Omega_s}{2})} e^{-\beta E_a}. \tag{3.16}$$

3.4 The Normal Mode Analysis

3.4.1 The Eigenvalue Problem

Having made the simplest possible analysis of the problem, we now proceed to make a rigorous multidimensional calculation of the rate. This requires a normal mode analysis [149] of vibrations of the chain around the equilibrium position as well as around the transition state. In the following, we make this for the transition state. The calculations are similar and simpler for vibrations around the equilibrium position. The transition state has one of the bonds stretched (the one that breaks) – the bond length is y_- which corresponds to the maximum of the potential $V(y)$. All the other bonds have an equilibrium bond length equal to y_+, which is the minimum of the potential $V(y)$. We denote the displacement of the jth atom from its equilibrium position by ξ_j and take the bond between the atom numbers $n - 1$ and n to be the one that breaks. Then, for small amplitude vibrations

around the transition state, under the harmonic approximation, we have the Hamiltonian

$$H = \frac{1}{2} \sum_{j=1}^{N} m\, \dot{\xi}_j^2 + \frac{1}{2} \sum_{j=1\neq n}^{N} m\omega_+^2 (\xi_j - \xi_{j-1})^2 - \frac{1}{2} m\omega_-^2 (\xi_n - \xi_{n-1})^2. \qquad (3.17)$$

The quantities ω_+ and ω_- are defined by the equation $m\omega_\pm^2 = \pm V''(y_\pm)$ and are given by

$$\omega_\pm^2 = \frac{D_e a^2}{m} \left(\sqrt{1 - F_1} \pm (1 - F_1) \right). \qquad (3.18)$$

We can write down the classical mechanical equations of motion for the atoms as

$$m\, \ddot{\xi}_1 = -2m\omega_+^2 \xi_1 + m\omega_+^2 \xi_2,$$

$$m\, \ddot{\xi}_j = -m\omega_+^2 (\xi_j - \xi_{j-1}) + m\omega_+^2 (\xi_{j+1} - \xi_j),$$

$$m\, \ddot{\xi}_{n-2} = -m\omega_+^2 (\xi_{n-2} - \xi_{n-3}) + m\omega_+^2 (\xi_{n-1} - \xi_{n-2}),$$
$$m\, \ddot{\xi}_{n-1} = -m\omega_+^2 (\xi_{n-1} - \xi_{n-2}) - m\omega_-^2 (\xi_n - \xi_{n-1}), \qquad\qquad (3.19)$$
$$m\, \ddot{\xi}_n = m\omega_-^2 (\xi_n - \xi_{n-1}) + m\omega_+^2 (\xi_{n+1} - \xi_n),$$
$$m\, \ddot{\xi}_{n+1} = -m\omega_+^2 (\xi_{n+1} - \xi_n) + m\omega_+^2 (\xi_{n+2} - \xi_{n+1}),$$

$$m\, \ddot{\xi}_N = m\omega_+^2 \xi_{N-1} - 2m\omega_+^2 \xi_N.$$

We can write solutions of the form

$$\xi_j = \xi_j^0 e^{i\omega t} \qquad (3.20)$$

where ω is the frequency with which the jth atom is vibrating. Using this in the sets of equations (3.19), we get the following equations.

$$\omega^2 \xi_1^0 = 2\omega_+^2 \xi_j^0 - \omega_+^2 \xi_{j+1}^0,$$

$$\cdots\cdots\cdots\cdots\cdots\cdots\cdots\cdots\cdots\cdots\cdots\cdots\cdots\cdots\cdots$$

$$\omega^2 \xi_j^0 = \omega_+^2 \left(\xi_j^0 - \xi_{j-1}^0 \right) - \omega_+^2 \left(\xi_{j+1}^0 - \xi_j^0 \right),$$

$$\cdots\cdots\cdots\cdots\cdots\cdots\cdots\cdots\cdots\cdots\cdots\cdots\cdots\cdots\cdots$$

$$\omega^2 \xi_{n-2}^0 = \omega_+^2 \left(\xi_{n-2}^0 - \xi_{n-3}^0 \right) - \omega_+^2 \left(\xi_{n-1}^0 - \xi_{n-2}^0 \right),$$
$$\omega^2 \xi_{n-1}^0 = \omega_+^2 \left(\xi_{n-1}^0 - \xi_{n-2}^0 \right) + \omega_-^2 \left(\xi_n^0 - \xi_{n-1}^0 \right),$$
$$\omega^2 \xi_n^0 = -\omega_-^2 \left(\xi_n^0 - \xi_{n-1}^0 \right) - \omega_+^2 \left(\xi_{n+1}^0 - \xi_n^0 \right),$$
$$\omega^2 \xi_{n-2}^0 = \omega_+^2 \left(\xi_{n+1}^0 - \xi_n^0 \right) - \omega_+^2 \left(\xi_{n+2}^0 - \xi_{n+1}^0 \right),$$

$$\cdots\cdots\cdots\cdots\cdots\cdots\cdots\cdots\cdots\cdots\cdots\cdots\cdots\cdots\cdots$$

$$\omega^2 \xi_N^0 = -\omega_+^2 \xi_{N-1}^0 + 2\omega_+^2 \xi_N^0.$$

(3.21)

We have N such equations. We write the above equations in the form of an eigen value problem as

$$\omega_+^2 \begin{bmatrix} - & - & - & - & - & - & - \\ -1 & 2 & -1 & 0 & 0 & 0 & 0 \\ 0 & -1 & 2 & -1 & 0 & 0 & 0 \\ 0 & -1 & 1-\gamma & \gamma & 0 & 0 & 0 \\ 0 & 0 & \gamma & 1-\gamma & -1 & 0 & 0 \\ 0 & 0 & 0 & -1 & 2 & 0 & 0 \\ - & - & - & - & - & - & - \end{bmatrix} \begin{bmatrix} - \\ \xi_{n-2}^0 \\ \xi_{n-1}^0 \\ \xi_n^0 \\ \xi_{n+1}^0 \\ \xi_{n+2}^0 \\ - \end{bmatrix} = \omega^2 \begin{bmatrix} - \\ \xi_{n-2}^0 \\ \xi_{n-1}^0 \\ \xi_n^0 \\ \xi_{n+1}^0 \\ \xi_{n+2}^0 \\ - \end{bmatrix}$$

(3.22)

where

$$\gamma = \omega_-^2 / \omega_+^2.$$

(3.23)

The equation can be written as

$$\mathcal{D}_N^\ddagger \xi^0 = \omega^2 \xi^0$$

(3.24)

where

$$
\mathcal{D}_N^\ddagger = \omega_+^2
\begin{bmatrix}
\mathbf{D}_{n-1} & -1 & & & \\
-1 & 1-\gamma & \gamma & & \\
& \gamma & 1-\gamma & \gamma & \\
& & \gamma & \mathbf{D}_{N-n-1}
\end{bmatrix},
\tag{3.25}
$$

the matrix $\mathbf{D}_{n-1}$ denoting an $(n-1) \times (n-1)$ square matrix having the form

$$
\mathbf{D}_{n-1} =
\begin{bmatrix}
2 & -1 & & & \\
-1 & 2 & -1 & & \\
& -1 & 2 & -1 & \\
& & -1 & 2 & -1
\end{bmatrix}
\tag{3.26}
$$

and

$$
\xi^0 =
\begin{bmatrix}
\xi_1^0 \\
\xi_2^0 \\
- \\
- \\
\xi_n^0 \\
\xi_{n+1}^0 \\
\xi_{n+2}^0 \\
- \\
- \\
\xi_N^0
\end{bmatrix}.
\tag{3.27}
$$

From equation (3.24), it follows that

$$
\left[\omega^2 \mathbf{I} - \mathcal{D}_N^\ddagger \right] \xi^0 = 0.
\tag{3.28}
$$

Here $\mathbf{I}$ is the identity matrix. This implies that

$$
\left| \omega^2 \mathbf{I} - \mathcal{D}_N^\ddagger \right| = 0.
\tag{3.29}
$$

We shall in the following assume that the polymer is fairly long and that it is a bond in the bulk that is broken, as this simplifies our analysis. In principle one can analyze other cases also, but it is tedious. Further, we do not expect the rates to be very different even if it is not a bond in the bulk that is broken. The above implies that n and $N - n$ are taken to be large numbers. We now have to find the frequency of the unstable mode and the ratios of the partition functions in the Eq. (3.1). These quantities are very conveniently found using the partitioning technique and Green's matrix. The formulae from the partitioning technique which we use are given in the appendix A.

3.4.2 The Green's Matrix.

We now consider the Green's matrix, which we define by:

$$\mathbf{G}^{0,n}(\overline{\omega}^2) = \left[\overline{\omega}^2 - \mathbf{D}_n\right]^{-1}. \tag{3.30}$$

Here $\overline{\omega}^2 = \omega^2/\omega_+^2$. Let us now evaluate the first diagonal element of the Green's matrix, which we denote as $G_{11}^{0,n}(\overline{\omega}^2)$. Partitioning the Green's matrix as in the following equation,

$$\mathbf{G}^{0,n}(\overline{\omega}^2) = \begin{bmatrix} \overline{\omega}^2 - 2 & 1 \\ 1 & \overline{\omega}^2 - \mathbf{D}_{n-1} \end{bmatrix}^{-1} \tag{3.31}$$

and using the formulae (A.2) of appendix A leads to the first diagonal element of the Green's matrix to be

$$G_{11}^{0,n}(\overline{\omega}^2) = \left(\overline{\omega}^2 - 2 - G_{11}^{0,n-1}(\overline{\omega}^2)\right)^{-1}. \tag{3.32}$$

In the limit where n is very large, the first diagonal element of the Green's matrix has to be independent of n. That is $G_{11}^{0,n}(\overline{\omega}^2) \approx G_{11}^{0,n-1}(\overline{\omega}^2)$. We shall then omit the superscripts n and $n-1$. Then we get the result

$$G_{11}^{0}(\overline{\omega}^2) = \left(\overline{\omega}^2 - 2 - G_{11}^{0}(\overline{\omega}^2)\right)^{-1}. \tag{3.33}$$

which can be solved for $G_{11}^{0}(\overline{\omega}^2)$, to get

$$G_{11}^0(\overline{\omega}^2) = \frac{\overline{\omega}^2 - 2 \pm \sqrt{(\overline{\omega}^2 - 2)^2 - 4}}{2}. \tag{3.34}$$

Using the condition that $G_{11}^0(\overline{\omega}^2) \longrightarrow 0$ as $\overline{\omega}^2 \longrightarrow \pm\infty$ leads to

$$G_{11}^0(\overline{\omega}^2) = \tfrac{1}{2}\left(\overline{\omega}^2 - 2 + \sqrt{\overline{\omega}^4 - 4\overline{\omega}^2}\right), \qquad \text{if } \overline{\omega}^2 < 0,$$

$$G_{11}^0(\overline{\omega}^2) = \tfrac{1}{2}\left(\overline{\omega}^2 - 2 + i\sqrt{4\overline{\omega}^2 - \overline{\omega}^4}\right), \qquad \text{if } 0 < \overline{\omega}^2 < 4 \text{ and}$$

$$G_{11}^0(\overline{\omega}^2) = \frac{1}{2}\left(\overline{\omega}^2 - 2 - \sqrt{\overline{\omega}^4 - 4\overline{\omega}^2}\right), \qquad \text{if } \overline{\omega}^2 > 4. \tag{3.35}$$

In determining the matrix element for $0 < \overline{\omega}^2 < 4$, we have assumed $\overline{\omega}^2$ to have a small negative imaginary part.

3.4.3 The Frequency of the Unstable Mode

The frequencies of the modes are determined by the determinantal equation (3.29). i.e. $\left|\omega^2 - \mathcal{D}_N^\ddagger\right| = 0$. Denoting $\overline{\omega}^2 = \omega^2/\omega_+^2$ this equation may be written as $\left|\overline{\omega}^2 - \mathbf{D}_N^\ddagger\right| = 0$, with

$$\left[\overline{\omega}^2 - \mathbf{D}_N^\ddagger\right] = \begin{bmatrix} \overline{\omega}^2 - \mathbf{D}_{n-1} & 1 & \\ 1 & \begin{matrix} \overline{\omega}^2 - 1 + \gamma & -\gamma \\ -\gamma & \overline{\omega}^2 - 1 + \gamma \end{matrix} & \begin{matrix} \\ 1 \end{matrix} \\ & 1 & \overline{\omega}^2 - \mathbf{D}_{N-n-1} \end{bmatrix}. \tag{3.36}$$

Using the partitioning technique (see Eq. (A.1) of appendix A), we get

$$\left|\overline{\omega}^2 - \mathbf{D}_N^\ddagger\right| = \left|\overline{\omega}^2 - \mathbf{D}_{n-1}\right| \left|\overline{\omega}^2 - \mathbf{D}_{N-n-1}\right|$$

$$\det \begin{bmatrix} \overline{\omega}^2 - 1 + \gamma - G_{11}^{0,n-1}(\overline{\omega}^2) & -\gamma \\ -\gamma & \overline{\omega}^2 - 1 + \gamma - G_{11}^{0,N-n-1}(\overline{\omega}^2) \end{bmatrix} = 0. \tag{3.37}$$

The unstable mode has an imaginary frequency. Hence we are looking for a solution of the above equation with $\overline{\omega}^2 = -\overline{\Omega}^2$, with $\overline{\Omega}$ real. If the breaking of the polymer occurs

not too near the ends, then we can replace the matrix elements of Green's matrix in the above equation with $G^0_{11}(-\overline{\Omega}^2)$ and this leads to the equation

$$\det \begin{bmatrix} -\overline{\Omega}^2 - 1 + \gamma - G^0_{11}(-\overline{\Omega}^2) & -\gamma \\ -\gamma & -\overline{\Omega}^2 - 1 + \gamma - G^0_{11}(-\overline{\Omega}^2) \end{bmatrix} = 0. \qquad (3.38)$$

Substituting for $G^0_{11}(\overline{\omega}^2)$ using the Eq. (3.35) gives

$$\left(-2\overline{\Omega}^2 - 2 + 2\gamma + \overline{\Omega}^2 + 2 - \sqrt{\overline{\Omega}^4 + 4\overline{\Omega}^2} + 2\gamma \right) \times$$

$$\left(-2\overline{\Omega}^2 - 2 + 2\gamma + \overline{\Omega}^2 + 2 - \sqrt{\overline{\Omega}^4 + 4\overline{\Omega}^2} - 2\gamma \right) = 0. \qquad (3.39)$$

i.e $\left(-\overline{\Omega}^2 + 4\gamma - \sqrt{\overline{\Omega}^4 + 4\overline{\Omega}^2} \right) \left(-\overline{\Omega}^2 - \sqrt{\overline{\Omega}^4 + 4\overline{\Omega}^2} \right) = 0.$ The second factor cannot be equal to zero for nonzero values of $\overline{\Omega}$. Therefore the first factor should be equal to zero. i.e.

$$-\overline{\Omega}^2 + 4\gamma = \sqrt{\overline{\Omega}^4 + 4\overline{\Omega}^2} \qquad (3.40)$$

From this we get $\overline{\Omega} = \frac{2\gamma}{\sqrt{1+2\gamma}}$, and hence

$$\Omega = \omega_+ \overline{\Omega} = \frac{2\omega_+ \gamma}{\sqrt{1 + 2\gamma}}. \qquad (3.41)$$

Substituting the value of γ from Eq. (3.23),

$$\Omega = \frac{2\omega_-^2}{\sqrt{\omega_+^2 + 2\omega_-^2}}. \qquad (3.42)$$

3.5   The Rate: Transition State Theory

We now proceed to the calculation of the rate of the reaction using the Eq. (3.2). Under the harmonic approximation, the rate given by this equation can be calculated exactly.

Using the infinite product representations

$$\sinh(x) = x \prod_{n=1}^{\infty} \left(1 + \frac{x^2}{n^2\pi^2}\right) \tag{3.43}$$

and

$$\sin(x) = x \prod_{n=1}^{\infty} \left(1 - \frac{x^2}{n^2\pi^2}\right) \tag{3.44}$$

for $\sin(x)$ and $\sinh(x)$, we can write the rate given by the Eq. (3.2) as

$$R = \frac{\Omega}{4\pi} e^{-\beta E_a} \frac{\Pi_j \left[\frac{\beta\hbar\omega_j}{2} \Pi_{l=1}^{\infty} \left\{1 + \left(\frac{\beta\hbar\omega_j}{2l\pi}\right)^2\right\}\right]}{\left(\frac{\beta\hbar\Omega}{2}\right) \Pi_{l=1}^{\infty} \left\{1 - \left(\frac{\beta\hbar\Omega}{2l\pi}\right)^2\right\} \Pi_k' \left[\frac{\beta\hbar\omega_k^\dagger}{2} \Pi_{l=1}^{\infty} \left\{1 + \left(\frac{\beta\hbar\omega_k^\dagger}{2l\pi}\right)^2\right\}\right]}. \tag{3.45}$$

In the above, the prime in the product Π_k' indicates that the unstable mode of the transition state is to be left out from the product. In the eigen value problem we had considered the unstable mode to have an imaginary frequency $i\Omega$. This means that if we include this mode also in the product in the denominator, $\left(\omega_i^\dagger\right)^2 = -\Omega^2$ where i denotes the index for the unstable mode, we can write the rate to be

$$R = \frac{\Omega}{4\pi} e^{-\beta E_a} \frac{\Pi_j \left[\frac{\beta\hbar\omega_j}{2} \Pi_{l=1}^{\infty} \left\{1 + \left(\frac{\beta\hbar\omega_j}{2l\pi}\right)^2\right\}\right]}{\Pi_j \left[\frac{\beta\hbar|\omega_j^\dagger|}{2} \Pi_{l=1}^{\infty} \left\{1 + \left(\frac{\beta\hbar\omega_j^\dagger}{2l\pi}\right)^2\right\}\right]}. \tag{3.46}$$

We define p_l by the equation

$$p_l = \frac{\prod_j \left(l^2 + \left(\frac{\beta\hbar\omega_j}{2\pi}\right)^2\right)}{\prod_j \left(l^2 + \left(\frac{\beta\hbar\omega_j^\dagger}{2\pi}\right)^2\right)}. \tag{3.47}$$

so that the expression for the rate can be written as

$$R = \frac{\Omega e^{-\beta E_a}}{4\pi} \sqrt{|p_0|} \prod_{l=1}^{\infty} p_l. \tag{3.48}$$

Now we calculate $\ln(p_l)$. Defining $z = \frac{\hbar\omega_+ \beta}{2\pi}$, we can write

$$\ln(p_l) = \sum_j \ln\left(l^2 + z^2 \frac{\omega_j^2}{\omega_+^2}\right) - \sum_j \ln\left(l^2 + z^2 \frac{\left(\omega_j^\ddagger\right)^2}{\omega_+^2}\right).$$ (3.49)

In the above, the second term on the right hand side contains summation over all the normal modes of the transition state, including the unstable mode. We know that $\frac{\omega_j^2}{\omega_+^2}$ are eigenvalues of the matrix $\mathbf{D}_N$ and $\frac{\left(\omega_j^\ddagger\right)^2}{\omega_+^2}$ are eigenvalues of the matrix $\mathbf{D}_N^\ddagger$. Therefore the Eq. (3.49) may be written as

$$\ln(p_l) = Trace\left[\ln\left(l^2 + z^2 \mathbf{D}_N\right)\right] - Trace\left[\ln\left(l^2 + z^2 \mathbf{D}_N^\ddagger\right)\right].$$ (3.50)

Hence $\ln(p_l) = \ln\left|l^2 + z^2 \mathbf{D}_N\right| - \ln\left|l^2 + z^2 \mathbf{D}_N^\ddagger\right|$. Thus we get

$$p_l = \frac{\left|l^2 + z^2 \mathbf{D}_N\right|}{\left|l^2 + z^2 \mathbf{D}_N^\ddagger\right|}.$$ (3.51)

Now,

$$\left[l^2 + z^2 \mathbf{D}_N^\ddagger\right] = \left[\begin{array}{c|cc|c} l^2 + z^2 D_{n-1} & & -z^2 & \\ \hline -z^2 & l^2 + z^2(1-\gamma) & \gamma z^2 & \\ & \gamma z^2 & l^2 + z^2(1-\gamma) & \gamma z^2 \\ \hline & & \gamma z^2 & l^2 + z^2 D_{N-n-1} \end{array}\right].$$ (3.52)

Similarly,

$$\left[l^2 + z^2 \mathbf{D}_N\right] = \left[\begin{array}{c|cc|c} l^2 + z^2 D_{n-1} & & -z^2 & \\ \hline -z^2 & l^2 + 2z^2 & -z^2 & \\ & -z^2 & l^2 + 2z^2 & -z^2 \\ \hline & & -z^2 & l^2 + z^2 D_{N-n-1} \end{array}\right].$$ (3.53)

Again using the same partitioning as in the Eq. (3.36) for both numerator and denominator of Eq. (3.51) gives

$$p_l = \frac{\begin{vmatrix} l^2 + 2z^2 - z^4 X_{n-1} & -z^2 \\ -z^2 & l^2 + 2z^2 - z^4 X_{N-n-1} \end{vmatrix}}{\begin{vmatrix} l^2 + z^2(1-\gamma) - z^4 X_{n-1} & \gamma z^2 \\ \gamma z^2 & l^2 + z^2(1-\gamma) - z^4 X_{N-n-1} \end{vmatrix}}. \tag{3.54}$$

In the above, X_{n-1} is the last diagonal element of $[l^2 + z^2 \mathbf{D}_{n-1}]^{-1}$. In the case where n and $N - n - 1$ are both large, this would be independent of n and we will denote it by X. Now, from the Eq. (A.2) of the appendix, $(l^2 + 2z^2 - z^4 X)^{-1}$ is the last diagonal element of $[l^2 + z^2 \mathbf{D}_n]^{-1}$. Thus $X = (l^2 + 2z^2 - z^4 X)^{-1}$ which on solving for X, we get

$$X = \frac{1}{2z^4} \left(l^2 + 2z^2 - \sqrt{(l^2 + 2z^2)^2 - 4z^4} \right). \tag{3.55}$$

Using this in the Eq. (3.54), we get

$$p_l = \frac{(l^2 + \sqrt{(l^2 + 2z^2)^2 - 4z^4} + 2z^2)^2 - 4z^2}{(l^2 + \sqrt{(l^2 + 2z^2)^2 - 4z^4} - 2\gamma z^2)^2 - 4\gamma^2 z^4}. \tag{3.56}$$

We can write p_l in a convenient form as

$$p_l = \frac{R[l, -1]}{R[l, \gamma]} \tag{3.57}$$

by defining $R[l, \gamma]$ as

$$R[l, \gamma] = (l^2 + \sqrt{(l^2 + 2z^2)^2 - 4z^4} - 2\gamma z^2)^2 - 4\gamma^2 z^4. \tag{3.58}$$

We can now find the value of p_0 by taking $l \to 0$ limit and this gives

$$p_0 = \lim_{l \to 0} \frac{(l^2 + \sqrt{(l^2 + 2z^2)^2 - 4z^4} + 2z^2)^2 - 4z^2}{(l^2 + \sqrt{(l^2 + 2z^2)^2 - 4z^4} - 2\gamma z^2)^2 - 2\gamma z^2} = -1/\gamma = -\omega_+^2/\omega_-^2 \ . \quad (3.59)$$

The product $\prod_{l=1} p_l$ has to be evaluated numerically. We can make the convergence faster by adopting the following procedure - We define

$$q_l = S[l, -1]/S[l, \gamma], \quad (3.60)$$

with

$$S[l, \gamma] = \left(2l^2 + 2z^2(1 - \gamma)\right)^2 - 4\gamma^2 z^4. \quad (3.61)$$

It is clear that as $l \to \infty$, $p_l \to q_l$. Then the infinite product $\prod_{l=1}^{\infty} p_l$ can be rewritten as below :

$$\prod_{l=1}^{\infty} p_l = \prod_{l=1}^{\infty} \frac{R[l, -1]}{R[n, \gamma]} = \prod_{l=1}^{\infty} \frac{S[l, -1]}{S[l, \gamma]} \prod_{m=1}^{\infty} \frac{R[m, -1]/S[m, -1]}{R[m, \gamma]/S[m, \gamma]} = \kappa_1 \prod_{l=1}^{\infty} q_l \quad (3.62)$$

with

$$\kappa_1 = \prod_{m=1}^{\infty} \frac{R[m, -1]/S[m, -1]}{R[m, \gamma]/S[m, \gamma]} = \prod_{m=1}^{\infty} \frac{\left\{1 + \frac{(R[m,-1]-S[m,-1])}{S[m,-1]}\right\}}{\left\{1 + \frac{(R[m,\gamma]-S[m,\gamma])}{S[m,\gamma]}\right\}} \quad (3.63)$$

which can be evaluated numerically and is found to be rapidly convergent. The infinite product $\prod_{l=1}^{\infty} q_l$ can be analytically evaluated, in terms of the Gamma function Γ [150, 151]. We can write

$$q_l = \frac{S[l, -1]}{S[l, \gamma]} = \frac{(l^2 + 2z^2)^2 - z^4}{(l^2 + z^2(1 - \gamma))^2 - \gamma^2 z^4}$$

$$= \frac{(l + iz\sqrt{3})(l - iz\sqrt{3})}{(l + z\sqrt{2\gamma - 1})(l - z\sqrt{2\gamma - 1})}. \quad (3.64)$$

Hence

$$\prod_{l=1}^{\infty} q_l = \frac{\Gamma\left(1 + z\sqrt{2\gamma - 1}\right)\Gamma\left(1 - z\sqrt{2\gamma - 1}\right)}{\Gamma\left(1 + iz\sqrt{3}\right)\Gamma\left(1 - iz\sqrt{3}\right)}. \quad (3.65)$$

We can also write the classical expression for the rate as

$$R_{classical} = \frac{\Omega}{4\pi}\sqrt{|p_0|}e^{-\beta E_a}.$$ (3.66)

Substituting the value of p_0 from Eq. (3.59) and Ω from Eq. (3.42) gives

$$R_{classical} = \frac{1}{4\pi}\frac{2\omega_+\omega_-}{\sqrt{\omega_+^2 + 2\omega_-^2}}e^{-\beta E_a}.$$ (3.67)

The fully quantum mechanical expression may be written as

$$R = \kappa R_{classical}$$ (3.68)

where

$$\kappa = \frac{\Gamma(1 + z\sqrt{2\gamma - 1})\Gamma(1 - z\sqrt{2\gamma - 1})}{\Gamma(1 + iz\sqrt{3})\Gamma(1 - iz\sqrt{3})}\kappa_1.$$ (3.69)

with $z = \frac{\beta\hbar\omega_+}{2\pi}$. We refer to κ as the quantum correction factor. The term κ_1 in the above equation is defined by the Eq. (3.63).

3.6   Calculations for the Lennard-Jones Potential:

If one assumes a Lennard-Jones potential for the interaction between two successive atoms, separated by a distance y, then the modified potential $V(y)$, is given by:

$$V(y) = \varepsilon\left[\left(\frac{a_{LJ}}{y}\right)^{12} - 2\left(\frac{a_{LJ}}{y}\right)^6\right] - Fy.$$ (3.70)

Just as in the case of the Morse potential, this also has a minimum (y_+) and a maximum (y_-) for real $y > 0$, $F > 0$. These values of $y_\pm$ can be calculated as follows. Differentiating Eq. (3.70) with respect to y, and equating the derivative to be equal to zero gives

$$12\varepsilon(-a_{LJ}^{12}y^{-13} + a_{LJ}^6 y^{-7}) - F = 0.$$ (3.71)

Putting $x = y/a_{LJ}$ gives

$$12\varepsilon \left(\frac{-1}{a_{LJ} x^{13}} + \frac{1}{a_{LJ} x^{7}} \right) - F = 0. \tag{3.72}$$

Multiplying throughout by $a_{LJ} x^{13}/12\varepsilon$ gives

$$f_1 x^{13} + 1 - x^6 = 0 \tag{3.73}$$

with

$$f_1 = \frac{F a_{LJ}}{12\varepsilon}. \tag{3.74}$$

Numerical investigation shows that the two roots coalesce at $f_1 = 0.2241584081$. Hence the potential would cease to have a minimum if the force at the end of the polymer exceeds $F_c = 12\varepsilon(0.2241584081)/a_{LJ}$.

3.7   Results

Having obtained the rate one can calculate the life-time of a bond as $\tau = (1/R)$. We now use the above expressions to calculate the rate of the dissociation of a bond of a polyethylene molecule that is subject to stress. For the calculations, following Oliveira and Taylor [46], we take the value of D_e to be 360 kJ/ mole. m is taken to be the mass of the $-CH_2-$ unit. For the Morse potential, the force constant for small amplitude vibrations near the minimum is $2D_e a^2$. Following Oliveira and Taylor [46], we take this to be 280 N/m, and use this to fix the value of the Morse parameter a. Thus the limiting force $D_e a/2$, for which breaking is no longer an activated force can be calculated to be 4.5738×10^{-9} dynes per molecule. We give in Fig. 3.3 a plot of the logarithm of the lifetime of the bond against the applied force for several temperatures.   The lifetimes calculated using Eq. (3.16) (single bond breaking rate) are compared with the results of multidimensional transition state theory in Fig. 3.5 for two temperatures 100K and 300K. We see that a very rough estimate of the rate can be obtained by a simple approximation that considers the dynamics of only the bond that breaks.
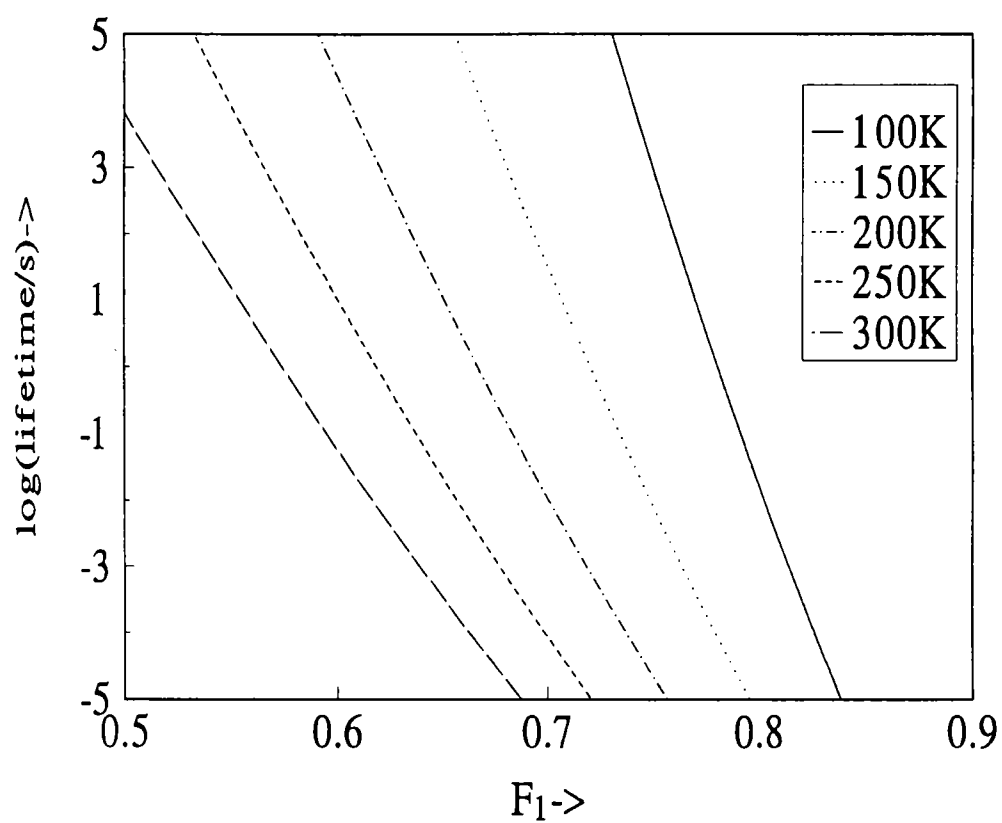
Figure 3.3: Plot of logarithm of lifetime/s against the applied force, for polyethylene at a range of temperatures, using the Morse potential. Note that $F_1 = F/(D_e a/2)$ and for polyethylene, the limiting force is $D_e a/2 = 4.574 \times 10^{-9} N$.

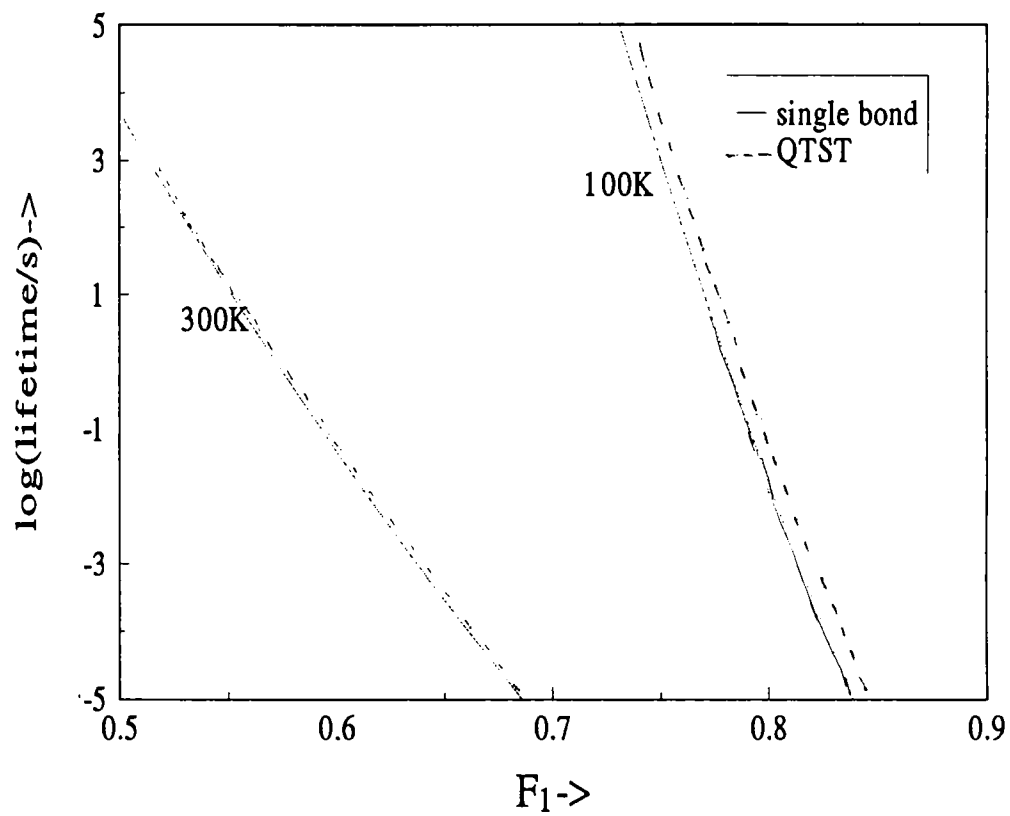Figure 3.4: The figure compares the lifetimes calculated using Eq. (3.16) and the result of multidimensional transition state theory. It shows that a rough estimate of the rate can be obtained by a simple approximation that considers the dynamics of only the bond that breaks.
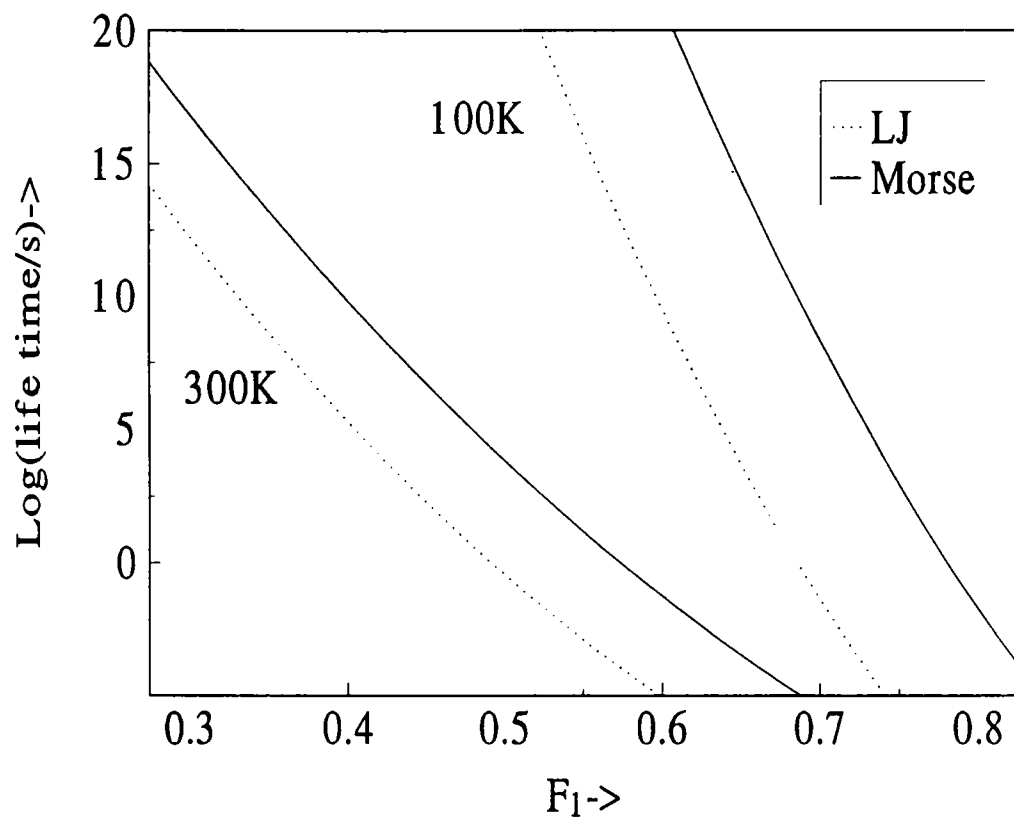
Figure 3.5: Plot of logarithm of the lifetime against the applied force, for polyethylene at 100K and 300K, using Morse and Lennard-Jones potentials.

The Fig. 3.4 compares the result for the Morse potential and the LJ potential (with the parameters ε and a_{LJ} chosen so as to reproduce the dissociation energy and force constant of the bond). The LJ potential leads to a much smaller lifetime, typically by a few orders of magnitude. This obviously means that the activation energy for breaking is sensitive to the actual potential that is used to fit / the way the fitting is done. The Fig. 3.6 gives plot of the quantum correction factor for the rate for a range of temperatures, estimated using the Morse potential. It is found that the quantum correction factor is always greater than unity – in all our calculations, quantum transition state theory leads to higher rates than classical transition state theory. The correction, however, is important only if the temperature is less than 150 K.

A general conclusion from the calculations is that at normal temperatures, if the force is somewhat greater than half the limiting force, then the bond would break in a matter of seconds. More specifically, we now look at the problem of breaking strain, to which quite a bit of attention is given in references [46] and [94]. We also did calculations for polyethylene, finding the lifetime of a bond as a function of the strain of the bond. Logarithm of the lifetime is plotted as a function of the amount of strain S (= the amount by which a bond is stretched). Fig. 3.7 plots logarithm of the lifetime against S. It is seen that the variation is exponential and that in a small range of S, the lifetime varies rapidly from 10^5 seconds to 10^{-5} seconds.

It has to be remembered that these results are for the lifetime of one bond. The polymer has a large number (N) of such bonds. All these bonds, except the ones near the two ends would have the same rate of breaking and therefore the rate of breaking of a polymer would be equal to N times the rate calculated by the Eq. (3.68). We now compare our results using the classical rate expression with the simulation results of Taylor and Oliveira [46]. For this we use the same conventions as they have used for choosing the units of energy, distance, time and temperature. i.e. energy in units of the binding energy ε, distance in units of the lattice parameter a_{LJ}, temperature in units of ε/k_B and time in units of the smallest period for phonon oscillations, $\tau_0 = 2\pi/\omega_0$ where $\omega_0 = 12\sqrt{\varepsilon/2ma_{LJ}^2}$. Fig. 3.8 compares logarithm of the lifetime for one bond calculated with the above theory
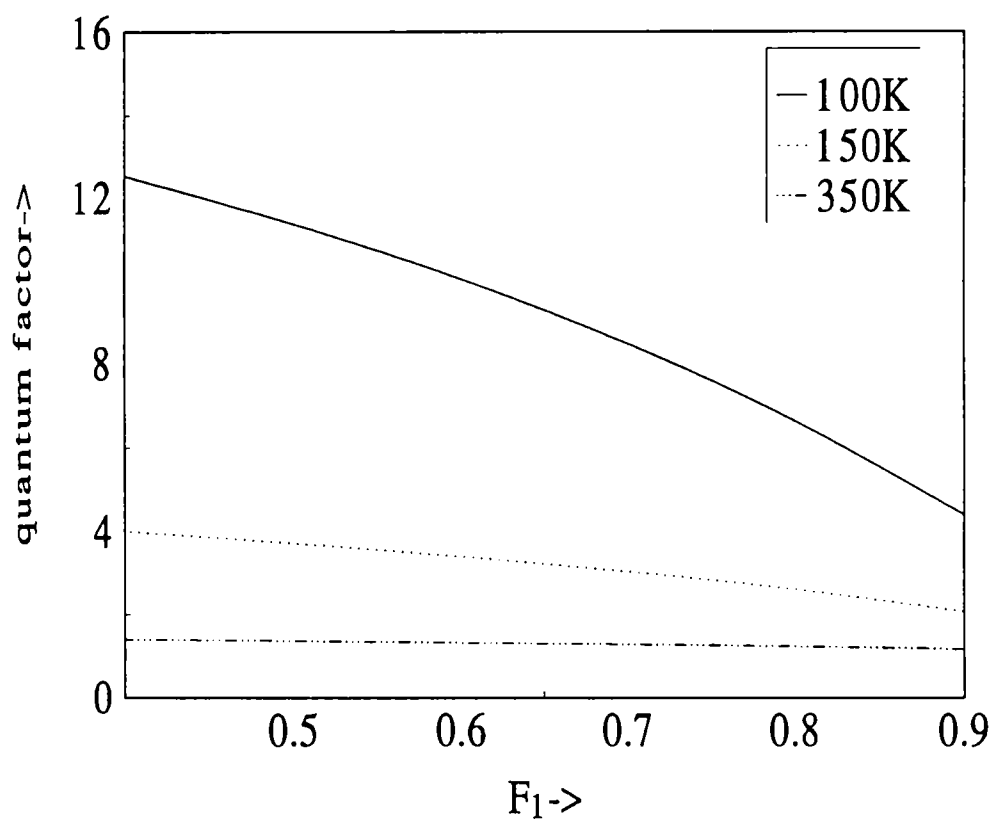
Figure 3.6: Plot of the quantum correction factor for the rate as a function of the force, for different temperatures. Calculations were done using the Morse potential.
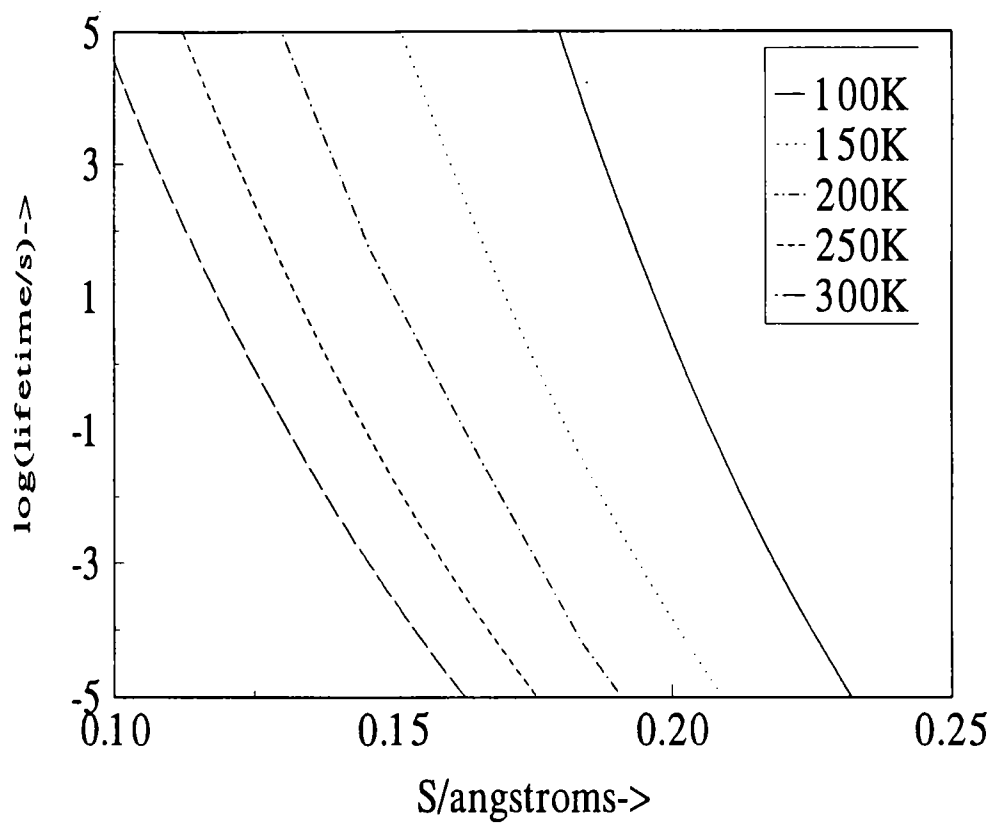
Figure 3.7: Logarithm of the (lifetime/s) of a single bond plotted against the strain for the Morse potential. S is the amount by which the bond is stretched. The plot shows that in a fairly narrow range of S the lifetime changes exponentially from 10^5 seconds to 10^{-5} seconds.
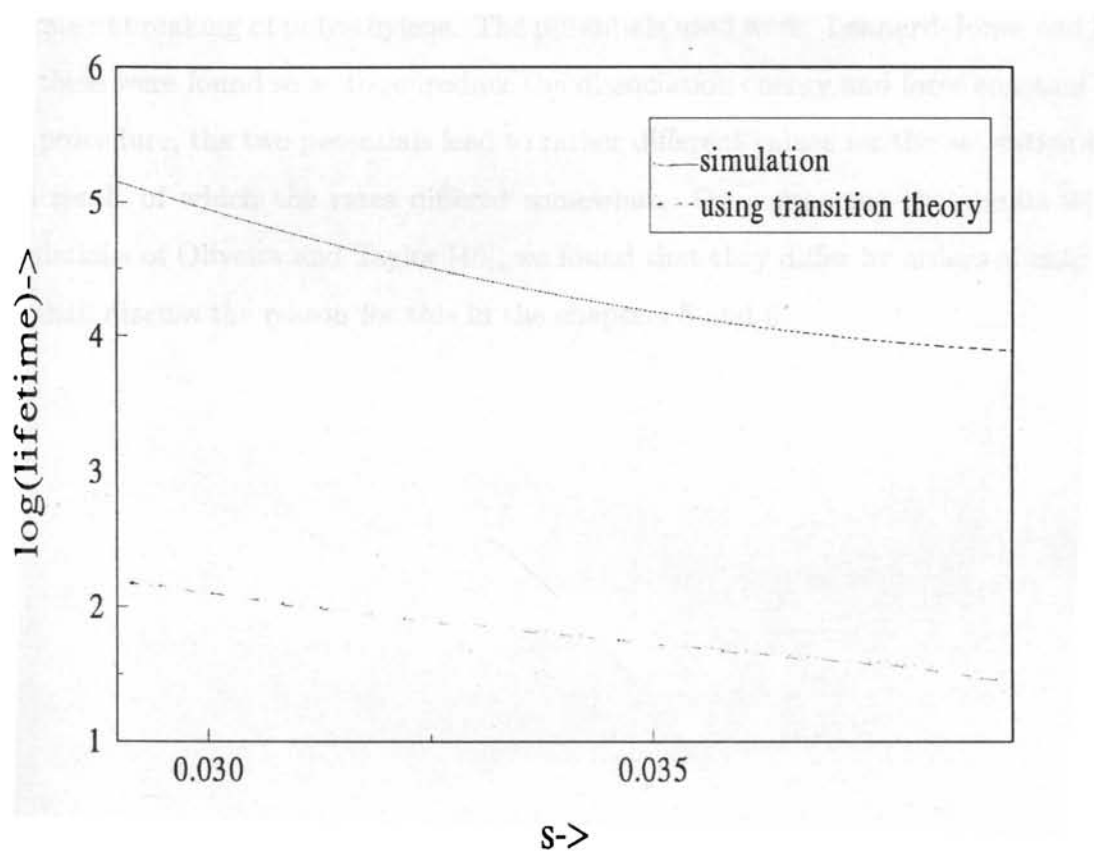
Figure 3.8: Plot of logarithm of the lifetime (dimensionless) against the strain for the Lennard Jones potential using simulation results of Oliveira and transition state thory. Energy is given in units of ε, distance in units of a_{LJ}, temperature in units of ε/k_B and time in units of τ_0. Here temperature $T = .05$.

th those of the simulation results. We find that result of transition state theory is

ghly 100–1000 times too large!

18 Conclusion

this chapter we derived an expression for the rate of breaking of a polymer using

ultidimensional quantum transition state theory. Using this expression, we calculated

e rate of breaking of polyethylene. The potentials used were: Lennard-Jones and Morse,

d these were found so as to reproduce the dissociation energy and force constant. With

is procedure, the two potentials lead to rather different values for the activation energy,

a result of which the rates differed somewhat. On comparing the results with the

mulations of Oliveira and Taylor [46], we found that they differ by orders of magnitude.

e shall discuss the reason for this in the chapters 5 and 6.

Chapter 4

Breaking when the Polymer
Contains a Foreign Atom in the
Main Chain

4.1   Introduction

In the last chapter we have applied the transition state theory for the breaking of a polymer. It is theoretically possible to get expression for the rate of breaking if there are diferent atoms present in the main chain of the polymer. In the experiments of Garnier et al. [152], they measured the single-polymer entropic elasticity and the single covalent bond force profile using two types of atomic force microscopes on a synthetic polymer molecule, polymethacrylic acid in water. The conventional atomic force microscope is well known for its good force resolution, allowing the investigation of an individual molecule's properties, such as entropic elasticity, [153, 154, 155] bond strength between biological receptors and ligands [156], and more recently, strength of a single covalent bond [157]. The conventional atomic force microscope allowed them to distinguish two types of interactions present in this system when doing force spectroscopic measurements: the first interaction is associated with adsorption sites of the polymer chains onto a bare gold surface, the second interaction is directly correlated to the rupture process of a single covalent bond. All

these bridging interactions allowed them to stretch the single polymer chain and to deter-mine the various factors playing a role in the elasticity of these molsecules. By optimizing the polymer length so as to fulfill the elastic stability conditions, they were able to map out the entire force profile associated with the cleavage of a single covalent bond. Exper-imental data coupled with molecular quantum mechanical calculations strongly suggest that the breaking bond is located at one end of the polymer chain.

Garnier's [152] experiment involved four types of bonds, Au–Au, Au–S, C–C and C–S bonds. It is difficult to get an analytic expression for the rate of breaking, though they have shown that breaking bonds are the Au–Au or Au–S bonds, both residing at the extremities of the polymer chain. In the following we try to derive an expression for the rate of breaking of a polymer which contains a foreign atom in the main chain itself but not towards the end. The model is given in Fig. 4.1.

4.2 Expression for the Rate

From chapter **3** we have the expression for the rate as

$$R = \frac{\Omega e^{-\beta E_a}}{4\pi} \sqrt{|p_0|} \prod_{l=1}^{\infty} p_l. \tag{4.1}$$

If we can neglect the quantum factor, the expression reduces to

$$R_{classical} = \frac{\Omega e^{-\beta E_a}}{4\pi} \sqrt{|p_0|}. \tag{4.2}$$

Here E_a represents the activation energy, Ω represents the frequency of the unstable mode and p_0 is the ratio of the product of the square of the frequencies in the equilibrium and transition states. Hence we need to calculate these.

4.2.1 Calculation of Activation Energy

Let the Morse parameters corresponding to this new bond be D_e' and a' and the mass of the new atom be M. We assume that the new bonds are weaker and hence when the force
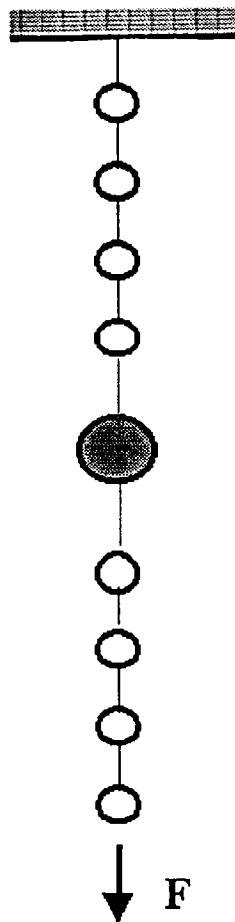
Figure 4.1: The model investigated consists of N units each of mass m, and another atom of mass M connected between the nth and $n+1^{th}$ units joined together by bonds obeying the Morse potential. It is fixed at one end and is acted upon by a force F acting at the other end.

; applied, one of these bonds will break. In Eq. (3.7) we have to add one more term i.e.

$$V(y') = D_e'(1 - e^{-a'y'})^2 - Fy'.$$ (4.3)

'here y' corresponds to the new atom. When the force is applied all bonds except the ew bond will be having $y = \frac{1}{a}\ln\left[\frac{2}{1+\sqrt{1-F_1}}\right]$. (see Eq. (3.10)). For the new bond the quilibrium extension will be $y_+' = \frac{1}{a'}\ln\left[\frac{2}{1+\sqrt{1-F_1'}}\right]$ and the transition state extension 'ill be $y_-' = \frac{1}{a'}\ln\left[\frac{2}{1-\sqrt{1-F_1'}}\right]$ where $F_1' = 2F/(D_e'a')$. The activation energy for the rocess is (see Eq. (3.12))

$$E_a' = D_e'\left[\sqrt{1-F_1'} + \frac{F_1'}{2}\ln\left\{\frac{1-\sqrt{1-F_1'}}{1+\sqrt{1-F_1'}}\right\}\right].$$ (4.4)

..2.2 Calculation of Ω

,s in the previous case we denote the displacement of the jth atom from its equilibrium osition by ξ_j and the new atom by ζ. We assume that the bond between the new atom nd the $(n+1)^{th}$ atom is breaking. Then, for small vibrations around the transition state, 'e have the Hamiltonian

$$l = \frac{1}{2}\sum_{j=1}^{N} m\,\dot{\xi}_j^2 + M\,\dot{\zeta}^2 + \frac{1}{2}\sum_{j=1\neq n+1}^{N} m\omega_0^2(\xi_j - \xi_{j-1})^2 + \frac{1}{2}M\omega_+^2(\zeta - \zeta_n)^2 - \frac{1}{2}M\omega_-^2(\zeta_{n+1} - \zeta)^2.$$ (4.5)

'he equations for the normal modes are :

$$m\omega^2\xi_{n-1}^0 = -m\omega_0^2\xi_{n-2}^0 + 2m\omega_0^2\xi_{n-1}^0 - m\omega_0^2\xi_n^0\,,$$

$$m\omega^2\xi_n^0 = -m\omega_0^2\xi_{n-1}^0 + m\omega_0^2\xi_n^0 + M\omega_+^2\xi_n^0 - M\omega_+^2\zeta^0\,,$$

$$M\omega^2\zeta^0 = -M\omega_+^2\xi_n^0 + M\omega_+^2\zeta^0 - M\omega_-^2\zeta^0 + M\omega_-^2\xi_{n+1}^0\,,$$

$$m\omega^2\xi_{n+1}^0 = M\omega_-^2\zeta^0 - M\omega_-^2\xi_{n+1}^0 + m\omega_0^2\xi_{n+1}^0 - m\omega_0^2\xi_{n+2}^0\,,$$ (4.6)

Dividing all equations by ω_0^2, third equation by M and other equations by m, and putting $\frac{\lambda^2}{\lambda_0^2} = \varpi^2$, $\frac{\omega_+^2}{\omega_0^2} = \gamma_+$ and $\frac{\omega_-^2}{\omega_0^2} = \gamma_-$ we get,

$$\varpi^2 \xi_{n-1}^0 = \xi_{n-2}^0 + 2\xi_{n-1}^0 - \xi_n^0 \ ,$$

$$\varpi^2 \xi_n^0 = -\xi_{n-1}^0 + \xi_n^0 + \frac{M}{m}\gamma_+\xi_n^0 - \frac{M}{m}\gamma_+\zeta^0 ,$$

$$\varpi^2 \zeta^0 = -\gamma_+\xi_n^0 + \gamma_+\zeta^0 - \gamma_-\zeta^0 + \gamma_-\xi_{n+1}^0 \ ,$$

$$\varpi^2 \xi_{n+1}^0 = \frac{M}{m}\gamma_-\zeta^0 - \frac{M}{m}\gamma_-\xi_{n+1}^0 + \xi_{n+1}^0 - \xi_{n+2}^0 \ ,$$

$$(4.7)$$

The above equations can be written in a matrix form as $\varpi^2 \xi^0 = D_{N+1}^{\ddagger} \xi^0$ where

$$D_{N+1}^{\ddagger} = \begin{bmatrix} 2 & -1 & & & & & \\ -1 & 2 & -1 & & & & \\ & -1 & 1+\frac{M}{m}\gamma_+ & -\frac{M}{m}\gamma_+ & & & \\ & & -\gamma_+ & \gamma_+ - \gamma_- & \gamma_- & & \\ & & & \frac{M}{m}\gamma_- & 1-\frac{M}{m}\gamma_- & -1 & - \\ & & & & -1 & 2 & - \\ - & - & - & - & - & - & - \end{bmatrix}. \qquad (4.8)$$

The frequencies of the modes are determined by the determinantal equation

$$\left| \varpi^2 I - D_{N+1}^{\ddagger} \right| = 0. \qquad (4.9)$$

where

$$\left[\varpi^2 \mathbf{I} - \mathbf{D}^\ddagger_{N+1}\right] = \tag{4.10}$$

$$\begin{bmatrix} \varpi^2 - \mathbf{D}_{n-1} & 1 & & & \\ 1 & \varpi^2 - 1 - \frac{M}{m}\gamma_+ & +\frac{M}{m}\gamma_+ & & \\ & \gamma_+ & \varpi^2 - \gamma_+ + \gamma_- & -\gamma_- & \\ & & -\frac{M}{m}\gamma_- & \varpi^2 - 1 + \frac{M}{m}\gamma_- & 1 \\ & & & 1 & \varpi^2 - \mathbf{D}_{N-n-1} \end{bmatrix}.$$

Using the partitioning technique we get

$$\left|\varpi^2 \mathbf{I} - \mathbf{D}^\ddagger_{N+1}\right| = \left|\varpi^2 \mathbf{I} - \mathbf{D}_{n-1}\right|\left|\varpi^2 \mathbf{I} - \mathbf{D}_{N-n-1}\right| \times$$

$$\begin{vmatrix} \varpi^2 - 1 - \frac{M}{m}\gamma_+ - G_{11}^{0,n-1} & +\frac{M}{m}\gamma_+ & \\ \gamma_+ & \varpi^2 - \gamma_+ + \gamma_- & -\gamma_- \\ -\frac{M}{m}\gamma_- & \varpi^2 - 1 + \frac{M}{m}\gamma_- - G_{11}^{0,N-n-1} \end{vmatrix} = 0. \tag{4.11}$$

The unstable frequency has an imaginary frequency. Hence we can look for a solution of the above equation with $\varpi^2 = -\overline{\Omega}^2$, with $\overline{\Omega}$ real. We take $G_{11}^{0,n-1} = G_{11}^{0,N-n-1} = G_{11}^0\left(-\overline{\Omega}^2\right)$. Thus the above equation reduces to

$$\begin{vmatrix} -\overline{\Omega}^2 - 1 - \frac{M}{m}\gamma_+ - G_{11}^0\left(-\overline{\Omega}^2\right) & +\frac{M}{m}\gamma_+ & \\ \gamma_+ & -\overline{\Omega}^2 - \gamma_+ + \gamma_- & -\gamma_- \\ -\frac{M}{m}\gamma_- & -\overline{\Omega}^2 - 1 + \frac{M}{m}\gamma_- - G_{11}^0\left(-\overline{\Omega}^2\right) \end{vmatrix} = 0.$$

$$\tag{4.12}$$

$\overline{\Omega}$ can be found out by solving the above equation. The frequency of the unstable mode can be calculated using $\Omega = \omega_+\overline{\Omega}$.

4.2.3 Calculation of p_0

We take p_l as

$$p_l = \frac{\left| l^2 + z^2 \mathbf{D}_{N+1} \right|}{\left| l^2 + z^2 \mathbf{D}_{N+1}^{\dagger} \right|} \tag{4.13}$$

where

$$\left| l^2 + z^2 \mathbf{D}_{N+1}^{\dagger} \right| = \tag{4.14}$$

$$\begin{vmatrix} l^2 + z^2 \mathbf{D}_{n-1} & -z^2 & & & & \\ -z^2 & l^2 + z^2 + z^2 \frac{M}{m}\gamma_+ & -z^2 \frac{M}{m}\gamma_+ & & & \\ & -z^2\gamma_+ & l^2 + z^2\gamma_+ - z^2\gamma_- & z^2\gamma_- & & \\ & & \frac{z^2 M}{m}\gamma_- & l^2 + z^2 - z^2 \frac{M}{m}\gamma_- & -z^2 & \\ & & & -z^2 & l^2 + z^2 \mathbf{D}_{N-n-1} \end{vmatrix} .$$

Using the partitioning technique we can write

$$p_l = \frac{\begin{vmatrix} l^2 + z^2 + z^2 \frac{M}{m}\gamma_+ - z^4 X_{n-1} & -z^2 \frac{M}{m}\gamma_+ & \\ -z^2\gamma_+ & l^2 + 2z^2\gamma_+ & -z^2\gamma_+ \\ & -\frac{z^2 M}{m}\gamma_+ & l^2 + z^2 + z^2 \frac{M}{m}\gamma_+ - z^4 X_{n-1} \end{vmatrix}}{\begin{vmatrix} l^2 + z^2 + z^2 \frac{M}{m}\gamma_+ - z^4 X_{n-1} & -z^2 \frac{M}{m}\gamma_+ & \\ -z^2\gamma_+ & l^2 + z^2\gamma_+ - z^2\gamma_- & z^2\gamma_- \\ & \frac{z^2 M}{m}\gamma_- & l^2 + z^2 - z^2 \frac{M}{m}\gamma_- - z^4 X_{n-1} \end{vmatrix}} .$$

$$\tag{4.15}$$

We can calculate p_0 by taking the limit of p_l in the limit $l \to 0$. It is found that

$$p_0 = \lim_{l \to 0} p_l = -\frac{\gamma_+}{\gamma_-} = -\frac{\omega_+^2}{\omega_-^2}. \tag{4.16}$$

4.3 An Example – Polyethylene Containing One Sulphur Atom

Using these expressions we have calculated the rate of breaking of polyethylene which contains one sulphur atom. We take the values of the Morse parameters D_e of C–C and
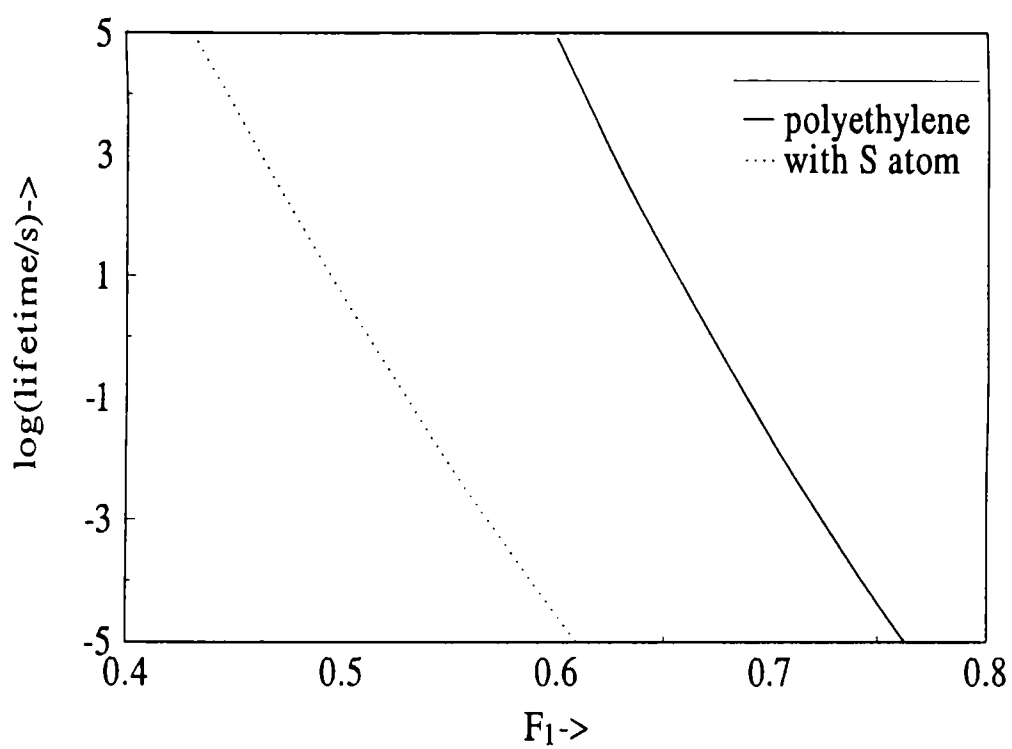
Figure 4.2: Plot of logarithm of lifetime against the applied force, for polyethylene and polyethylene containing one S atom at temperature 200K using the Morse potential.

C-S to be 360 kJ/mol and 250 kJ/ mol [158] and the force constants of C–C and C–S to be 280 N/m [46] and 300 N/m [159]. Fig. 4.2 compares the logarithm of life time in the two cases. We can see that the rate has been increased by many orders of magnitude. This is not surprising since there is a change in the exponential factor due to the decrease in the activation energy.

4.4 Conclusion

In this chapter, we derived an expression for the breaking of a polymer molecule which contains one foreign atom in the main chain of the molecule. Using this, we performed the calculations for polyethylene which contains a sulphur atom. The rate of breaking of the C-S bond was found to be three orders of magnitude greater than that of the C–C bond. This is due to the lower activation energy for breaking the C-S bond. If the polymer contains N C–C bonds, the probability of breaking will be N times that of a single bond. Usually, there are thousands of C–C bonds in the polymer and therefore, we expect that the probability of breaking a C–C bond will be greater than that of the C–S bond and it will be a C–C bond that is likely to break when a force is applied.

Chapter 5

Polymer-Plus-Reservoir Model

5.1 Introduction

In Chapter **3** we have seen that our transition state results for the breaking of the polymer do not agree with the simulation results of Oliveira and Taylor [46]. This is not very surprising because the simulations (see Eq. 3 in [46]) contain a damping force introduced to represent the interchange of kinetic energy between a monomer and its neighbours on other chains which is assumed to take the form of a viscous force. A random force term is also included to model the interaction with a thermal reservoir at temperature T. This force is generally assumed to have the property that its value at one position and time will be uncorrelated with that at other positions and times. We expect that our transition state theory results may agree with the simulations if we account for these two forces. This is not difficult to do, using the method given in Weiss [160]. A brief account of the method is given in the following section.

5.2 Classical Langevin Equation

A vast number of situations in nature can be adequately described by a system with one or few degrees of freedom in contact with a rather complex environment whose number of degrees of freedom tends to infinity. In the classical limit the dynamics is described by a

Langevin equation which contains a frictional force which is proportional to the velocity and an additional random force arising from the fluctuations of the environment. The fluctuating force $f(t)$ is usually taken to be Gaussian and is characterised completely by the ensemble averages

$$\langle f(t) \rangle = 0. \tag{5.1}$$

$$\langle f(t) f(t') \rangle = K_{cl}(t - t'). \tag{5.2}$$

For a white noise source, the frictional force is local in time, and the Langevin equation for a particle of mass M, having position q, has the Markovian form

$$M\,\ddot{q}\,(t) + M\gamma\,\dot{q}\,(t) + V'(q) = f(t) \tag{5.3}$$

where the stochastic force $f(t)$ is δ-correlated according to

$$K_{cl}(t - t') = 2M\gamma k_B T \delta(t - t') \tag{5.4}$$

where T is the temperature of the environment. The Langevin equation (5.3) describes a heavy Brownian particle M immersed in a fluid of light particles and driven by a systematic force $F = -V'(q)$, where $V(q)$ is an externally applied potential. The average effect on the heavy particle is contained in the friction force and the fluctuating force vanishes on an average. If the heat reservoir is a source of coloured noise as in many practical cases, the Langevin equation has the form

$$M\,\ddot{q}\,(t) + M \int_{-\infty}^{t} dt'\gamma(t - t')\,\dot{q}\,(t') + V'(q) = f(t). \tag{5.5}$$

5.3 System-Plus-Reservoir Models

For many complex systems we do not have a clear understanding of the microscopic origin of damping. However, sometimes one might be able to acquire knowledge of the power

spectrum of the stochastic force in the classical regime. Therefore, it is interesting to set up phenomenological system-plus-reservoir models which reduce in the appropriate limit to a description of the stochastic process in terms of a quasiclassical Langevin equation of the form (5.5). To make the elimination of the reservoir tractable, it is necessary to impose the restriction of linearity, i.e., any one degree of freedom of the environment is sufficiently weakly perturbed that it is permitted to put up a system-reservoir coupling which is linear in the reservoir coordinates. The simplest model of a dissipative quantum-mechanical system that one can envisage is a particle of mass M coupled linearly via its displacement q to a collection of Harmonic oscillators.

The Hamiltonian for the system is

$$H = \frac{p^2}{2M} + V(q) + \frac{1}{2} \sum_{\alpha=1}^{N} \left\{ \frac{p_\alpha^2}{m_\alpha} + m_\alpha \omega_\alpha^2 \left(x_\alpha - \frac{c_\alpha}{m_\alpha \omega_\alpha^2} q \right)^2 \right\}. \tag{5.6}$$

The above Hamiltonian has been used to model dissipation by many authors. A harmonic potental was used for $V(q)$ by Rubin [161] for classical systems and Senitzky [162], Ford et al. [163] and Ullersma [164] for quantum systems. Zwanzig [129] treated the model in the classical regime for a nonlinear potential. From this Hamiltonian, one derives the equation of motion as

$$M \ddot{q} + \frac{\partial V}{\partial q} + M \int_0^t \gamma(t - \tau) \dot{x}(\tau) d\tau = \xi(t) \tag{5.7}$$

(see Eq. (3.31) in [122]) with the heat bath prepared initially in thermal equilibrium, $\xi(t)$ obeying

$$\langle \xi(t)\xi(s) \rangle = k_B T \gamma(t - s)$$

and

$$\gamma(t) = \frac{1}{M} \sum_{i=1}^{N} \frac{c_i^2}{m_i \omega_i^2} \cos(\omega_i t).$$

Defining

$$J(\omega) = \frac{\pi}{2} \sum_{i=1}^{N} \frac{c_i^2}{m_i \omega_i} \delta(\omega - \omega_\alpha), \tag{5.8}$$

e can write

$$\gamma(t) = \frac{2}{\pi M} \int_0^\infty \frac{J(\omega)}{\omega} \cos(\omega t)\, d\omega \ . \tag{5.9}$$

n putting

$$J(\omega) = M\gamma\omega, \tag{5.10}$$

e get

$$\gamma(t) = \gamma \tag{5.11}$$

hich leads to ohmic damping, which is the case considered by Oliveira and Taylor [46]. his approach is very powerful and has been used extensively to solve the classical and quantum Kramers' problem [122].

.4 Polymer Molecule Connected to a Bath of Harmonic Oscillators

ow we consider a polymer molecule containing N monomer units. To introduce dissiation each unit is imagined to be connected to $\mathcal{N}$ harmonic oscillators ($\mathcal{N} \to \infty$). The lamiltonian for the system can be written as

$$H = \frac{1}{2}\sum_{j=1}^{N} M\,\dot{\xi}_j^2 + \frac{1}{2}\sum_{j=1\neq n+1}^{N} M\omega_+^2(\xi_j - \xi_{j-1})^2 - \frac{1}{2}M\omega_-^2(\xi_{n+1} - \xi_n)^2$$

$$+ \frac{1}{2}\sum_{i=1}^{\mathcal{N}}\sum_{j=1}^{N} m_{ij}\,\dot{x}_j^2 + \frac{1}{2}\sum_{i=1}^{\mathcal{N}}\sum_{j=1}^{N} m_{ij}\omega_{ij}^2 \left(x_{ij} - \frac{c_{ij}}{m_{ij}\omega_{ij}^2}\xi_j\right)^2 . \tag{5.12}$$

Ve can write the equations of motion for the system and find normal modes. The equaons for normal modes can be written in a matrix form as $\omega^2\zeta_0 = \mathcal{D}_N^\ddagger\, \zeta_0$. The matrix $\mathcal{D}_N^\ddagger$ e have to consider will be a $\mathbf{N} \times \mathbf{N}$ square matrix where $\mathbf{N} = N + N\mathcal{N}$; ζ_0 repesents the coordinate vector defined as $\zeta_0^\mathsf{T} = \begin{bmatrix} \xi_1^0 & \xi_2^0 & \cdots \xi_N^0 & x_{11}^0 & x_{12}^0 & \cdots & x_{21}^0 & x_{22}^0 & \cdots & \cdots & x_{N\mathcal{N}}^0 \end{bmatrix}$

here ζ_0^T is the tanspose of ζ_0. The angular frequencies of the normal modes for the trantion state are the eigen values of the matrix $\mathcal{D}_N^{\ddagger}$ and those for the equilibrium state re the eigen values of the matrix $\mathcal{D}_N^0$. If we take the bond between the atom numbers and $n+1$ to be the one that will break, (which is what is assumed in the Eq. (5.12)) ie two matrices differ only for four elements which are $(n,n)^{th}$, $(n,n+1)^{th}$, $(n+1,n)^{th}$ id $(n+1,n+1)^{th}$ elements. The matrix $\mathcal{D}_N^{\ddagger}$ would have one unstabe mode, which is ie reaction coordinate. The frequencies are determined by the determinental equation $^2 - \mathcal{D}_N^{\ddagger}\big| = 0$, where

$$\mathcal{D}_N^{\ddagger} = \begin{bmatrix} \mathbf{A} & \mathbf{B} \\ \mathbf{C} & \mathbf{D} \end{bmatrix}. \tag{5.13}$$

he matrices $\mathbf{A}$, $\mathbf{B}$, $\mathbf{C}$ and $\mathbf{D}$ are defined as $\mathbf{A} =$

$$\begin{bmatrix} 2\omega_+^2 + \sum_{i=1}^{\mathcal{N}} \frac{c_{i1}^2}{Mm_{i1}\omega_{i1}^2} & -\omega_+^2 & - & - & - \\ -\omega_+^2 & - & - & - & - \\ - & - & \omega_+^2 - \omega_-^2 + \sum_{i=1}^{\mathcal{N}} \frac{c_{in}^2}{Mm_{in}\omega_{in}^2} & \omega_-^2 & - \\ - & - & \omega_-^2 & \omega_+^2 - \omega_-^2 + \sum_{l=1}^{\mathcal{N}} \frac{c_{in+1}^2}{Mm_{i,n+1}\omega_{i,n+1}^2} & - \\ - & - & - & - & - \end{bmatrix}$$

$$\mathbf{B} = \begin{bmatrix} \mathbf{B}_1 & 0 & - & - \\ 0 & \mathbf{B}_2 & 0 & - \\ - & - & - & - \\ - & - & 0 & \mathbf{B}_N \end{bmatrix}, \tag{5.14}$$

$$\mathbf{C} = \begin{bmatrix} \mathbf{C}_1 & 0' & - & - \\ 0' & \mathbf{C}_2 & 0' & - \\ - & - & - & - \\ - & - & 0' & \mathbf{C}_N \end{bmatrix},$$

ınd

$$
\mathbf{D} = \begin{bmatrix} \mathbf{D}_1 & \mathbf{0}^\dagger & - & - \\ \mathbf{0}^\dagger & \mathbf{D}_2 & \mathbf{0}^\dagger & - \\ - & - & - & - \\ - & - & \mathbf{0}^\dagger & \mathbf{D}_N \end{bmatrix}.
$$

ʋhere the matrices $\mathbf{B}_i$, $\mathbf{C}_i$ and $\mathbf{D}_i$ are defined as

$$
\mathbf{B}_i = \begin{bmatrix} -\frac{c_{1i}}{M} & -\frac{c_{2i}}{M} & - & - & -\frac{c_{\mathcal{N}i}}{M} \end{bmatrix},
$$

$$
\mathbf{C}_i^\mathsf{T} = \begin{bmatrix} -\frac{c_{1i}}{m_{1i}} & -\frac{c_{2i}}{m_{2i}} & - & - & -\frac{c_{\mathcal{N}i}}{m_{\mathcal{N}i}} \end{bmatrix},
$$

$$
\mathbf{D}_i = \begin{bmatrix} \omega_{1i}^2 & 0 & - & - & - \\ 0 & \omega_{2i}^2 & - & - & - \\ - & - & - & - & - \\ - & - & - & - & - \\ - & - & - & - & \omega_{\mathcal{N}i}^2 \end{bmatrix}.
$$

Ɔ is a row matrix of order $\mathcal{N}$ given by $\mathbf{0} = \begin{bmatrix} 0 & 0 & - & - & 0 \end{bmatrix}$, $\mathbf{0}' = \mathbf{0}^\mathsf{T}$ and $\mathbf{0}^\dagger$ is an $\mathcal{N} \times \mathcal{N}$ ʑero matrix.

We can write

$$
\left| \omega^2 - \mathcal{D}_\mathbf{N}^\dagger \right| = \det \begin{bmatrix} \overline{\mathbf{A}} & \overline{\mathbf{B}} \\ \hline \overline{\mathbf{C}} & \overline{\mathbf{D}} \end{bmatrix} = \det \left[\overline{\mathbf{A}} - \overline{\mathbf{B}}\,\overline{\mathbf{D}}^{-1}\overline{\mathbf{C}} \right] \times \det \overline{\mathbf{D}}. \tag{5.15}
$$

$\overline{\mathbf{D}}^{-1}$ is a diagonal matrix with elements of the form $\frac{1}{\omega^2 - \omega_{ij}^2}$. $\overline{\mathbf{B}}\,\overline{\mathbf{D}}^{-1}\overline{\mathbf{C}}$ is a $N \times N$ square matrix with only diagonal elements of the form $\sum\limits_{i=1}^{\mathcal{N}} \dfrac{c_{ij}^2}{M m_{ij}(\omega^2 - \omega_{ij}^2)}$. To find the normal modes, one has to put the left hand side of Eq. (5.15) equal to zero and solve for ω. Since $\det \overline{\mathbf{D}}$ cannot be zero, the other determinant should be equal to zero. i.e.,

$$
\begin{vmatrix}
\omega^2 - 2\omega_+^2 - \sum_{i=1}^{N} \frac{c_{i1}^2}{Mm_{i1}}\left(\frac{1}{\omega_{i1}^2} + \frac{1}{\omega^2 - \omega_{i1}^2}\right) & \omega_+^2 & 0 & - \\[2ex]
\omega_+^2 & \omega^2 - 2\omega_+^2 - \sum_{i=1}^{N} \frac{c_{i1}^2}{Mm_{i2}}\left(\frac{1}{\omega_{i2}^2} + \frac{1}{\omega^2 - \omega_{i2}^2}\right) & \omega_+^2 & - \\[2ex]
- & \omega_+^2 & - & - \\[2ex]
- & - & & - \quad -
\end{vmatrix} = 0.
$$

$$\qquad\qquad\qquad (5.16)$$

5.4.1 Calculation of Ω

For this we have to solve Eq. (5.16) with $\omega = i\Omega$. Now the diagonal elements can be written in a simple form since

$$
\frac{1}{\omega_{ij}^2} + \frac{1}{-\Omega^2 - \omega_{ij}^2} = \frac{\Omega^2}{(\Omega^2 + \omega_{ij}^2)\omega_{ij}^2}. \qquad (5.17)
$$

We write

$$
\sum_{i=1}^{N} \frac{c_{ij}^2}{Mm_{ij}(\Omega^2 + \omega_{ij}^2)\omega_{ij}^2} = \frac{2}{\pi M}\int_0^\infty \frac{J_j(\omega)}{\omega(\omega^2 + \Omega^2)}d\omega \qquad (5.18)
$$

where

$$
J_j(\omega) = \frac{\pi}{2}\sum_{i=1}^{N} \frac{c_{ij}^2}{m_{ij}\omega_{ij}}\delta(\omega - \omega_{ij}).
$$

Assuming $J_j(\omega) = M\gamma\omega$, to have ohmic friction, we get

$$
\sum_{i=1}^{N} \frac{c_{ij}^2}{Mm_{ij}(\Omega^2 + \omega_{ij}^2)\omega_{ij}^2} = \frac{2}{\pi M}\int_0^\infty \frac{J_j(\omega)}{\omega(\omega^2 + \Omega^2)}d\omega = \gamma\frac{2}{\pi}\int_0^\infty \frac{1}{(\omega^2 + \Omega^2)}d\omega = \gamma\Omega.
$$

Now we write Eq. (5.16) with $\omega = i\Omega$.

$$\det \mathcal{D} = \begin{vmatrix} -\Omega^2 - 2\omega_+^2 - \Omega\gamma & \omega_+^2 & 0 & - & - & - \\ - & - & - & - & - & - \\ & \omega_+^2 & -\Omega^2 - \omega_+^2 + \omega_-^2 - \Omega\gamma & -\omega_-^2 & & \\ & & -\omega_-^2 & -\Omega^2 - \omega_+^2 + \omega_-^2 - \Omega\gamma\,\omega_+^2 & & \\ & & & & \,'_- & \\ - & - & - & - & - & - \end{vmatrix} = 0$$

$$(5.19)$$

where $\mathcal{D}$ is a $N \times N$ square matrix. We take the Green's matrix $G^0 = [-\Omega^2 - \mathbf{D}_n]^{-1}$ where $\mathbf{D}_n$ is the $n \times n$ matrix having the form

$$\mathbf{D}_n = \begin{bmatrix} 2\omega_+^2 + \Omega\gamma & -\omega_+^2 & & \\ -\omega_+^2 & 2\omega_+^2 + \Omega\gamma & -\omega_+^2 & \\ & -\omega_+^2 & 2\omega_+^2 + \Omega\gamma & \\ - & - & - & - \end{bmatrix}.$$

As discussed in chapter 3 if G_{11}^0 represents the first diagonal element of the Green's matrix we have the relation

$$G_{11}^0 = \frac{1}{-\Omega^2 - 2\omega_+^2 - \Omega\gamma - \omega_+^4 G_{11}^0}$$

$$(5.20)$$

which on solving gives

$$G_{11}^0 = \frac{(-\Omega^2 - 2\omega_+^2 - \Omega\gamma) + \sqrt{(-\Omega^2 - 2\omega_+^2 - \Omega\gamma)^2 - 4\omega_+^4}}{2\omega_+^4}.$$

$$(5.21)$$

As in chapter 3 we simplify Eq. (5.19) using the partition technique and we get

$$\begin{vmatrix} -\Omega^2 - \omega_+^2 + \omega_-^2 - \Omega\gamma - G_{11}^0 \omega_+^4 & -\omega_-^2 \\ -\omega_-^2 & -\Omega^2 - \omega_+^2 + \omega_-^2 - \Omega\gamma - G_{11}^0 \omega_+^4 \end{vmatrix} = 0.$$

$$(5.22)$$

On solving, we find

$$\Omega = \frac{\sqrt{2\omega_-^2 + \omega_+^2}\sqrt{16\omega_-^4 + 2\gamma^2\omega_-^2 + \gamma^2\omega_+^4} - \gamma(2\omega_-^2 + \omega_+^2)}{2(2\omega_-^2 + \omega_+^2)}. \qquad (5.23)$$

5.4.2 Calculation of p_0

p_0 is the ratio of the product of the square of the frequencies in the equilibrium and transition states. But the squares of the frequencies of the normal modes in the transition state are the eigen values of the matrix $\mathcal{D}_N^\ddagger$ and we know that the product of the eigenvalues of a matrix is equal to the value of its determinant. Now we try to evaluate $\det \mathcal{D}_N^\ddagger$. The matrix $\mathcal{D}_N^\ddagger$ is defined by Eqs. (5.13) and (5.14). We use the identity $\det \begin{bmatrix} \mathbf{A} & \mathbf{B} \\ \mathbf{C} & \mathbf{D} \end{bmatrix} = \det \begin{bmatrix} \mathbf{A} - \mathbf{B}\mathbf{D}^{-1}\mathbf{C} \end{bmatrix} \times \det \mathbf{D}$. Now $\mathbf{A}$ is an $N \times N$ matrix, $\mathbf{B}$ is an $N \times (\mathcal{N}N)$ matrix, $\mathbf{C}$ is an $(\mathcal{N}N) \times N$ matrix and $\mathbf{D}$ is an $(\mathcal{N}N) \times (\mathcal{N}N)$ matrix. The matrix $\mathbf{B}\mathbf{D}^{-1}\mathbf{C}$ will be an $N \times N$ matrix given by

$$\mathbf{B}\mathbf{D}^{-1}\mathbf{C} = \begin{bmatrix} \sum_{i=1}^{\mathcal{N}} \frac{c_{i1}^2}{Mm_{i1}\omega_{1i}^2} & 0 & & \\ 0 & \sum_{i=1}^{\mathcal{N}} \frac{c_{i2}^2}{Mm_{i2}\omega_{i2}^2} & & \\ - & - & - & - \\ - & - & - & \sum_{i=1}^{\mathcal{N}} \frac{c_{i1}^2}{Mm_{iN}\omega_{iN}^2} \end{bmatrix}.$$

Hence the matrix $\mathbf{A} - \mathbf{B}\mathbf{D}^{-1}\mathbf{C}$ will be the same as the matrix if there is no friction. Now we have to find only the ratio of the determinants. $\det \mathbf{D}$ is the same for both the numerator and denominator. Hence we see that the value of p_0 is the same as the case where there is no friction. i.e.

$$p_0 = -\frac{\omega_+^2}{\omega_-^2}.$$

The above result and Eq. (5.23) gives

$$R_{classical} = \frac{1}{4\pi}\frac{\omega_+}{\omega_-}\frac{\sqrt{2\omega_-^2 + \omega_+^2}\sqrt{16\omega_-^4 + 2\gamma^2\omega_-^2 + \gamma^2\omega_+^4} - \gamma(2\omega_-^2 + \omega_+^2)}{2(2\omega_-^2 + \omega_+^2)}e^{-\beta E_a}. \qquad (5.24)$$
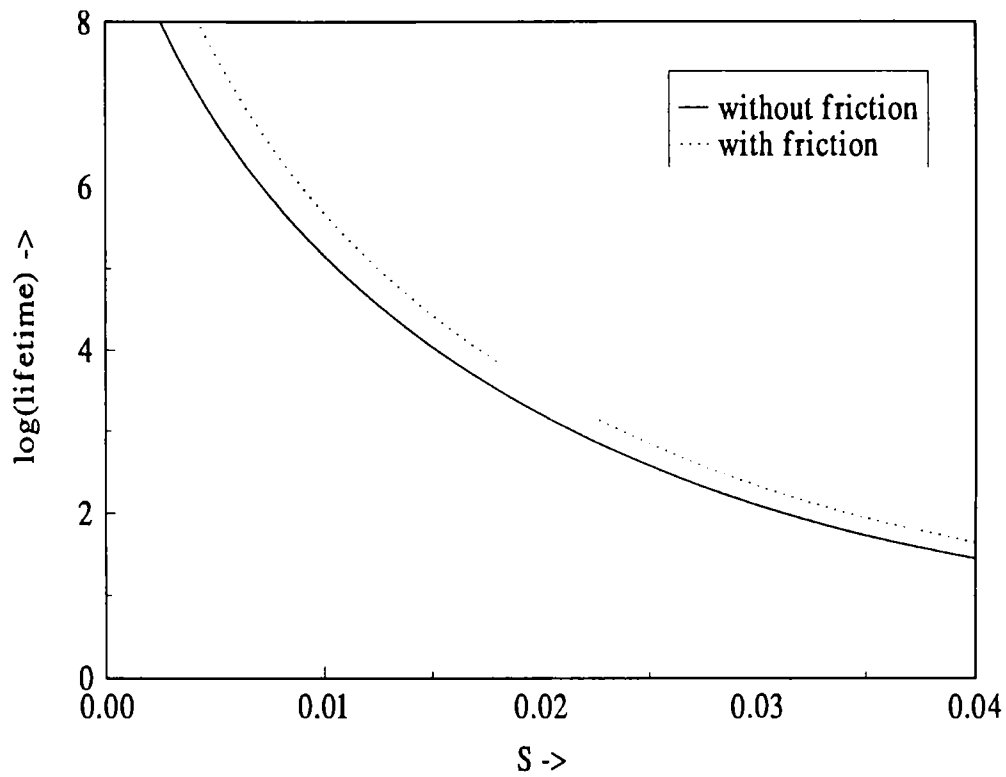
Figure 5.1: Plot of logarithm of the lifetime against the strain for the Lennard Jones potential for the two cases: without damping (solid curve) and with damping (dotted curve). Energy is given in units of ε, distance in units of a_{LJ}, temperature T in units of ε/k_B and time in units of τ_0. Here $T = .05$ and $\gamma = 0.25\omega_0$. The figure shows that damping can increase the lifetime by only one order of magnitude.
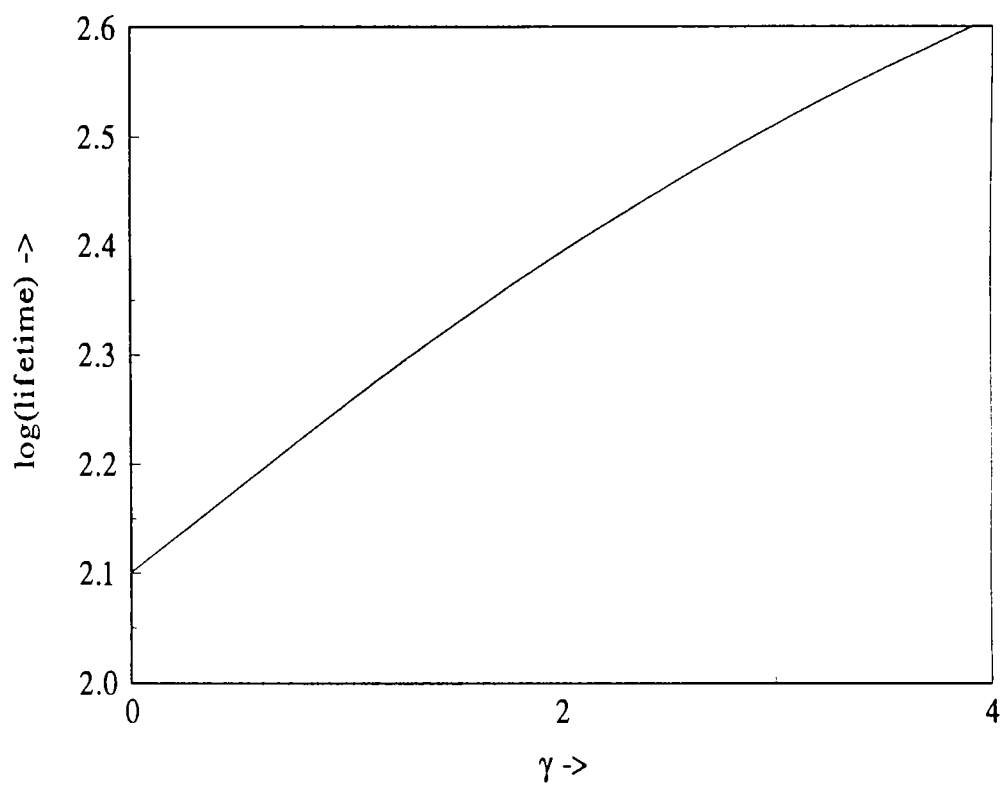
Figure 5.2: Variation of the lifetime against the viscosity parameter γ in units of $\omega_0/2\pi$. Energy is given in units of ε, distance in units of a_{LJ}. temperature T in units of ε/k_B and time in units of τ_0. Here $T = .05$ and $S = .03$.

Using this expression we have calculated the rate of breaking of the polymer.We use the same units of energy, distance, time and temperature that Oliveira and Taylor [46] have made. i.e. energy in units of the binding energy ε, distance in units of the lattice parameter a_{LJ}, temperature in units of ε/k_B and time in units of the smallest period for phonon oscillations, $\tau_0 = 2\pi/\omega_0$ where $\omega_0 = 12\sqrt{\varepsilon/2ma_{LJ}^2}$. Fig. 5.1 shows a plot of logarithm of the lifetime for one bond calculated with the above theory. The viscosity parameter γ is taken to be equal to $0.25\omega_0$ as in the simulations of Oliveira and Taylor [46]. We can see that though the lifetime increases, the increase is very small, especially, in the large force regimes. Fig. 5.2 gives the variation of the life time with the viscosity parameter γ in units of $\omega_0/2\pi$.

5.5   Conclusion

Oliveira and Taylor [46] included friction from the surroundings in the simulations. Therefore, in our transition state theory approach, it is necessary to include friction. For this, we assumed that each atom in the chain is coupled to a collection of harmonic oscillators, with the coupling adjusted so that each atom is subject to Ohmic friction and the noise. Using this approach, we calculated the rate of breaking of the polymer. Although the rates were found to be lower, the results still were not in agreement with the simulations. The reason for this is that the bonds, once broken can still come back and heal. In the next chapter, we analyse this process.

Chapter 6

Beyond Transition State Theory: Rate of Separation of the Broken Ends

6.1 Introduction

In the third chapter we have seen that the rates calculated using quantum transition state theory do not agree with the simulation results of Oliveira and Taylor [46]. We incorporated damping into the system in the previous chapter by introducing the idea that each unit of the polymer is connected to a large number of harmonic oscillators. Though we found that the rate is decreased, the agreement with the simulations is still poor.

In this chapter we look more closely at the actual dynamics taking place during the breaking process. The breaking of the polymer requires activation energy to be possessed by a bond to dissociate, the probability of this being $e^{-\beta E_a}$. If thermal fluctuations give the bond the energy E_a, then it can dissociate, with a frequency $\frac{\Omega}{4\pi}\sqrt{|p_0|}$ (see the Eq. (3.66)). The time of crossing the barrier is $t_{cross} = 1/\left(\frac{\Omega}{4\pi}\sqrt{|p_0|}\right)$. However, even if crossing (i.e. the bond is broken) has occurred, it is not necessary that the reaction should occur. Once the crossing has occurred, the two ends have to separate by a minimum distance, within

which it is possible for the broken ends to come back and heal the bond. We now calculate the time required for the two broken ends to separate by this minimum distance. The two broken ends separate from one another by translational motion. The potential energy of the system decreases as a function of the separation of the two ends and since the bond is already broken, this decrease is mostly due to the externally applied force. This is obviously linearly dependent on the separation. Denoting the minimum distance as d_c, we find the average time required to move apart by this distance.

6.2 Connection with Brownian Particle

The classical Hamiltonian describing the motion is:

$$H = \frac{1}{2}\sum_{j=1}^{N} m\,\dot{\xi}_j^2 + \frac{1}{2}\sum_{j=1 \neq n}^{N} m\omega_+^2(\xi_j - \xi_{j-1})^2 - \alpha(\xi_n - \xi_{n-1}). \tag{6.1}$$

In the above, α is the slope of the potential energy curve, in the region where the potential is linear in distance of separation (i.e. linear in $(b + \xi_n - \xi_{n-1})$). On looking at the equations of motion, one realizes that they separate into two uncoupled parts, one for each broken part. It is enough to analyze only one of them, as the behavior of the other is identical (provided both the chains are long). So we consider the part of the Hamiltonian corresponding to $j \geq n$. Renumbering the atoms $(n, n+1, n+2, \dots)$ as $(0, 1, 2 \dots)$, and taking the chain to be very long $(N \to \infty)$, we can write the Hamiltonian as

$$H_{broken} = \frac{1}{2}\sum_{j=0}^{\infty} m\,\dot{\xi}_j^2 + \frac{1}{2}\sum_{j=1}^{\infty} m\omega_+^2(\xi_j - \xi_{j-1})^2 - \alpha\xi_0. \tag{6.2}$$

The problem now is to calculate the time that it takes ξ_0 to exceed the value ξ_c given that its initial value was zero, and that the chain is at a temperature T. Obviously, as both the ends are executing translational motion, the distance that each one has to cover would be $\xi_c = d_c/2$. The time should be determined mainly by the long wavelength modes of the chain. To describe these modes, one can use a continuum approximation to the above Hamiltonian. The continuum version has the advantage that one can obtain analytical

results. The Hamiltonian is

$$H_{broken} = \frac{1}{2}\rho \int_0^\infty dx \xi_t(x,t)^2 + \frac{1}{2}\mathcal{T} \int_0^\infty dx \xi_x(x,t)^2 - \alpha\xi(0,t). \tag{6.3}$$

In the above, subscripts t and x indicate partial differentiation with respect to these variables, ρ is the density of the chain per unit length ($= m/b_+$, b_+ being the length of a stretched bond, at its equilibrium position) and $\mathcal{T} = mb_+\omega_+^2$ is the tension in the chain. The speed of sound in the chain is given by $c = \sqrt{\mathcal{T}/\rho}$. We imagine that $\xi(0,t) = 0$ until $t = 0$, with the rest of the chain at thermal equilibrium, appropriate to a temperature T. Up to this time, the last term in the Eq. (6.3) is not present in the Hamiltonian. At $t = 0$, the chain is broken, and the last term is now present, and it represents the fact that the chain can lower its potential energy by moving its end. Writing the equation of motion for the string gives forced wave equation

$$\rho\xi_{tt}(x,t) = \mathcal{T}\xi_{xx}(x,t) + \alpha\delta(x). \tag{6.4}$$

To solve the above equation, we use transform techniques. We first define the Fourier cosine transform of $\xi(x,t)$ by

$$\overline{\xi}(w,t) = \int_0^\infty dx \xi(x,t)\cos(wx). \tag{6.5}$$

We take the Fourier cosine transform of equation (6.4) to get

$$\rho\overline{\xi}_{tt}(w,t) + \mathcal{T}w^2\overline{\xi}(w,t) = \alpha - \mathcal{T}\xi_x(0,t). \tag{6.6}$$

Once the chain is broken, the end of the chain is not under strain and hence we put $\left(\frac{\partial\xi(x,t)}{\partial x}\right)_{x=0} = 0$. Now we introduce the Laplace transform of $\overline{\xi}(w,t)$ by

$$\Xi(w,s) = \int_0^\infty dt \overline{\xi}(\omega,t)e^{-st}. \tag{6.7}$$

This obeys the equation

$$\left(\rho s^2 + \mathcal{T}w^2\right)\overline{\Xi}(w,s) = \frac{\alpha}{s} + \rho\overline{\xi}_t(w,0) + \rho s\overline{\xi}(w,0),\tag{6.8}$$

where

$$\overline{\xi}_t(w,0) = \int_0^\infty dx\,\xi_t(x,0)\cos(wx).\tag{6.9}$$

Solving for $\overline{\Xi}(w,s)$

$$\overline{\Xi}(w,s) = \frac{1}{(\rho s^2 + \mathcal{T}w^2)}\left(\frac{\alpha}{s} + \rho\overline{\xi}_t(w,0) + s\rho\overline{\xi}(w,0)\right).$$

Taking the inverse transforms leads to

$$\xi(x,t) = \mathcal{L}^{-1}\left[\frac{2}{\pi}\int_0^\infty dw\cos(wx)\frac{1}{(\rho s^2 + \mathcal{T}w^2)}\left(\frac{\alpha}{s} + \rho\overline{\xi}_t(w,0) + s\rho\overline{\xi}(w,0)\right)\right]\tag{6.10}$$

where $\mathcal{L}^{-1}$ stands for the Laplace inverse. As we are interested only in the motion of the end of the chain, we put $x = 0$ in the above to get

$$\xi(0,t) = \frac{\alpha}{\sqrt{\mathcal{T}\rho}}t + \zeta(t)\tag{6.11}$$

with

$$\zeta(t) = \zeta_1(t) + \zeta_2(t).\tag{6.12}$$

Here

$$\zeta_1(t) = \frac{2}{\pi}\int_0^\infty dw\overline{\xi}(w,0)\mathcal{L}^{-1}\frac{\rho s}{(\rho s^2 + \mathcal{T}w^2)}$$

$$= \frac{2}{\pi}\int_0^\infty dw\overline{\xi}(w,0)\cos(c\omega t).$$

Thus

$$\zeta_1(t) = \xi(x,0)_{x=ct}\tag{6.13}$$

and

$$\zeta_2\left(t\right) = \frac{2}{\pi} \int_0^\infty dw \bar{\xi}_t\left(w,0\right) \mathcal{L}^{-1} \frac{\rho}{\left(\rho s^2 + \mathcal{T}w^2\right)} = \frac{2}{\pi} \int_0^\infty dw \bar{\xi}_t\left(w,0\right) \frac{\sin\left(cwt\right)}{cw}. \qquad (6.14)$$

The equation (6.11) shows that the broken end of the chain undergoes translational motion with a uniform velocity equal to $\frac{\alpha}{\sqrt{\mathcal{T}\rho}}$. In addition, it undergoes diffusive motion, due to thermal fluctuations which is represented by the term $\zeta\left(t\right)$. In the appendix, we calculate the correlation function for this and show that

$$\left\langle \zeta\left(t\right)\zeta\left(t_1\right)\right\rangle = \frac{2k_B T}{\rho c} \min\left(t,t_1\right). \qquad (6.15)$$

The above correlation function is just that for Brownian motion, with a diffusion coefficient $D = \frac{k_B T}{\rho c}$. Thus the motion of the end of the chain is the same as that of a Brownian particle of mass unity, drifting with a velocity v in the positive direction, having the diffusion coefficient D.

6.3 The First Passage Time:

In our problem we need the average time that such a Brownian particle spends in a region with $\xi < \xi_c$ before going out for the first time from this region. It is given that it started at $\xi = 0$ and is drifting in the positive direction with a velocity v towards the point $\xi_c \left(> 0\right)$ and it is also undergoing diffusive motion. This is essentially a first passage problem and may be solved by finding the probability density $P\left(\xi,t\right)$ for the particle to be at ξ at the time t, given that it was at $\xi = 0$ at the time $t = 0$. $P\left(\xi,t\right)$ obeys the diffusion equation

$$P_t\left(\xi,t\right) = DP_{\xi\xi}\left(\xi,t\right) - vP_\xi\left(\xi,t\right). \qquad (6.16)$$

This has to be solved subject to the condition that $P(\xi_c, 0) = 0$. Then, one has to calculate the survival probability

$$P_{surv}(t) = \int_{-\infty}^{\xi_c} d\xi P(\xi, t) \tag{6.17}$$

from which the average time that it spends in the region may be obtained as

$$\langle t \rangle = \int_0^\infty dt P_{surv}(t). \tag{6.18}$$

To solve the equation (6.16) we use Laplace transform techniques. We first define $\overline{P}(\xi, s) = \int_0^\infty dt P(\xi, t) e^{-st}$. It obeys the differential equation

$$s\overline{P}(\xi, s) - D\overline{P}_{\xi\xi}(\xi, s) + v\overline{P}_\xi(\xi, s) = \delta(\xi). \tag{6.19}$$

This equation is to be solved, subject to the condition that $\overline{P}(\xi_c, s) = 0$. We give the details of the solution in the appendix. The solution is found to be

$$\overline{P}(\xi, s) = \frac{\exp\left[\frac{v\xi - |\xi|\sqrt{v^2 + 4Ds}}{2D}\right]}{\sqrt{v^2 + 4Ds}} - \frac{\exp\left[\frac{v\xi - (\xi_c + |\xi - \xi_c|)\sqrt{v^2 + 4Ds}}{2D}\right]}{\sqrt{v^2 + 4Ds}}. \tag{6.20}$$

From this, we obtain the Laplace transform of the survival probability

$$\overline{P}(s) = \int_{-\infty}^{+\infty} d\xi \overline{P}(\xi, s) = \frac{1}{s}\left[1 - \exp\left[\frac{v\xi_c - \xi_c\sqrt{v^2 + 4Ds}}{2D}\right]\right]. \tag{6.21}$$

The average survival time is then

$$\langle t \rangle = \int_0^\infty P(t)\, dt$$

$$= \lim_{t \to 0} \int_0^\infty e^{-st} P(t)\, dt = \lim_{s \to 0} \overline{P}(s) = \xi_c/v.$$

In the last step we have used the L' Hospital's rule. Interestingly, this is just the time that one would have estimated neglecting the diffusive motion of the chain end [165]. Now,

Chapter 6. Beyond Transition State Theory: Rate of Separation of the Broken Ends99

taking $\xi_c = d_c/2$ and using $v = \frac{\alpha}{\sqrt{T}\rho}$, we find the average passage time of the two ends, over the distance d_c to be

$$\langle t \rangle = d_c \rho c / (2\alpha).$$

(6.22)

Now one has the problem of choosing the value of d_c. The simplest estimate that one can make is that the ends should be separated by a distance equal to the stable bond length. Let b_c represents the position corresponding to the bond length such that energy of the final state is equal to the energy of the initial state (see Fig. 6.1). We take the potential between b_- and b_c to be linear, neglecting the curved portion near the top of the barrier. Let $l = b_c - b_-$. Then, the slope α of the potential is given by $\alpha = \Delta E/l$, which leads to the crossing time as: $\langle t \rangle = l d_c \rho c / (2\Delta E)$. Using this expression, we have estimated the time of crossing the distance d_c for the Lennard Jones model. This is compared with the time of crossing the barrier ($= 1$/prefactor of the rate in the classical equation) in Fig.6.2. The results show that in the small force regime, the first passage rate is considerably lower than that of the crossing rate and hence is the rate determining step. The actual crossing frequency may be obtained by adding the two times and then taking its inverse. The logarithm of the lifetime so obtained is plotted in Fig.6.3. On comparing the results with those of the simulation, we find that the agreement is still poor. The modification in the rate is small and is still about 100 times the result of the simulation! What could be the reason for this?

6.4 First Passage with Friction

While our calculations till now have considered the vibrational motion of the atoms of the chain in isolation, Oliveira and Taylor has an external friction and fluctuating force in their simulations (see their Eq. 3) [46]. So perhaps it is not surprising that our results are not in agreement with the simulation. We now make the same kind of analysis for the chain in presence of friction. Due to the presence of friction, the problem can no longer be described by a Hamiltonian. But we write the continuum version of their equations of
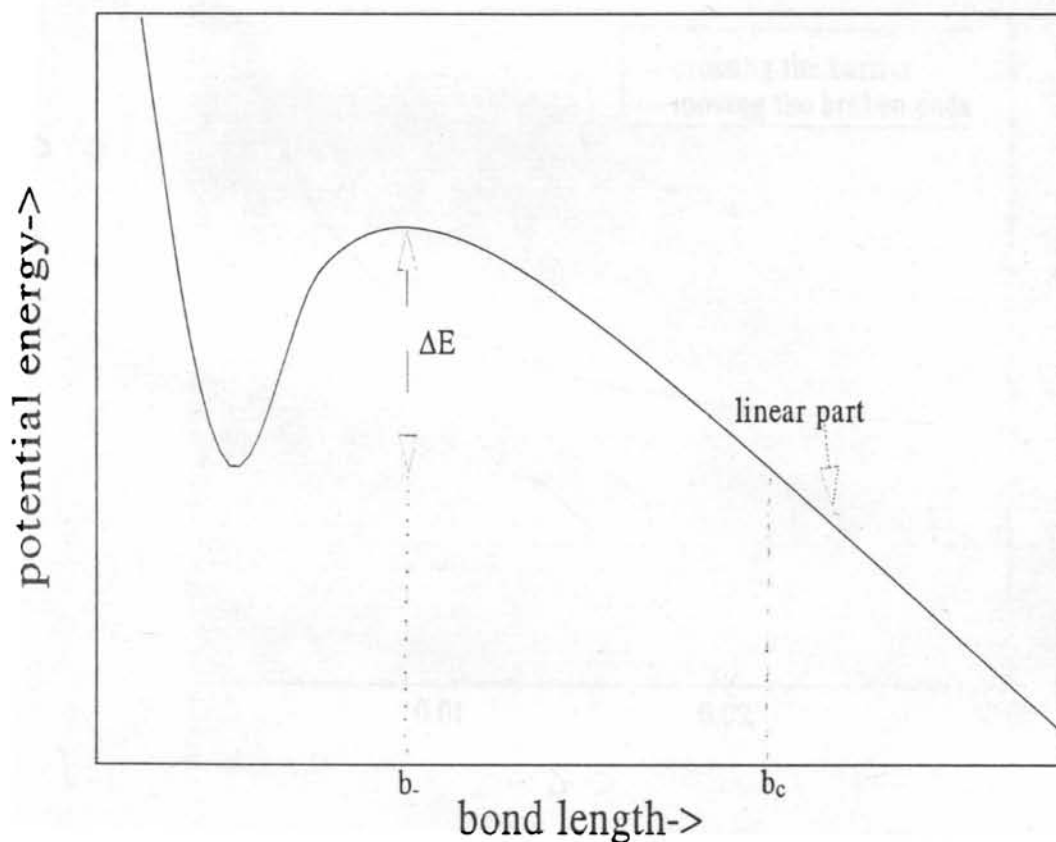
Figure 6.1: The figure shows that beyond the transition state potential energy is approximately a linear function of bond length. At b_c the potential energy of the bond is equal to its equilibrium value.
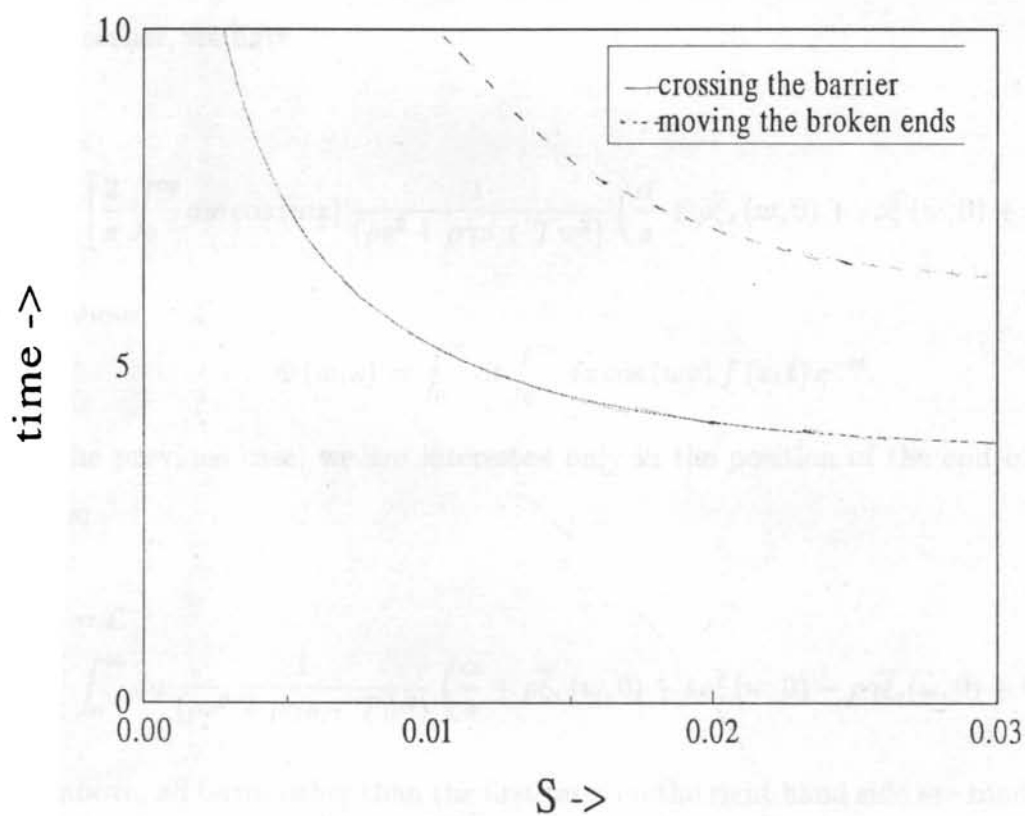
Figure 6.2: The figure compares the time required for crossing the barrier (t_{cross}) and the time required for the broken ends to separate to the critical distance. The distance is in units of a_{LJ} and time in units of τ_0.

motion, which is:

$$\rho \xi_{tt}\left(x, t\right) + \rho \gamma \xi_t\left(x, t\right) = \mathcal{T} \xi_{xx}\left(x, t\right) + \alpha \delta\left(x\right) + f(x, t), \tag{6.23}$$

γ is the friction coefficient, and $f(x, t)$ is the fluctuating force, having the mean zero and correlation

$$\langle f(x_1, t_1) f(x_2, t_2)\rangle = 2\rho\gamma k_B T \delta\left(x_1 - x_2\right)\delta\left(t_1 - t_2\right). \tag{6.24}$$

This stochastic wave equation can be analyzed just as earlier. Following the same procedure as earlier, we have

$$\xi\left(x, t\right) = \tag{6.25}$$
$$\mathcal{L}^{-1}\left[\frac{2}{\pi}\int_0^\infty dw \cos\left(wx\right)\frac{1}{\left(\rho s^2 + \rho\gamma s + \mathcal{T}w^2\right)}\left(\frac{\alpha}{s} + \rho\bar{\xi}_t\left(w, 0\right) + s\rho\bar{\xi}\left(w, 0\right) + \Phi\left(w, s\right)\right)\right].$$

In the above,

$$\Phi\left(w, s\right) = \int_0^\infty dt \int_0^\infty dx \cos\left(wx\right) f\left(x, t\right) e^{-st}. \tag{6.26}$$

As in the previous case, we are interested only in the position of the end of the chain, which is:

$$\xi\left(0, t\right) = \mathcal{L}^{-1} \tag{6.27}$$
$$\left[\frac{2}{\pi}\int_0^\infty dw\frac{1}{\left(\rho s^2 + \rho\gamma s + \mathcal{T}w^2\right)}\left(\frac{\alpha}{s} + \rho\bar{\xi}_t\left(w, 0\right) + s\rho\bar{\xi}\left(w, 0\right) - \rho\gamma\bar{\xi}_t(\omega, 0) + \Phi\left(w, s\right)\right)\right].$$

In the above, all terms other than the first term on the right hand side are random, arising from thermal fluctuations. So on calculating the averages of both the sides, we get

$$\langle \xi\left(0, t\right)\rangle = \mathcal{L}^{-1}\left[\frac{2}{\pi}\int_0^\infty dw\frac{\alpha}{s\left(\rho s^2 + \rho\gamma s + \mathcal{T}w^2\right)}\right]$$
$$= \mathcal{L}^{-1}\left[\frac{\alpha}{\rho c s\sqrt{s^2 + \gamma s}}\right] = \frac{\alpha}{\rho c}te^{-\gamma t/2}\left(I_0\left(\gamma t/2\right) + I_1\left(\gamma t/2\right)\right). \tag{6.28}$$

In the above, $I_n\left(\gamma t/2\right)$ denotes modified Bessel function of order n [166]. As earlier, the average survival time is given by solving the equation $\langle \xi\left(0, t\right)\rangle = d_c/2$ for the time t to

find the time for travelling a distance $d_c/2$ by one end of the chain. This is the survival probability of the chain. This result, is only an approximation. Strictly speaking, we should write down an analogue of the diffusion equation (6.16) for this problem and solve it to find the survival time. As the random terms in this equation are more complex than the ones in the equation (6.16), we have not done this. In the earlier problem we saw that the random terms had no effect on the average survival probability. So we neglect their influence in this problem too.

Using this, we have estimated the time of crossing the distance d_c in the presence of friction. In the small force regime the calculated time is two-three orders greater than the time taken for crossing the barrier. Applying this correction we have calculated the lifetimes for a polymer under LJ potential. In Fig. 6.3 we compare the values of the logarithms of lifetimes for the three cases- (1) without considering the motion of the broken ends (2) considering the motion of the broken ends but without friction and (3) with friction. Our calculations which takes account of friction differs only one order of magnitude from the simulations of Oliveira and Taylor [46].

6.5   Conclusion

In this chapter, we analysed the motion of the broken ends after the breaking has occured. The two ends have to be separated by a minimum distance, within which it is possible for the two broken ends to come back and heal the bond. We calculated the time required for the two broken ends to separate from one another by this critical distance. In the absence of friction, for the range of parameters considered in the simulation, this time is of the same order of magnitude as that is required for crossing the barrier. However, in the presence of friction, the calculated time is two to three orders of magnitude greater than the time taken for crossing the barrier, thus making our results in agreement with the simulations within an order of magnitude.
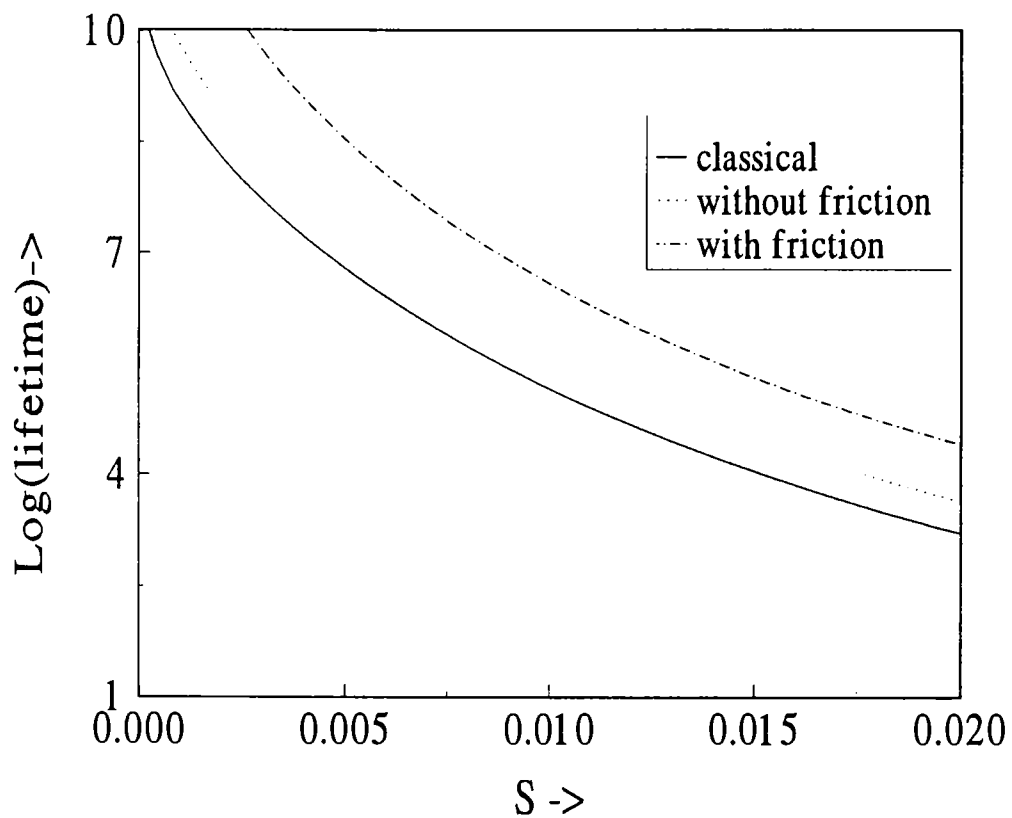
Figure 6.3: Plot of logarithm of the lifetime against the strain for the Lennard Jones potential for the three cases: transition state theory (solid curve), motion of broken ends without friction (dotted curve) and with friction (dashed curve). Energy is given in units of ε, distance in units of a_{LJ}, temperature T in units of ε/k_B and time in units of τ_0. Here $T = .05$ and $\gamma = 0.25\omega_0$. The figure shows that the damped motion of the broken ends can increase the lifetime by two orders of magnitude.

Chapter 7

Summary and Conclusions

In this chapter we summarise the entire work that had been done in this thesis.

7.1 Expression for the Rate Using QTST

We considered a single polymer molecule which is imagined to be a chain of N units of mass m joined together by bonds obeying the Morse potential. It has one end fixed and a force F is acting on the other end. We use multidimensional quantum transition state theory (QTST) to derive expressions for the rate of breaking of the polymer. The force modifies the potential of each bond so that for any nonzero value for the force F, the potential has two extrema, one being a minimum and the other a maximum. If a bond gets a certain activation energy, it can go over the barrier resulting in the breaking of the bond and consequently of the polymer. The activation energy can be easily calculated as the difference in the potential of the two extrema. As the simplest approach, we consider the vibrational motion of just one bond that may break and neglect coupling to the rest of the system. If coupling is included, the partition function will involve N frequency factors. But we need to consider only the ratio of the partition functions at the two extrema. The unstable frequency in the transition state and the ratio of the square of the frequencies of the equilibrium and transition states can be found using partion technique. The rate expression is derived also for the special case in which there is a foreign atom

105

along the main chain of the polymer. The calculations are repeated for a polymer whose units interact by Lennard–Jones potential. On comparing our results with the simulation results of Oliveira and Taylor, we see that our results are larger by orders of magnitude.

7.2   Polymer Molecule in the Presence of a Bath of Harmonic Oscillators

Oliveira and Taylor [46] have included friction in their starting equation for the simulations and so and we consider our system to be present in a bath of harmonic oscillators which can interact linearly with every unit. To be in agreement with Oliveira and Taylor [46] we take the friction to be Ohmic and also neglect quantum effects. We do the normal mode analysis for this and obtain an expression for the rate. But although the rate is found to be decreased, the decrease is only of one order of magnitude, and still the final result is not in agreement with the simulations.

7.3   Rate of Separation of the Broken Ends

To understand this discrepancy, we go beyond TST. We assume that even if the crossing over the barrier has occured, it is not necessary that the reaction should occur. After the crossing, the two ends have to separate by a minimum distance, within which it is possible for the two broken ends to come back and heal the bond. We calculate the time required for the two broken ends to separate from one another through this critical distance. For this we assume that after the breaking, the potential energy decrease is linearly dependent on the separation of the two ends. Using a continuum approximation we write the equation of motion for the system in the form of a forced wave equation. The solution of the wave equation shows that the broken end of the chain undergoes translational motion with a uniform velocity. In addition, it undergoes diffusive motion due to thermal fluctuations. Calculation of correlation function shows that the motion of the end of the chain is similar to that of a Brownian particle. We calculate the average

time that such a particle spends within the critical distance before going out for the first time from this region. This is compared with the time of crossing the barrier. The results show that in the small force regime, the first passage rate is considerably lower than that of the crossing rate and hence the rate determining step. The actual frequency may be obtained by adding the two times and then taking the inverse. On comparing the results with those of the simulations, we find that the agreement is still poor.

7.4 Separation in the Presence of Friction

We attribute this discrepancy to the fact that as the broken ends are moving, they suffer damping due to the friction of the surrounding medium. We analyse the motion of the broken ends in presence of friction by solving the continuum version of the equations used by Oliveira and Taylor. We obtain an expression for the mean position of the broken end as a function of time from which we can calculate the time needed for the end to travel the critical distance. It is seen that in the small force regime the calculated time is two-three orders greater than the time taken for crossing the barrier thus making our results in agreement with the simulations within an order of magnitude.

7.5 Conclusions

The main findings of our work are summarised below.

1. The life time of the bond is somewhat sensitive to the potential that is used in the calculations – using Lennard-Jones or the Morse potential lead to rather different answers.

2. For a given potential, a rough estimate of the rate can be obtained by a simple approximation that considers the dynamics of only the bond that breaks and neglects the coupling to neighboring bonds. Dynamics of neighboring bonds would decrease the rate, but usually not more than by one order of magnitude.

3. For the breaking of polyethylene, quantum effects are important only for temperatures below 150 K.

4. The lifetime strongly depends on the strain and as the strain varies over a narrow range, the lifetime varies rapidly from 10^5 seconds to 10^{-5}seconds.

5. If we change one unit of the polymer by a foreign atom, say by one sulphur atom, in the main chain itself, by a weaker bond, the rate is found to increase by orders of magnitude.

6. Introducing friction into Multidimensional transition state theory can decrease the rate but by only one order of magnitude.

7. The rate determining step for the process in most cases is the separation of the broken ends from one another. This is particularly true, if there is friction on the two ends from the surroundings.

Appendix A

Partitioning Formulae

The matrix identities that we use in the text are given below. For any square matrix of the form $\begin{bmatrix} \mathbf{A} & \mathbf{B} \\ \mathbf{C} & \mathbf{D} \end{bmatrix}$, with $\mathbf{A}$ and $\mathbf{D}$ square matrices, one has

$$\det \begin{bmatrix} \mathbf{A} & \mathbf{B} \\ \mathbf{C} & \mathbf{D} \end{bmatrix} = \det \mathbf{A} \det \begin{bmatrix} \mathbf{D} - \mathbf{C}\mathbf{A}^{-1}B \end{bmatrix} \tag{A.1}$$

and

$$\begin{bmatrix} \mathbf{A} & \mathbf{B} \\ \mathbf{C} & \mathbf{D} \end{bmatrix}^{-1} = \begin{bmatrix} \left(\mathbf{A} - \mathbf{B}\mathbf{D}^{-1}\mathbf{C}\right)^{-1} & -\mathbf{A}\left(\mathbf{A} - \mathbf{B}\mathbf{D}^{-1}\mathbf{C}\right)^{-1}\mathbf{B}\mathbf{D}^{-1} \\ -\left(\mathbf{D} - \mathbf{C}\mathbf{A}^{-1}\mathbf{B}\right)^{-1}\mathbf{C}\mathbf{A}^{-1} & \left(\mathbf{D} - \mathbf{C}\mathbf{A}^{-1}\mathbf{B}\right)^{-1} \end{bmatrix}. \tag{A.2}$$

109

Appendix B

The Correlation Functions

For calculating the correlation functions $\langle \zeta_1(t_1)\zeta_1(t_2)\rangle$, $\langle \zeta_2(t_1)\zeta_2(t_2)\rangle$ and $\langle \zeta_2(t_1)\zeta_1(t_2)\rangle$, we need the correlation functions $\langle \xi_t(x_1,0), \xi_t(x_2,0)\rangle$, $\langle \xi_x(x_1,0), \xi_x(x_2,0\rangle$ and $\langle \xi_t(x_1,0), \xi_x(x_2,0\rangle$. To find these, we consider the chain to be semi-infinite, with the end of the chain held fixed, and the Hamiltonian to be

$$H_{fixed} = \frac{1}{2}\rho \int_0^\infty dx \xi_t(x,t)^2 + \frac{1}{2}\mathcal{T}\int_0^\infty dx \xi_x(x,t)^2. \qquad (B.1)$$

Before the breaking, the chain is at equilibrium at a temperature T and at the time of breaking ($t = 0$), the positions $\xi(x,o)$ and velocities $\xi_t(x,0)$ have the probability distribution functional [167]

$$P[\xi(x,0),\xi_t(x,0)] = N\exp\left[-\frac{1}{k_B T}(\frac{1}{2}\rho \int_0^\infty dx \xi_t(x,t)^2 + \frac{1}{2}\mathcal{T}\int_0^\infty dx \xi_x(x,t)^2)\right] \qquad (B.2)$$

where

$$N = \left[\int D\xi(x,0)\int D\xi_t(x,0)\exp\left[-\frac{1}{k_B T}(\frac{1}{2}\rho \int_0^\infty dx \xi_t(x,0)^2 + \frac{1}{2}\mathcal{T}\int_0^\infty dx \xi_x(x,0)^2]\right]\right]^{-1} \qquad (B.3)$$

is the normalization factor. In the above, $\int D\xi_t(x,0)\int D\xi(x,0)$ stands for functional integration over all possible $\xi_t(x,0)$ and $\xi(x,0)$. Any correlation function involving $\xi_t(x,0)$

and $\xi_x(x,0)$ may be calculated as functional derivatives of the generating functional

$$G[j(x),k(x)] = N \int D\xi(x,0)D\xi_t(x,0)P[\xi(x,0),\xi_t(x,0)]$$

$$exp\left[\left(\int_0^\infty dx\xi_t(x,0)j(x) + \int_0^\infty dx\xi_x(x,0)k(x)\right)\right]. \qquad (B.4)$$

The functional can be easily evaluated and one obtains

$$G[j(x),k(x)] = exp\left[\frac{k_BT}{2}\left(\frac{1}{\rho}\int_0^\infty dxj(x)^2 + \frac{1}{\mathcal{T}}\int_0^\infty dxk(x)^2\right)\right]. \qquad (B.5)$$

Now we evaluate the correlation functions of $\xi_t(x,0)$ and $\xi_x(x,0)$ as functional derivatives of the generating functional. Thus,

$$\langle\xi_t(x_1,0),\xi_t(x_2,0)\rangle = \left[\frac{\delta^2 G(j(x),k(x))}{\delta j(x_1)\delta j(x_2)}\right]_{j=0,k=0}. \qquad (B.6)$$

$$\frac{\delta^2 G(j(x),k(x))}{\delta j(x_1)\delta j(x_2)} = \frac{\delta^2}{\delta j(x_1)\delta j(x_2)}\left(exp\left[\frac{k_BT}{2}\left(\frac{1}{\rho}\int_0^\infty dx_2j(x_2)^2 + \frac{1}{\mathcal{T}}\int_0^\infty dxk_2(x_2)^2\right)\right]\right)$$

$$= \frac{\delta}{\delta j(x_1)}\left(\frac{k_BT}{\rho}j(x_2)exp\left[\frac{k_BT}{2}\left(\frac{1}{\rho}\int_0^\infty dx_2j(x_2)^2 + \frac{1}{\mathcal{T}}\int_0^\infty dxk_2(x_2)^2\right)\right]\right)$$

$$= \frac{k_BT}{\rho}\left(\delta(x_2-x_1)\right)exp\left[\frac{k_BT}{2}\left(\frac{1}{\rho}\int_0^\infty dx_2j(x_2)^2 + \frac{1}{\mathcal{T}}\int_0^\infty dx_2k(x_2)^2\right)\right]$$

$$+ \left(\frac{k_BT}{\rho}\right)^2 j(x_2)j(x_1)\exp\left[\frac{k_BT}{2}\left(\frac{1}{\rho}\int_0^\infty dx_1j(x_1)^2 + \frac{1}{\mathcal{T}}\int_0^\infty dx_2k(x_1)^2\right)\right].$$

Hence, from Eq. (B.7),

$$\langle\xi_t(x_1,0),\xi_t(x_2,0)\rangle = \left[\frac{\delta^2 G(j(x),k(x))}{\delta j(x_1)\delta j(x_2)}\right]_{j=0,k=0} = \frac{k_BT\delta(x_2-x_1)}{\rho}. \qquad (B.7)$$

Similarly,

$$\langle\xi_x(x_1,0),\xi_x(x_2,0)\rangle = \left[\frac{\delta^2 G[j(x),k(x)]}{\delta k(x_1)\delta k(x_2)}\right]_{j=0,k=0} = \frac{k_BT\delta(x_2-x_1)}{\mathcal{T}}. \qquad (B.8)$$

$$\langle \xi_t(x_1, 0), \xi_x(x_2, 0) \rangle = \left[\frac{\delta^2 G\left[j(x), k(x)\right]}{\delta j(x_1)\delta k(x_2)} \right]_{j=0, k=0}.$$

$$\left[\frac{\delta^2 G\left[j(x), k(x)\right]}{\delta j(x_1)\delta k(x_2)} \right] = \frac{\delta}{\delta j(x_1)} \left(\frac{k_B T}{\mathcal{T}} k(x_2) exp \left[\frac{k_B T}{2} \left(\frac{1}{\rho} \int_0^\infty dx_2 j(x_2)^2 + \frac{1}{\mathcal{T}} \int_0^\infty dx_2 k(x_2)^2 \right) \right] \right)$$

$$= \frac{k_B T}{\mathcal{T}} k(x_2) j(x_1) \exp \left[\frac{k_B T}{2} \left(\frac{1}{\rho} \int_0^\infty dx_1 j(x_1)^2 + \frac{1}{\mathcal{T}} \int_0^\infty dx_1 k(x_1)^2 \right) \right].$$

i.e.,

$$\langle \xi_t(x_1, 0), \xi_x(x_2, 0) \rangle = \left[\frac{\delta^2 G\left[j(x), k(x)\right]}{\delta j(x_1)\delta k(x_2)} \right]_{j=0, k=0} = 0. \tag{B.9}$$

B.1   The Correlation Function for $\zeta_1(t)$

Now we consider $\langle \zeta_1(t_1)\zeta_1(t_2) \rangle$. Using the Eq. (6.13), we write

$$\langle \zeta_1(t_1)\zeta_1(t_2) \rangle = \langle \xi(x_1, 0)\xi(x_2, 0) \rangle_{x_1 = ct_1, x_2 = ct_2}.$$

As $\xi(0, 0) = 0$, we can write

$$\xi(x, 0) = \int_0^x dx' \xi_{x'}(x', 0).$$

Hence

$$\langle \xi(x_1, 0), \xi(x_2, 0) \rangle = \int_0^{x_1} dx' \int_0^{x_2} dx'' \langle \xi_{x'}(x', 0), \xi_{x''}(x'', 0) \rangle = \frac{k_B T}{\mathcal{T}} min(x_1, x_2). \tag{B.10}$$

$$\langle \zeta_1(t_1)\zeta_1(t_2) \rangle = \langle \xi(x_1, 0)\xi(x_1, 0) \rangle_{x_1 = ct_1, x_2 = ct_2} = \frac{k_B T}{\mathcal{T}} min(ct_1, ct_2).$$

i.e.,

$$\langle \zeta_1(t_1)\zeta_1(t_2) \rangle = \frac{k_B T c}{\mathcal{T}} min(t_1, t_2) = \frac{k_B T}{\rho c} min(t_1, t_2). \tag{B.11}$$

B.2   The Correlation Function of $\zeta_2(t)$

Now we consider the correlation function of $\zeta_2(t)$, which is defined by the Eq. (6.14) of the text

$$\langle \zeta_2(t_1)\zeta_2(t_2)\rangle = \left(\frac{2}{\pi}\right)^2 \int_0^\infty d\omega_1 \frac{\sin(c\omega_1 t_1)}{c\omega_1} \int_0^\infty d\omega_2 \frac{\sin(c\omega_2 t_2)}{c\omega_2} \left\langle \overline{\xi_t}(\omega_1,0)\overline{\xi_t}(\omega_2,0)\right\rangle. \quad (B.12)$$

Now,

$$\left\langle \overline{\xi_t}(\omega_1,0)\overline{\xi_t}(\omega_2,0)\right\rangle = \int_0^\infty dx_1 \cos(\omega_1 x_1) \int_0^\infty dx_2 \cos(\omega_2 x_2) \left\langle \xi_t(x_1,0),\xi_t(x_2,0)\right\rangle.$$

$$= \frac{k_B T}{\rho}\int_0^\infty dx_1 \cos(\omega_1 x_1)\cos(\omega_2 x_1) = \frac{k_B T}{2\rho}\int_0^\infty dx_1(\cos(\omega_1 - \omega_2)x_1 + \cos(\omega_1 + \omega_2)x_1).$$

Using the cosine representation of δ function gives

$$\left\langle \overline{\xi_t}(\omega_1,0)\overline{\xi_t}(\omega_2,0)\right\rangle = \frac{\pi k_B T}{2\rho}\left[\delta(\omega_1 - \omega_2) + \delta(\omega_1 + \omega_2)\right].$$

Using the above in the Eq. (B.12) gives

$$\langle \zeta_2(t_1)\zeta_2(t_2)\rangle = \frac{k_B T}{\rho}\frac{2}{\pi}\int_0^\infty d\omega_1 \frac{\sin(c\omega_1 t_1)}{c\omega_1}\frac{\sin(c\omega_1 t_2)}{c\omega_1} = \frac{k_B T}{\rho c}\min(t_1, t_2). \quad (B.13)$$

B.3   The Cross-Correlation Function of $\zeta_1(t)$ and $\zeta_2(t)$

$$\langle \zeta_2(t_1)\zeta_1(t_2)\rangle = \left(\frac{2}{\pi}\right)^2 \int_0^\infty d\omega_1 \frac{\sin(c\omega_1 t_1)}{c\omega_1}\int_0^\infty dx_1 \cos(\omega_1 x_1)\times$$

$$\int_0^\infty d\omega_2 \cos(c\omega_2 t_2)\int_0^{x_2} dx' \left\langle \xi_t(x_1,0),\xi_{x'}(x',0)\right\rangle = 0. \quad (B.14)$$

Appendix C

Solution for $\overline{P}(\xi, s)$

We write the Eq. (6.19)

$$s\overline{P}(\xi,s) - D\overline{P}_{\xi\xi}(\xi,s) + v\overline{P}_{\xi}(\xi,s) = \delta(\xi). \tag{C.1}$$

The equation has to be solved for the two regions, $\xi < 0$ and $\xi > 0$.

We rewrite the Eq. (C.1) for $\xi < 0$ as

$$\overline{P}_{\xi\xi}(\xi,s) - \frac{v}{D}\overline{P}_{\xi}(\xi,s) - \frac{s}{D}\overline{P}(\xi,s) = 0. \tag{C.2}$$

The general solution is

$$\overline{P}(\xi,s)_- = c_1 \exp\left(\frac{v + \sqrt{v^2 + 4sD}}{2D}\xi\right) + c_2 \exp\left(\frac{v - \sqrt{v^2 + 4sD}}{2D}\xi\right). \tag{C.3}$$

Since when $\xi \to -\infty$, $\overline{P}(\xi,s)_-$ should be zero, we have

$$\overline{P}(\xi,s)_- = c_1 \exp\left(\frac{v + \sqrt{v^2 + 4sD}}{2D}\xi\right). \tag{C.4}$$

Similarly for $\xi > 0$, the general solution is

$$\overline{P}(\xi,s)_+ = c_3 \exp\left(\frac{v + \sqrt{v^2 + 4sD}}{2D}\xi\right) + c_4 \exp\left(\frac{v - \sqrt{v^2 + 4sD}}{2D}\xi\right). \tag{C.5}$$

Here we use the boundary condition that at ξ_c, $\overline{P} = 0$. Hence,

$$c_3 \exp\left(\frac{v + \sqrt{v^2 + 4sD}}{2D}\xi_c\right) + c_4 \exp\left(\frac{v - \sqrt{v^2 + 4sD}}{2D}\xi_c\right) = 0. \qquad (C.6)$$

Therefore we get,

$$c_3 = -c_4 \exp\left(\frac{-2\sqrt{v^2 + 4sD}}{2D}\xi_c\right). \qquad (C.7)$$

Since the two solutions match at $\xi = 0$, we have,

$$c_1 = c_3 + c_4. \qquad (C.8)$$

Now we integrate Eq. (C.1) between the limits $-\epsilon$ and $+\epsilon$ with the result that

$$\int_{-\epsilon}^{\epsilon} s\overline{P}(\xi, s)d\xi - D\left(\overline{P}_\xi(\xi, s)\Big|_{-\epsilon}^{\epsilon}\right) + v\left(\overline{P}(\xi, s)\Big|_{-\epsilon}^{\epsilon}\right) = 1. \qquad (C.9)$$

Since $\overline{P}(\xi, s)$ is continous, as $\epsilon \to 0$, the first and third terms on the left hand side become equal to zero and hence

$$-D\left(\overline{P}_\xi(\xi, s)\Big|_{-\epsilon}^{\epsilon}\right) = 1, \qquad (C.10)$$

as $\epsilon \to 0$. i.e.

$$-D(\overline{P}_\xi(\epsilon, s) - \overline{P}_\xi(-\epsilon, s)) = 1, \qquad (C.11)$$

as $\epsilon \to 0$. i.e.

$$-D\left[c_3\left(\frac{v}{2D} + \frac{\sqrt{v^2 + 4sD}}{2D}\right) + c_4\left(\frac{v}{2D} - \frac{\sqrt{v^2 + 4sD}}{2D}\right) - c_1\left(\frac{v}{2D} + \frac{\sqrt{v^2 + 4sD}}{2D}\right)\right] = 1. \qquad (C.12)$$

Substituting the value of c_1 from Eq. (C.8) and simplifying we get,

$$c_4 = \frac{1}{\sqrt{v^2 + 4sD}}. \qquad (C.13)$$

Using Eq. (C.7) we get,

$$c_3 = -\frac{1}{\sqrt{v^2 + 4sD}} \exp\left(\frac{-2\sqrt{v^2 + 4sD}}{2D}\xi_c\right).$$ (C.14)

Thus, by substituting the values of the constants in the Eqs. (C.4) and (C.5), the solution for $\overline{P}(\epsilon, s)$ becomes,

for $\xi > 0$,

$$\overline{P}(\xi, s) = \frac{1}{\sqrt{v^2 + 4sD}}\left[\exp\left(\frac{v - \sqrt{v^2 + 4sD}}{2D}\xi\right) - \exp\left(\frac{v + \sqrt{v^2 + 4sD}}{2D}\xi - \frac{2\sqrt{v^2 + 4sD}}{2D}\xi_c\right)\right]$$ (C.15)

and for $\xi < 0$,

$$\overline{P}(\xi, s) = \frac{1}{\sqrt{v^2 + 4sD}}\left[\exp\left(\frac{v + \sqrt{v^2 + 4sD}}{2D}\xi\right) - \exp\left(\frac{v + \sqrt{v^2 + 4sD}}{2D}\xi - \frac{2\sqrt{v^2 + 4sD}}{2D}\xi_c\right)\right].$$ (C.16)

Eqs. (C.15) and (C.16) can be combined together as

$$\overline{P}(\xi, s) = \frac{\exp\left[\frac{v\xi - |\xi|\sqrt{v^2 + 4Ds}}{2D}\right]}{\sqrt{v^2 + 4Ds}} - \frac{\exp\left[\frac{v\xi - (\xi_c + |\xi - \xi_c|)\sqrt{v^2 + 4Ds}}{2D}\right]}{\sqrt{v^2 + 4Ds}}.$$ (C.17)

References

[1] H. H. Kausch, *Polymer Fracture*, Springer–Verlag, Berlin (1978).

[2] N. J. Capiati and R. S. Porter, J. Polym. Sci., Polym. Phys. Ed. **13**, 1177 (1975).

[3] S. N. Zhurkov, Intern. J. Fracture Mech. **1**, 311 (1965).

[4] L. Holliday and W. A. Holmes–Walker, J. Appl. Polym. Sci. **16**, 139 (1972).

[5] B. Crist, M. A. Ratner, A. L. Brower, and J. R. Sabin, J. Appl. Phys. **50**, 6047 (1979).

[6] A. D. Chevychelov, Polym. Sci. **8**, 49 (1966).

[7] A. Peterlin, Int. J. Fract. **11**, 761 (1975).

[8] A. I. Gubanov, Polym. Mech. **3**, 408 (1967).

[9] J. Smook, W. Hamersma and A. J. Pennings, J. Mater. Sci. **19**, 1359 (1984).

[10] B. D. Coleman and D.W. Marquardt, J. Appl. Phys. **28**, 1065 (1975).

[11] B. Epstein, J. Appl. Phys. **19**, 140 (1948).

[12] T. Yokobori, Kolloid–Z **166**, 20 (1959).

[13] A. Stuart and O. L. Anderson, J. Am. Ceramic Soc. **36**, 416 (1953).

[14] A. Tobolsky, H. Eyring, J. Chem. Phys. **11**, 125 (1943).

[15] Y. C. Huang, Proc. Int. Conf. Compos. Mater. Energy, 156 (1995).

[16] A.A. Griffith, Phil.Trans. Roy. Soc. A **221**, 163 (1921).

[17] C.E. Inglis, Tran. Roy. Inst. Nav. Archit. **60**, 219 (1913).

[18] G. R. Irwin, J. Appl. Mech. **61**, 449 (1939).

[19] R. P. Kambour and R.E. Robertson, *Polymer Thermal Analysis*, A.D. Jenkins (Ed.), North–Holland Publishing Co., Amsterdam, 1972, Chap. 11.

[20] T. L. Smith, *Reology*, Vol. 5, F. R. Erich (ed.), New York, Academic Press (1969), p. 127.

[21] P. J. Blatz, S. C. Sharda and N. W. Tschoegl, Trans. Soc. Rheol. **18**, 145 (1974).

[22] S. Glasstone, K. J. Laidler and H. Eyring, *The Theory of Rate Processses*, New York: McGraw Hill (1941).

[23] S. N. Zhurkov and B. N. Narzullayev, Zhur. Techn. Phys. **23**, 1677 (1953).

[24] F. Bueche, J. Appl. Phys. **26**, 1133 (1955), F. Bueche, J. Appl. Phys. **28**, 784 (1957), F. Bueche, J. Appl. Phys. **29**, 1231 (1958).

[25] A. I. Gubanov and A. D. Checychelov, Sov. Phys. Solid State **4**, 681 (1962).

[26] G. M. Bartenev, Polym. Mech. (USA) **6**, 393 (1970).

[27] A. V. Dobrodumov and A. M. El'yashevich, Sov. Phys. Solid State **15**, 1258 (1973).

[28] C. C. Hsiao, J. Appl. Phys. **30**, 1492 (1959).

[29] H. H. Kausch and C. C. Hsiao, J. Appl. Phys. **39**, 4915 (1968).

[30] R. L. Salganik, Int. J. Fracture Mech. **6**, 1 (1970).

[31] B. D. Goikhman, Strength Mater. (USA) **4**, 918 (1972).

[32] Yu. Ya. Gotlib, A. V. Dobrodumov, A. M. El'yashevich and Yu. E. Svetlov, Sov. Phys. Solid State **15**, 555 (1973).

[33] K. C. Valanis, Report G 378–ChME–001 (1974), University of Iowa, Iowa City, USA.

[34] Y. Termonia and P. Smith, Macromolecules **20**, 835 (1987).

[35] F. Bueche and J. C. Halpin, J. Appl. Phys. **35**, 36 (1964).

[36] W. Pechhold and S. Blasenbrey Kolloid–Z. Z. Polymers **241**, 955 (1970).

[37] Z–G. Wang, U. Landman, R. L. Blumberg–Selinger, and W. M. Gelbart, Phys. Rev. B **44**, 378 (1991).

[38] R. L. Blumberg Selinger, R. M. Lynden–Bell and W. M. Gelbart, J. Chem. Phys. **98**, 9808 (1993).

[39] R. W. Welland, M. Shin, D. Allen and J. B. Ketterson, Phys. Rev. B **46**, 503 (1992).

[40] L. I. Manevitch, L. S. Zarkhin and N. S. Enikolopian, J. Appl. Polym. Sci. **39**, 2245 (1990).

[41] R. C.Baljon Arlette and M. O. Robbins, Comput. theor. Polym. Sci. **9**, 35(1999).

[42] K. D. Knudsen, J. G. Hernandez Cifre and J. Garcia de la Torre, Colloid Polym. Sci. **275**, 1001 (1997).

[43] Sheng Yu–Jane, Lai Pik–Yin and Tsao Heng–Kwong, Phy. Rev. E **56**, 1900 (1997).

[44] T. Matsuda and K. Tai, Polymer **38**, 1669 (1997).

[45] R. W. Smith and D. J. Scrolovitz, Modell. Simul. Mater. Sci. Eng. **2**, 1153 (1994).

[46] F. A. Oliveira and P. L. Taylor, J. Chem. Phys. **101**, 10118 (1994).

[47] F. A. Oliveira, Phy. Rev. B. **57**, 10576 (1998).

[48] Kim Bolton, Stur Nordholm, H. W. Schranz, J. Phy. Chem. **99**, 2477 (1995).

[49] B. K. Chakrabarti, D. Chowdhury and D. Stauffer, Z. Phys. B. - Condensed Matter **62**, 343 (1986).

[50] M. R. Nyden and D. W. Noid, J. Phys. Chem. **95**, 940 (1991).

[51] J. J. Lopez Cascales and J. Garcia de la Torre, J. Chem. Phys. **95** , 9384 (1991).

[52] Cleri Fabrizio, S. R. Phillpot, D. Wolf and S.Yip, J. Am. Ceram. Soc. **81**, 501 (1998).

[53] R. L. Blumberg–Selinger, Z.-G. Wang, W. M. Gelbart and A. Ben–Shaul, Phys. Rev. A **43**, 4396 (1991).

[54] R. L. Blumberg–Selinger, Z.-G. Wang, and W. M. Gelbart , J. Chem. Phys. **95**, 9128 (1991), R. L. Blumberg–Selinger, R. M. Lynden–Bell and W. M. Gelbart, J. Chem. Phys. **98**, 9808 (1993).

[55] P. Meakin, Science **252**, 226 (1991).

[56] A. J. Kinloch and R. J. Young, *Fracture Behaviour of Polymers*, Applied Science, London (1983).

[57] R. O. Ritchie, W. W. Geberich and J..H. Underwood, *Encyclopedia of Physical Science And Technology*, Academic Press, New York (1987), vol. 5, p. 594.

[58] D. S. Dugdale, J. Mech. Phys. Solids **8**, 100 (1960).

[59] L. M. Schwartz, S. Feng, M. F. Thorpe and P. N. Sen, Phys. Rev. B **32**, 4607 (1985).

[60] R. Garcia-Molina, F. Guiinea and E. Louis, Phys. Lett **60**, 124 (1988).

[61] M. Born and K. Huang, *Dynamical Theory of Crystal Lattices*, Oxford University Press, New York (1954).

[62] P. N. Sen and M.F. Thorpe, Phys. Rev. B **15**, 4030 (1977).

[63] G. N. Hassold and D. J. Srolovitz, Phys. Rev. B **39,** 9273 (1989).

[64] C. Tang, Phys. Rev. A 31, 1977 (1986), J. Kertesz and T. Vicsek, J. Phys. A **19**, L257 (1986).

[65] J. Nittmann and H. E. Stanley, Nature **321**, 663 (1986).

[66] T. A Witten and L. M. Sander, Phys. Rev. Lett. **47**, 1400 (1981).

[67] J. D. Chen and D. Wilkinson, Phys. Rev. Lett. **55**, 1892 (1985).

[68] K. J. Maloy, F. Boger, J. Feder, T. Jossang and P. Meakin, Phys. Rev. A **36**, 318 (1987).

[69] K. J. Maloy, J. Feder and T. Jossang, Phys. Rev. Lett. **55**, 2688 (1985).

[70] W. A. Curtin and H. Sher, J. Matter. Res. **5**, 535 (1990).

[71] H. J. Herrmann, J. Kertesz and L. de Arcangelis, Europhys. Lett. **10**, 147 (1989).

[72] P. Meakin, J. Phys. A **18**, L661 (1985).

[73] R. C. Ball and R. M. Brady, J. Phys. A **18**, L809 (1985).

[74] S. Tolman and P. Meakin, Phys. Rev. A **40**, 428 (1989).

[75] L. Niemeyer, L. Pictronero and H. J. Weismann, Phys. Rev. Lett. **52**, 1033 (1984).

[76] P. Meakin, Thin Solid Films **151**, 165 (1987).

[77] G. M. Barteenev and Yu. S. Zuyev, *Strength and Failure of Viscoelastic Materials*, Oxford: Pergamon Press (1968), p. 143ff., E. H. Andrews, *Fracture in Polymers*, Edinburgh: Oliver and Boyd (1968).

[78] D. C. Prevorsek, J. Polym. Sci. C **32**, 343 (1971).

[79] G. Mikos Antonios and A. Peppas Nikolaos, J. Chem. Phys. **88**, 1337 (1988).

[80] M. Sambasivam, A. Klein and L. H. Sperling, J. Appl. Polym. Sci. **58**, 357 (1995).

[81] C. Y. Hui and E. J. Kamer, Polym. Eng. Sci. **35**, 419 (1995).

[82] B. Crist, M. A. Ratner, A. L. Brower and J. R. Sabin, J. Appl. Phys. **50**, 6047 (1979).

[83] B. Crist Jr., Jens Oddershede, J. R. Sabin, J. W. Perram and M. A. Ratner, J. Polym. Sci. **22**, 881 (1984).

[84] LiuYongning, Int. J. Fract. **86** L3 (1997).

[85] Pla Oscar, Modell. Simul. Mater. Sci. Eng. **4**, 193 (1996).

[86] Moon chay-Kwon and G. Mcdonough Walter, J. Appl. Polym. Sci. **67**, 1701 (1998).

[87] Li Qiang, He Ziru, Song Mingshi and Tang Aoqing, Macromol. Theory Simul. **5**, 183 (1996).

[88] A. Chudnovsky, Y. Shulkin, D. Baron and K. P. Lin, J. Appl. Polym. Sci. **56**, 1465 (1995).

[89] B. N. J. Persson, J. Chem. Phys. **110**, 9713 (1999).

[90] L. S. Levitov, A. V. Shytovand and A. Yu. Yakovets, Phys. Rev. Lett. **75**, 370 (1995).

[91] M. Sambasivam, A. Klein, T. N. Thomas, N. Mohammadi and L. H. Sperling, Polym. Mater. Sci. Eng. **68**, 161 (1993).

[92] L. H. Sperling, M. Sambasivam and A. Klein, Polym. Mater. Sci. Eng. **73**, 45 (1995).

[93] S. D. Sjoerdsma, J. P. H. Boyens, Polym. Eng. Sci. **34**, 86 (1994).

[94] T. P. Doerr and P. L. Taylor, J. Chem. Phys. **101**, 10107 (1994).

[95] I. E. Govaert and T. Peijs, Polymer **36**, 4425 (1995).

[96] S. Arrhenius, Z. Phys. Chem. (Leipzig) **4**, 226 (1889).

[97] H. Eyring, J. Chem. Phys. **3**, 107 (1935).

[98] E. Wigner, J. Chem. Phys. **5**, 720 (1937).

[99] M. Polanyi and E. Wigner, Z. Phys. Chem. Abt. A **139**, 439 (1928).

[100] H. Petzer and E. Wigner, Z. Phys. Chem. Abt. B**15**, 445 (1932).

[101] W. F. K. Wynne–Jones and H. Eyring, J. Chem. Phys. **3**, 492 (1935).

[102] M. G. Evans and M. Polanyi, Trans. Faraday Soc. **31**, 875 (1935).

[103] O. K. Rice and H. C. Ramsperger, J. Am. Chem. Soc. **49**, 1617 (1927).

[104] L. S. Kassel, Proc. Nat. Acad. Sci. USA A14, 23 (1928).

[105] R. A. Marcus, J. Chem. Phys. 20, 359 (1952); R. A. Marcus, J. Chem. Phys. 43, 2658 (1965).

[106] W. L. Hase, *Dynamics of Molecular Collisions*, Part B, Plenum New York (1976) p. 121.

[107] E. E. Nikitin, *Theory of Elementary Atomic and Molecular Processes in Gases* Oxford: Clarendon (1974), Chapter 1.

[108] P. Pechukas and F. J. McLafferty, J. Chem. Phys. 58, 1622 (1973).

[109] B. C. Garrett and D. G. Truhler, J. Chem. Phys. 70, 1593 (1979).

[110] R. A. Marcus, J. Chem. Phys. 45, 2138 (1966); ibid. 2630 (1966).

[111] D. G. Truhlar and B. C. Garrett, Acc. Chem. Res. 13, 440 (1980).

[112] D. M. Bishop and K. J. Laidler, Trans. Faraday Soc. 66, 1685 (1970).

[113] J. C. Keck, J. Chem. Phys. 32, 1035 (1960).

[114] W. L. Hase, J. Chem. Phys. 64, 2442 (1976).

[115] B. H. Mahan, J. Chem. Ed. 51, 709 (1974); W. H. Miller, Acc. Chem. Res. 9, 306 (1976).

[116] H. S. Johnston and D. Rapp, J. Am. Chem. Soc. 83, 1 (1961).

[117] R. A. Marcus and M. E. Coltrin, J. Chem. Phys. 67, 2609 (1977).

[118] W. H. Miller, N. C. Handy and J. E. Adams, J. Chem. Phys. 72, 99 (1980).

[119] R. T. Skodje, D. G. Truhlar and B. C. Garett, J. Chem. Phys. 85, 3019 (1981); B. C. Garett and D. G. Truhlar, J. Chem. Phys. 81, 309 (1984).

[120] L. D. Landau and E. M. Lifshitz, *Quantum mechanics* (2nd edn.) Pergamon Press, Oxford (1965).

[121] H. A. Kramers, Physica **7**: 284 (1940).

[122] P. Hänggi, P. Talkner and M.Borkovec, Rev. Mod. Phys. **62**, 251 (1990).

[123] E. Pollak, H. Grabert, and P. Hänggi, J. Chem. Phys. **91**, 4073 (1989).

[124] J. S. Langer, Ann. Phys. **54**, 258 (1969).

[125] B. J. Matkowsky, Z. Schuss and E. Ben–Jacob, SIAM J. Appl. Math. **42**, 835 (1982).

[126] B. J. Matkowsky, Z. Schuss and C. Tier, SIAM J. Appl. Math. **43**, 673 (1983).

[127] E. Pollak and E. Hershkowitz, Chem. Phys. **180**, 191 (1994).

[128] R. F. Grote and J. T. Hynes, J. Chem.Phys. **73**, 2715 (1980).

[129] R. Zwanzig, J. Stat. Phys. **9**, 215 (1973).

[130] E. Pollak, J. Chem. Phys. **85**, 865 (1986); (b) E. Pollak, S.C. Tucker and B. J. Berne, Phys. Rev. Lett. **65**, 1399 (1990).

[131] J. B. Strauss and G. A. Voth, J. Chem. Phys. **96**, 5460 (1992); (b) J.B. Strauss, J.M. Gomez Llorente, and G. A. Voth, ibid. **98**, 4082 (1993).

[132] S. D. Schwartz, J. Chem. Phys. **105**, 6871 (1996).

[133] G. A. Voth, D. Chandler and W. H. Miller, J. Chem. Phys. **91**, 7749 (1989).

[134] G.A. Voth, Chem. Phys. Lett. **170**, 289 (1990).

[135] M. Messina, G. K. Schenter, and B. C. Garrett, J. Chem. Phys. **99**, 8644 (1993).

[136] M. Topaler and N. Makri, J. Chem. Phys. **101**, 7500 (1994).

[137] Y. Georgievskii and E. Pollak, J. Chem. Phys. **103**, 8910 (1995).

[138] S. Jang, A.G.Voth, J. Chem. Phys. **112**, 8747 (2000).

[139] D. M. Wardlaw and R. A. Marcus, Chem. Phys. Lett. **110**, 230 (1984); J. Chem. Phys. **83**, 3462 (1985).

[140] W. L. Hase and D. M. Wardlaw, *Biomolecular Collisions* Chemical Society, London (1989); D. M. Wardlaw and R. A. Marcus, Adv. Chem. Phys. **70**, 231 (1988), Part 1.

[141] E. E. Aubanel and D. M. Wardlaw, J. Phys. Chem. **93**, 3117 (1989).

[142] (a). S. J. Klippenstein and R. A. Marcus, J. Chem. Phys. **87**, 3410 (1987); (b) J. Phys. Chem. **92**, 3105 (1988).

[143] S. J. Klippenstein, Chem. Phys. Lett. **170**, 71 (1990); **214**, 418 (1993); J. Chem. Phys. **94**, 6469 (1991); **96**, 367 (1992); J. Phys. Chem. **98**, 11459 (1994).

[144] (a) S. C. Smith, J. Chem. Phys. **95**, 3404 (1991); (b) **97**, 2406 (1992); (c) J. Phys. Chem. **97**, 7034 (1993).

[145] S. H. Robertson, A. F. Wagner and D. M. Wardlaw, J. Chem. Phys. **103**, 2917, (1995); Robertson et al., Faraday Discuss. Chem. Soc. **102**, 65 (1995).

[146] S. H. Robertson, A. F. Wagner and D. M. Wardlaw, J. Chem. Phys. **113**, 2648 (2000).

[147] A.A. Ovichinnikov and Yu. I. Dakhnoskii, J. Electroanal. Chem. 202, 1 (1989).

[148] K. L. Sebastian, J. Chem. Phys. 90, 5056 (1989).

[149] A. A. Maradudin, *Theory of Lattice Dynamics in the Harmonic Approximations, Solid State Physics Supplement 3*, Academic Press (1964).

[150] M. Abramowitz, I. A. Stegun, *Handbook of Mathematical Functions*, Dover Publications, Inc, New York (1964).

[151] E. T. Whittaker and G. N. Watson, *A Course of Modern Analysis*, 4th edition, Cambridge University Press, New York (1927).

[152] L. Garnier, B G Manuel, E. W. van der Vegte, J. Snijders and G. Hadziioannou, J. Chem. Phys. **113**, 2497 (2000).

[153] C. Ortiz and G. Hadziioannou, Macromolecules **32**, 780 (1999).

[154] M. Rief, J. Pascual, M. Saraste and H. E. Gaub, J. Mol. Biol. **286**, 553 (1999).

[155] J. E. Bemis, B. B. Akhremitchev and G. C. Walker, Langmuir **15**, 2799 (1999).

[156] E. L. Florin, V. T. Moy and H. E. Gaaub, Science **264**, 415 (1994).

[157] M. Grandbois, M. Beyer, M. Rief, H. Classen-Schaumann and H. E. Gaub, Science **283**, 1727 (1999).

[158] R. C. Weast (Ed.), *CRC Handbook of Chemistry and Physics*, CRC Press Inc. Florida (1982).

[159] A. Vijay and D. N. Sathyanarayana, Journal of Molecular Structure, **327**, 181 (1994).

[160] U.Weiss, *Quantum Dissipative Systems*, World Scientific (1993).

[161] R. J. Rubin, J. Math. Phys. **11**, 309 (1960); *ibid.* **2**, 373 (1961).

[162] J. R. Senitzky, Phys. Rev. **119**, 670 (1960).

[163] G. W. Ford, M. Kac and P. Mazur, J. Math. Phys. **46**, 504 (1965).

[164] P. Ullersma, Physica (Utrecht) **32**, 27, 56, 74, 90 (1966).

[165] K. L. Sebastian and R. Puthur, Chemical Physics Letters **304**, 399 (1999).

[166] Abramowitz, I. Stegun, *Handbook of Mathematical Functions*, equations (4.3.89) and (4.5.69), Dover Publications, Inc, New York (1964).

[167] J. Zinn-Justin, Quantum Field Theory and Critical Phenomena, Third edition, chapters 1-6, Clarendon Press, Oxford (1996).